



ICONAT 2023

V. International Conference on Natural Science
and Technologies
Sunny Beach-Bulgaria
1st-3th June 2023



CONFERENCE BOOK
2023

ISBN: 978-625-00-1543-8

CHAIRMAN OF CONFERENCE

Prof. Dr. Abidin KILIÇ, Eskişehir Technical University

ORGANIZING COMMITTEE

Prof. Dr. Abidin KILIÇ, Eskişehir Technical University

Prof. Dr. Murad Omarov, Vice Rector, Kharkiv National University of Radio Electronics

Prof. Dr. Zafer Demir, Eskişehir Technical University

International Scientific Committee

Prof. Dr. Andrii Chukhrai (Ukraine)

Prof. Dr. Arturas Mickus (Lithuania)

Dr. Asif Pashayev (Azerbaijan)

Prof. Dr. Cengiz Türe (Turkey)

Prof. Dr. Dmytro Fedasyuk (Ukraine)

Prof. Dr. Dursun Aydın (Turkey)

Prof. Dr. Ekrem Aydiner (Turkey)

Prof. Dr. Ekrem Gürel (Turkey)

Prof. Dr. Feridun Ay (Turkey)

Prof. Dr. Hakan Dal (Turkey)

Prof. Dr. Hüseyin Sarı (Turkey)

Prof. Dr. Igor Nevlidov (Ukraine)

Prof. Dr. Igor Ruzhentsev (Ukraine)

Prof. Dr. İsmail Sökmen (Turkey)

Dr. Sofija S. Bekić (Serbia)

Prof. Dr. Kadir Aslan (USA)

Prof. Dr. Khanmammadov Agil (Azerbaijan)

Dr. Latifa Agamalieva (Azerbaijan)

Prof. Dr. Marzena S. Miichalowska (Poland)

Prof. Dr. Mehmet Candan (Turkey)

Prof. Dr. Meryem Akbelen (Turkey)

Prof. Dr. Murat Tanışlı (Turkey)

Prof. Dr. Mustafa Hoştut (Turkey)

Prof. Dr. Nihal Kus (Turkey)

Prof. Dr. Oguz Gülseren (Turkey)

Prof. Dr. Oleg Lazarenko (Ukraine)

Prof. Dr. Oleh Avrunin (Ukraine)

Prof. Dr. Oleksandr Lemeshko (Ukraine)

Prof. Dr. Oleksandr Tsopa (Ukraine)

Dr. Aygün IŞIK YILDIZ (Turkey)

Dr. Rahul M. Mane (India)

Prof. Dr. Rauf Amirov (Turkey)

Prof. Dr. Saliha Ilican (Turkey)

Prof. Dr. Sedef Dikmen (Turkey)

Prof. Dr. Sevil Çetinkaya Güner (Turkey)

Prof. Dr. Svetlana Kashuba (Poland)

Prof. Dr. Tayfun Akın (Turkey)

Prof. Dr. Urfat Nuriyev (Turkey)

Prof. Dr. Valentin Filatov (Ukraine)

Prof. Dr. Volodymyr Storozhenko (Ukraine)

Prof. Dr. Yevgenii Bodyansky (Ukraine)

Prof. Dr. Yevgen Nelin (Ukraine)

Prof. Dr. Yuri Machekhin (Ukraine)

Prof. Dr. Yüksel Ergün (Turkey)

MEETING LINK INFORMATION

HALL

<https://teams.microsoft.com/l/meetup->

[join/19%3ameeting_MTQ3OGU2MTAtOGExNC00ZGUzLWFIOWMtNmQ5M2Y2NTQ5NjZj%40thread.v2/0?context=%7b%22Tid%22%3a%22e24840f1-c171-4007-ae2d-ffc773f3119f%22%2c%22Oid%22%3a%2251bed7dc-4824-40c8-94e8-2672fe661cd7%22%7d](https://teams.microsoft.com/l/meetup-join/19%3ameeting_MTQ3OGU2MTAtOGExNC00ZGUzLWFIOWMtNmQ5M2Y2NTQ5NjZj%40thread.v2/0?context=%7b%22Tid%22%3a%22e24840f1-c171-4007-ae2d-ffc773f3119f%22%2c%22Oid%22%3a%2251bed7dc-4824-40c8-94e8-2672fe661cd7%22%7d)

Official Opening of the ICONAT-2023
01 June 2023 Meeting Salon I–Royal Castle Hotel

ICONAT 2023 PROGRAMME

- 09.00 The Start of Registration Process
- 09.30 Official Opening of the ICONAT-2023
Welcome by Conference
- Prof. Dr. Abidin Kılıç,
Eskisehir Technical University, Türkiye
Chairman of Organization Committee
- Prof. Dr. Omarov Murad,
Vice-Rector, NURE, Ukraine
- Prof. Dr. Zafer Demir,
Eskisehir Technical University, Türkiye
Chairman of Organization Committee
- Invited Speaker
Prof. Dr. Cengiz Türe
- Invited Speaker
Prof. Dr. Cem Cevik
- Invited Speaker
Prof. Dr. Igor Grebennik
“Solution strategy for some pickup and delivery problems based on the cyclic transfer approach”
- Invited Speaker
Assoc. Prof. Yurii Romashov
- 12.00 **Lunch Break**
- 19.00 **Conference Dinner-Bulgarian Tradational Dinner**

POSTER PRESENTATION SEASION: 01.06.2023 Thursday-15.00-17.00

01.06.2023 Thursday-14.00-15.00

ORAL PRESENTATIONS		
Chairing Abidin Kılıç		
01	AA Christy <i>Norway</i>	Desiccant Properties of Natural Bio-polymers studied by NIR Spectroscopy
02	Okan Külköylüoğlu, İsmail Ömer Yılmaz, Oğuz Mülayim, Süphan Karaytuğ, Serdar Sak, Serdar Sönmez <i>Türkiye</i>	Correlational Analyses Amid Water-Sediman Samples and Species From The Islands of Antarctica
03	Mete Özkurt <i>Türkiye</i>	Nilco Interaction May Play an Important Role in The Progression of Colorectal Cancer
04	Igor Nevliudov, Igor Badanyuk, Dmytro Nikitin <i>Ukraine</i>	Topological image processing for comprehensive defect and deviation analysis using adaptive binarisation

01.06.2023 Thursday-15.15-16.15

ORAL PRESENTATIONS		
Chairing Zafer Demir		
05	Oleksandr Miahkyi, Volodymyr Storozhenko, Roman Orel, Sergey Meshkov <i>Ukraine</i>	Reducing The Level Of Interference Considering The Morphological Characteristics of Objects in Thermal Nondestructive Testing
06	Oleksander Chubukin <i>Ukraine</i>	The Effect of Heat Treatment on The Structure of Niobium Oxide Films
07	Lili Arabuli, Ketevan Tavamaishvili, Tomas Macek, Petra Lovecka, Rudolf Jezek, Hristo Najdenski <i>Georgia</i>	Synthesis, Characterization and Evaluation of Anti-Tuberculosis Potential of Novel Hybrid Compounds Based on Isoniazid and Pyrazinamide

01.06.2023 Thursday-15.15-16.15

ORAL PRESENTATIONS		
Chairing A.A. Christy		
08	Tuğçe Pekdoğan <i>Türkiye</i>	The Power of Green Walls: A Sustainable Design Solution
09	Igor Nevliudov, Vladyslav Yevsieiev, Svitlana Maksymova, Oleksandr Klymenko, Maksym Vzhesniewski <i>Ukraine</i>	Shuttle-Based Storage and Retrieval System 3d Model Improvement and Development
10	Igor Nevliudov, Serhii Novoselov, Oksana Sychova <i>Ukraine</i>	Control Automation of Assembly Operations Using A Computer Vision System in Intelligent Production

11	Onur Şahin <i>Türkiye</i>	Efficiency of Smart Trans... Disorders in The... network
----	------------------------------	---

withdrawn

01.06.2023 Thursday-16.30-17.30

ORAL PRESENTATIONS		
Chairing Okan Külköylüoğlu		
12	Emine Nur Ünveren Bilgiç, Nazire Burçin Hamutoğlu, Emre Çam <i>Türkiye</i>	Examination of The Relationship Between The Occupational Identity Perceptions of Primary School Mathematics Teacher Candidates and TPCK
13	Victoria Nevlyudova, Nikolay Starodubtsev <i>Ukraine</i>	Mathematical Modelling of The Informative Feature Choice for Lifecycle State Analysis of Radio-Electronic Means Processes
14	Igor NEVLIUDOV, Murad OMAROV, Yurii ROMASHOV <i>Ukraine</i>	Numerical Methods to Solve Optimal Control Problems for Technical Applications Under Novel Global Challenges
15	Yurdakul AYGÖRMEZ <i>Türkiye</i>	Effect of Magnesium Sulfate... Metal Zeolite Based Geopolymer Mortars Produced with... powder

withdrawn

02.06.2023 Friday-9.30-10.30

ORAL PRESENTATIONS		
Chairing Emre Aytuğ Özsoy		
16	Hülya Kuru Mutlu, Mustafa Kulakci, Uğur Serincan <i>Türkiye</i>	High Selective Etching Gaas/Al _{0.3} ga _{0.7} as For Pn Junction Solar Cell Using Citric Acid Solution
17	Mehmet Fidan <i>Türkiye</i>	Two-Dimensional Data Generation Method From Multiple Time Series For 2d-Cnn-Based Rul Estimation Of Lithium-Ion Batteries
18	Nihal Kuş <i>Türkiye</i>	Analysis of C-H...O Interaction Between Anion and Cation of 1,3-Dimethylimidazolium Methylsulphate Using Natural Bond Orbital Method
19	Nazire Burçin Hamutoğlu, Emrah Bilgiç, Emine Nur Ünveren-Bilgiç <i>Türkiye</i>	An Evaluation on Inclusive Education During Distance Education Process: Classroom Teachers' Perceptions

02.06.2023 Friday-10.45-11.45

ORAL PRESENTATIONS		
Chairing Nihal Kuş		
20	Aslı Kaya, Nazire Burçin Hamutoğlu, Emre Çam, Emine Nur Ünveren-Bilgiç <i>Türkiye</i>	The Importance of The Planning Cycle for An Effective Structuring of Online Teaching Processes
21	Turan Teymurbaylı, Utku Kaya <i>Türkiye</i>	Deep Learning Advancements in Railway Track Segmentation: Previous Studies and Improvements
22	Fehmi Aslan <i>Türkiye</i>	Investigation of The Efficiency Of DSSC For Saffron Extract
23	Sara Abdolmaleki, Samad Khaksar <i>Georgia</i>	Evaluation of The Central-Metal Effect on Anticancer Activity and Mechanism of Action of Isostructural Cu(II) and Ni(II) Complexes Containing Pyridine-2,6-Dicarboxylate.

02.06.2023 Friday-14.00-15.00

ORAL PRESENTATIONS		
Chairing Lili Arabuli		
24	Igor Nevlidov, Iryna Zharikova, Sergiy Novoselov, Dmytro Nikitin <i>Ukraine</i>	Simulation of Flexible Printed Structures Design for Mobile Robot Platform
25	Svitlana Maksymova, Viktoriia Nevliudova, Oleksandr Klymenko, Gennadii Makarenko <i>Ukraine</i>	Voice Control Using in Pharmaceutical Products Logistics Systems
26	Cihangir KALE, Hikmet ESEN <i>Türkiye</i>	Investigation of Hydrogen Production by Using Concentrated Photovoltaic/Thermal Hybrid Collector with Spectral Beam Splitting
27	Murad Omarov, Vusala Muradova <i>Ukraine</i>	Bayesian Regularization of Learning

02.06.2023 Friday-15.15-16.15

ORAL PRESENTATIONS		
Chairing Mehmet Fidan		
28	Sergii Makovetskyi, Kauk Viktor <i>Ukraine</i>	Research of The Stability of The Secure Radio-Frequency Communication in The Distributed Systems by Using Multy-Channel IOT LPWAN Technologies
29	L. Arabuli, I. A. Iashchishyn, N. V. Romanova, G. Musteikyte V. Smirnovas, H. Chaudhary, Ž. M. Svedruži'c, And L. A. Morozova-Roche <i>Georgia</i>	Co-Aggregation Of S100a9 Protein With L- Dopa And Cyclen-Based Compounds – Effect On The Amyloid Fibril Self-Assembly
30	Peyman Salahshour, Samad Khaksar <i>Georgia</i>	3,5-Bis(trifluoromethyl) phenylammonium triflate: a new and green organocatalyst for the synthesis of indeno[1,2-b]pyridines
31	Olena Kovalenko, Olga Yunakova, Mykola Yunakov <i>Ukraine</i>	Peculiarities of $CS_{1-x}Rb_xCu_2Cl_3$ Solid Solutions Absorption Spectra

02.06.2023 Friday-16.30-17.30

ORAL PRESENTATIONS		
Chairing N. Burçin Hamudoğlu		
32	Igor Nevlidov, Dmytro Nikitin, Igor Badanyuk, Roman Strelets, Yegor Korotun <i>Ukraine</i>	Factor Analysis of Photopolymer Resins for 3D Printing
33	Hatice Güney, Abidin Kılıç <i>Türkiye</i>	Examining The Symmetry Operations of The DNA Molecule with Clifford Algebra
34	Abidin Kılıç <i>Türkiye</i>	Investigation of Transformation' Symmetric Molecules with Clifford Algebra
35	Murad Omarov, Vladyslav Korobskyi, Viktoriia Nevliudova <i>Ukraine</i>	Ensuring the robot snake's movement on slippery surfaces
36	Emre Aytuğ ÖZSOY <i>Türkiye</i>	A Geotechnical Examination of Kahramanmaras (Turkey) Pazarcık & Ekinözü 6 February 2023 Earthquakes
37	Çetin Yavuz, Ali Tarokh, Aydın Dikici <i>Türkiye</i>	Numerical Analysis of A New Thermosyphon Heat Pipe

38	Igor NEVLIUDOV, Shakhin OMAROV, Olena CHALA, Serhii TESLIUK <i>Ukraine</i>	Study of manufacturing defects in the technology of manufacturing moems semiconductor substrates for technical automation means
39	Igor NEVLIUDOV, Andriy SLUSAR, Kyrylo KRUSTALOV, Sofia KRUSTALOVA, Shakhin OMAROV <i>Ukraine</i>	Intelligent energy supply management system in the municipal sector"

01.06.2023 Thursday-14.00-17.0

POSTER PRESENTATIONS		
		Poster Presentation Hall
P1	Imane Bouguenoun, Widad Bouguenoun, Dalila Bendjeddou, Marie-Claire De Pauw-Gillet, Edwin De Pauw <i>Algeria</i>	The Stimulating Effect of The Cupressus Sempervirens Major Allergen (Cup S1) on Bronchial Epithelial Cells (Beas -2B)
P2	Tarana Poladova <i>Azerbaijan</i>	Synthesis and Study of New Surface-Active Polymer Complex with Catanionic Salt
P3	A.N. Mammadov, U.N. Sharifova, F.S. Ibrahimova, A.M. Qasimova, Mustafayeva A.N. <i>Azerbaijan</i>	Synthesis of Sodium Titanates Using Chitosan in The Environment
P4	Ulkar Shiraliyeva, Elmira Huseynova, Aida Rzayeva, Zarifa Mammadova, Saida Nadjafova, Nurana Mardanova <i>Azerbaijan</i>	Study of Activity and Selectivity of Oxide Catalysts in Hydrocarbon Oxidation Reactions
P5	Nur Uluhan, Abidin Kılıç <i>Türkiye</i>	The Importance of Earthquake Education in Science Center
P6	Almila Selcen Uray, Abidin Kılıç <i>Türkiye</i>	An Approach to the Representation of Platonic Solids with Geometric Algebra

ABSTRACTS

CONTENTS

NO	AUTHORS	TITLE	PAGE
01	Christy A.A. <i>Norway</i>	DESICCANT PROPERTIES OF NATURAL BIO-POLYMERS STUDIED BY NIR SPECTROSCOPY	10
02	Okan KÜLKÖYLÜOĞLU, İsmail Ömer YILMAZ, Oğuz MÜLAYİM, Süphan KARAYTUĞ, Serdar SAK, Serdar SÖNMEZ <i>Türkiye</i>	CORRELATIONAL ANALYSES AMID WATER-SEDIMAN SAMPLES AND SPECIES FROM THE ISLANDS OF ANTARCTICA	10
03	Mete Özkurt, <i>Türkiye</i>	NILCO INTERACTION MAY PLAY AN IMPORTANT ROLE IN THE PROGRESSION OF COLORECTAL CANCER	11
04	Igor Nevliudov, Igor Badanyuk, Dmytro Nikitin <i>Ukraine</i>	TOPOLOGICAL IMAGE PROCESSING FOR COMPREHENSIVE DEFECT AND DEVIATION ANALYSIS USING ADAPTIVE BINARISATION	11
s0 5	Oleksandr MIAHKYI, Volodymyr STOROZHENKO, Roman OREL, Sergey MESHKOV <i>Ukraine</i>	REDUCING THE LEVEL OF INTERFERENCE CONSIDERING THE MORPHOLOGICAL CHARACTERISTICS OF OBJECTS IN THERMAL NONDESTRUCTIVE TESTING	12
06	Oleksandr CHUBUKIN <i>Ukraine</i>	THE EFFECT OF HEAT TREATMENT ON THE STRUCTURE OF NIOBIUM OXIDE FILMS	13
07	Lili Arabuli ^{1*} , Ketevan Tavamaishvili ² , Tomas Macek ³ , Petra Lovecka ³ , Rudolf Jezek ³ , Hristo Najdenski ⁴ <i>Georgia, Czech Republic, Bulgaria</i>	SYNTHESIS, CHARACTERIZATION AND EVALUATION OF ANTI-TUBERCULOSIS POTENTIAL OF NOVEL HYBRID COMPOUNDS BASED ON ISONIAZID AND PYRAZINAMIDE	14
08	Tugce Pekdogan <i>Türkiye</i>	THE POWER OF GREEN WALLS: A SUSTAINABLE DESIGN SOLUTION	14
09	Igor Nevliudov, Vladyslav Yevsieiev, Svitlana Maksymova, Oleksandr Klymenko, Maksym Vzhesniewski <i>Ukraine</i>	SHUTTLE-BASED STORAGE AND RETRIEVAL SYSTEM 3D MODEL IMPROVEMENT AND DEVELOPMENT	15
10	Igor Nevliudov, Serhii Novoselov, Oksana Sychova <i>Ukraine</i>	CONTROL AUTOMATION OF ASSEMBLY OPERATIONS USING A COMPUTER VISION SYSTEM IN INTELLIGENT PRODUCTION	15
11	Onur Şahin withdrawn <i>Türkiye</i>	AKILLI ULAŞIM SİSTEMLERİNİN ULAŞIM AĞINDAKİ YAPISAL BOZULMALARIN TESPİTİNDEKİ ETKİNLİĞİ	15
12	Emine Nur Ünveren Bilgiç, Nazire Burçin Hamutoğlu , Emre Çam <i>Türkiye</i>	EXAMINATION OF THE RELATIONSHIP BETWEEN THE OCCUPATIONAL IDENTITY PERCEPTIONS OF PRIMARY SCHOOL MATHEMATICS TEACHER CANDIDATES AND TPCK	16
13	Victoria Nevlyudova, Nikolay Starodubtsev <i>Ukraine</i>	MATHEMATICAL MODELLING OF THE INFORMATIVE FEATURE CHOICE FOR LIFECYCLE STATE ANALYSIS OF RADIO-ELECTRONIC MEANS PROCESSES	16
14	Igor NEVLIUDOV, Murad OMAROV, Yurii ROMASHOV <i>Ukraine</i>	NUMERICAL METHODS TO SOLVE OPTIMAL CONTROL PROBLEMS FOR TECHNICAL APPLICATIONS UNDER NOVEL GLOBAL CHALLENGES	17
15	Yurdakul AYGÖRMEZ withdrawn <i>Türkiye</i>	KAOLİN KİLİ TOZU İLE ÜRETİLEN METAZEOLİT TABANLI GEOPOLİMER HARÇLARDA MAGNEZYUM SÜLFAT ETKİSİ	17
16	Hülya KURU MUTLU, Mustafa KULAKCI, Uğur SERİNCAN <i>Türkiye</i>	HIGH SELECTIVE ETCHING GAAS/AL _{0.3} GA _{0.7} AS FOR PN JUNCTION SOLAR CELL USING CITRIC ACID SOLUTION	18
17	Mehmet Fidan <i>Türkiye</i>	TWO-DIMENSIONAL DATA GENERATION METHOD FROM MULTIPLE TIME SERIES FOR 2D-CNN-BASED RUL ESTIMATION OF LITHIUM-ION BATTERIES	18
18	Nihal KUŞ <i>Türkiye</i>	ANALYSIS of C-H-O INTERACTION BETWEEN ANION and CATION of 1,3-DIMETHYLIMIDAZOLIUM METHYLSULPHATE USING NATURAL BOND ORBITAL METHOD	19
19	Emrah BİLGİÇ, Emine Nur ÜNVEREN-BİLGİÇ, Nazire Burçin HAMUTOĞLU <i>Türkiye</i>	AN EVALUATION on INCLUSIVE EDUCATION DURING DISTANCE EDUCATION PROCESS: CLASSROOM TEACHERS' PERCEPTIONS	19
20	Ash KAYA, Nazire Burçin HAMUTOĞLU, Emre ÇAM, Emine Nur ÜNVEREN-BİLGİÇ <i>Türkiye</i>	THE IMPORTANCE OF THE PLANNING CYCLE FOR AN EFFECTIVE STRUCTURING OF ONLINE TEACHING PROCESSES	20
21	Turan TEYMURBAYLI, Utku KAYA <i>Türkiye</i>	DEEP LEARNING ADVANCEMENTS IN RAILWAY TRACK SEGMENTATION: PREVIOUS STUDIES AND IMPROVEMENTS	20

22	Fehmi ASLAN <i>Türkiye</i>	INVESTIGATION OF THE EFFICIENCY OF DSSC FOR SAFFRON EXTRACT	21
23	Sara Abdolmaleki, Samad Khaksar <i>Georgia</i>	EVALUATION OF THE CENTRAL-METAL EFFECT ON ANTICANCER ACTIVITY AND MECHANISM OF ACTION OF ISOSTRUCTURAL Cu(II) AND Ni(II) COMPLEXES CONTAINING PYRIDINE-2,6-DICARBOXYLATE	21
24	Igor Nevliudov, Iryna Zharikova, Sergiy Novoselov, Dmytro Nikitin <i>Ukraine</i>	SIMULATION OF FLEXIBLE PRINTED STRUCTURES DESIGN FOR MOBILE ROBOT PLATFORM	22
25	Svitlana Maksymova, Viktoriia Nevliudova, Oleksandr Klymenko, Gennadii Makarenko <i>Ukraine</i>	VOICE CONTROL USING IN PHARMACEUTICAL PRODUCTS LOGISTICS SYSTEMS	22
26	Cihangir Kale, Hikmet Esen <i>Türkiye</i>	INVESTIGATION OF HYDROGEN PRODUCTION BY USING CONCENTRATED PHOTOVOLTAIC/THERMAL HYBRID COLLECTOR WITH SPECTRAL BEAM SPLITTING	23
27	Murad Omarov, Vusala Muradova <i>Ukraine</i>	BAYESIAN REGULARIZATION OF LEARNING	23
28	Makovetskyi Sergii, Kauk Viktor <i>Ukraine</i>	RESEARCH OF THE STABILITY OF THE SECURE RADIO-FREQUENCY COMMUNICATION IN THE DISTRIBUTED SYSTEMS BY USING MULTY-CHANNEL IOT LPWAN TECHNOLOGIES	24
29	L. Arabuli, I. A. Iashchishyn, N. V. Romanova, G. Musteikyte V. Smirnovas, H. Chaudhary, Ž. M. Svedružić, and L. A. Morozova-Roche <i>Georgia</i>	CO-AGGREGATION OF S100A9 PROTEIN WITH L- DOPA AND CYCLEN-BASED COMPOUNDS – EFFECT ON THE AMYLOID FIBRIL SELF-ASSEMBLY	24
30	Peyman Salahshour, Samad Khaksar <i>Georgia</i>	3,5-BIS(TRIFLUOROMETHYL) PHENYLAMMONIUM TRIFLATE: A NEW AND GREEN ORGANOCATALYST FOR THE SYNTHESIS OF INDENO[1,2-B]PYRIDINES	25
31	Olena Kovalenko, Olga Yunakova, Mykola Yunakov <i>Ukraine</i>	PECULIARITIES OF Cs _{1-x} Rb _x Cu ₂ Cl ₃ SOLID SOLUTIONS ABSORPTION SPECTRA	25
32	Igor Nevliudov, Dmytro Nikitin, Roman Strelets, Yegor Korotun <i>Ukraine</i>	FACTOR ANALYSIS OF PHOTOPOLYMER RESINS FOR 3D PRINTING	26
33	Hatice Güney, Abidin KILIÇ <i>Türkiye</i>	EXAMINING THE SYMMETRY OPERATIONS OF THE DNA MOLECULE WITH CLIFFORD ALGEBRA	27
34	Abidin KILIÇ <i>Türkiye</i>	INVESTIGATION OF TRANSFORMATION SYMMETRIC MOLECULES WITH CLIFFORD ALGEBRA	27
35	Murad Omarov, Vladyslav Korobskiy, Viktoriia Nevliudova <i>Ukraine</i>	ENSURING THE ROBOT SNAKE'S MOVEMENT ON SLIPPERY SURFACES	27
36	Emre Aytuğ ÖZSOY <i>Türkiye</i>	A GEOTECHNICAL EXAMINATION OF KAHRAMANMARAS (TURKEY) PAZARCIK & EKİNOZU 6 FEBRUARY 2023 EARTHQUAKES	28
37	Çetin YAVUZ, Ali TAROKH, Aydın DİKİCİ <i>Türkiye</i>	NUMERICAL ANALYSIS OF A NEW THERMOSYPHON HEAT PIPE	28
38	Igor NEVLIUDOV, Shakhin OMAROV, Olena CHALA, Serhii TESLIUK <i>Ukraine</i>	STUDY OF MANUFACTURING DEFECTS IN THE TECHNOLOGY OF MANUFACTURING MOEMS SEMICONDUCTOR SUBSTRATES FOR TECHNICAL AUTOMATION MEANS	29
39	Igor NEVLIUDOV, Andriy SLUSAR, Kyrylo KRUSTALOV, Sofia KRUSTALOVA, Shakhin OMAROV <i>Ukraine</i>	INTELLIGENT ENERGY SUPPLY MANAGEMENT SYSTEM IN THE MUNICIPAL SECTOR"	29
P1	Imane Bouguenoun, Widad Bouguenoun, Dalila Bendjeddou, Marie-Claire De Pauw-Gillet, Edwin De Pauw <i>Algeria, Belgium</i>	THE STIMULATING EFFECT OF THE <i>CUPRESSUS SEMPERVIRENS</i> MAJOR ALLERGEN (CUP S1) ON BRONCHIAL EPITHELIAL CELLS (BEAS -2B)	30
P2	Poladova Tarana Ali <i>Azerbaijan</i>	SYNTHESIS AND STUDY OF NEW SURFACE-ACTIVE POLYMER COMPLEX WITH CATIONIC SALT	30
P3	A.N. Mammadov, U.N. Sharifova, F.S. Ibrahimova, A.M. Qasimova, Mustafayeva A.N. <i>Azerbaijan</i>	SYNTHESIS OF SODIUM TITANATES USING CHITOSAN IN THE ENVIRONMENT	31
P4	Ulkar Shiralyeva, Elmira Huseynova, Aida Rzaeva, Zarifa Mammadova, Saida Nadjafova, Nurana Mardanova <i>Azerbaijan</i>	STUDY OF ACTIVITY AND SELECTIVITY OF OXIDE CATALYSTS IN HYDROCARBON OXIDATION REACTIONS	31
P5	Nur ULUHAN, Abidin Kılıç <i>Türkiye</i>	THE IMPORTANCE OF EARTHQUAKE EDUCATION IN SCIENCE CENTER	32
P6	Almila Selcen Uray, Abidin Kılıç <i>Türkiye</i>	AN APPROACH TO THE REPRESENTATION OF PLATONIC SOLIDS WITH GEOMETRIC ALGEBRA	32

01

DESICCANT PROPERTIES OF NATURAL BIO-POLYMERS STUDIED BY NIR SPECTROSCOPY

Christy A.A.

Department of Science, Faculty of Engineering and Science, University of Agder, Norway

alfred.christy@uia.no

ABSTRACT

Desiccants are substances used in the dehumidification process which is vital in order to avoid the degradation of materials. Silica gel is the most prominent type of desiccant used and today the world has developed an interest in bio-polymers due to certain demerits of silica. Hence this study was conducted to investigate the desiccant properties of the four commercial flours wheat, corn, potato and gram and to compare them with the common silica gel desiccant. The bio-polymers were dried under vacuum at 120 °C and were studied over time using Near-Infrared (NIR) spectroscopy for their –OH combination peak which appears at around 5200 cm⁻¹ and the derivative spectra were analyzed to recognize the specific –OH groups involved in hydrogen bonding process. Further, the gravimetric analysis was used to study the rate of adsorption and their long-term efficacies were detected using data loggers. The results clearly indicated that adsorption of water occurs at C1, C2+C3, C4 and C6-OH groups of the glucose units for wheat and corn flour while potato and gram flour showed only three peaks attributing to C1, C2+C3 and C6-OH. Further it was observed that C1 and C2+C3-OH groups have a similar and the highest rates. The rates of adsorption of all flours were greater than both analytical grade and commercial silica and corn flour was found to be an outstanding desiccant compared to conventional silica desiccant.

Keywords: Adsorption, bio-desiccant, Near-Infrared (NIR) spectroscopy, Gravimetric

02

CORRELATIONAL ANALYSES AMID WATER-SEDIMAN SAMPLES AND SPECIES FROM THE ISLANDS OF ANTARCTICA

Okan KÜLKÖYLÜOĞLU¹, İsmail Ömer YILMAZ², Oğuz MÜLAYİM³, Süphan KARAYTUĞ⁴, Serdar SAK⁵,
Serdar SÖNMEZ⁶

¹²³ Bolu Abant İzzet Baysal University, Middle East Technical University, Türkiye Petrolleri A.O., Adıyaman
⁴⁵⁶MersinUniversity, BalıkesirUniversity, AdıyamanUniversity,

ABSTRACT

Total of 32 water and sediman samples collected from four islands (Horseshoe, Nansen, Dismal, Livingstone) of Antarctica during the sixth Turkish Antarctica Expedition to Western Antarctica (TAE-6) were evaluated for providing ternary plot models among the variables. Although biodiversity (e.g., ostracods, copepods) of the sampling sites were low, unique species assemblages are valued with reporting a new ostracod species and two other reports of copepodid species. Models of ternary plots suggested that sampling sites divided in two groups based on anion and cation dominancy. First grup includes Na>Ca>K and Ca>Mg>K while the second group includes Cl>HCO₃>SO₄. Also, the same (Na>Ca>K) dominancy was found in sediman samples while correlation was positive amid some major anions of water and sedimant such as Na, Ca and K. However, there was no significant correlation between Ca and K values of water and sediman samples. According to the log Na and log K comparison, freshwater sampling sites are separated from the sites with highly saline sea water. Thus, correlation analyses and ternary plot models suggest that species reported from these sampling sites differ in their tolerance and optimum estimates. Further models are discussed for future possibilities.

Keywords: Antarctica islands, TAE-6, water and sediman chemistry, biodiversity, correlational analyses

Acknowledgment: This study was carried under the auspices of the Presidency of the Republic of Turkey, supported by the Ministry of Industry and Technology, and coordinated by TÜBİTAK MAM Polar Research Institute.

NILCO INTERACTION MAY PLAY AN IMPORTANT ROLE IN THE PROGRESSION OF COLORECTAL CANCER

Mete ÖZKURT

Physiology Department, Mecidal Faculty, Eskisehir Osmangazi University, Eskisehir, Turkey

ABSTRACT

Aim: NILCO is a novel mechanism that interacts with proinflammatory and proangiogenic signals, which are critical for cell proliferation and angiogenesis in cancer. We aimed to show the mechanisms of NILCO interaction in the colorectal cancer with a in-vitro study.

Material and Methods: We treated HT29 cells, a colorectal carcinoma cell line, with NOTCH1, Leptin and IL-1 siRNAs. Form the medium of the cells we made ELISA experiment for Leptin, IL-1 and VEGFA. We isolated mRNA and performed qRT-PCR for IL-1, NOTCH1, Leptin, VEGFA, MMP2, VEGFR2, Caspase9, E-Cad, IL-1R. We also isolated protein from the cells and performed western-blot analysis for IL-1, MMP2, NOTCH1, TIMP-1, VEGFA, VEGFR2 and OB-R .

Results: ELISA results showed no difference in all groups. Insignificant but folded increase was observed in IL-1, E-Cad and Leptin mRNA in all siRNA treated group. Leptin was significantly increased when Leptin siRNA was given. VEGFA, VEGFR2, IL-1R and MMP2 mRNAs were significantly increased when IL-1 siRNA was given. Caspase9 mRNA was significantly increased in both leptin and IL-1 siRNA treated groups. MMP2, VEGFA, OB-R proteins were higher while VEGFR were lower in IL-1 siRNA treated groups. NOTCH1 protein showed an increase in Leptin siRNA group.

Conclusion: Our results conclude that interaction of NILCO pathway but critically IL-1 may play an important role in the progression of colorectal cancer.

Keywords: NILCO, NOTCH1, Leptin, IL-1, Colorectal cancer, HT29

TOPOLOGICAL IMAGE PROCESSING FOR COMPREHENSIVE DEFECT AND DEVIATION ANALYSIS USING ADAPTIVE BINARISATION

Igor Nevludov, Igor Badanyuk, Dmytro Nikitin

¹ Department of Computer-Integrated Technologies, Automation and Mechatronics;
Kharkiv National University of Radio Electronics, Kharkiv, Ukraine

ABSTRACT

PCB topology image processing is an important component of Industry 4.0, as images can be used for automated quality control and visual inspection of manufacturing processes related to PCB production. Image processing can be used to control the quality of printed circuit boards, for example, to detect defects that may be invisible to the human eye. The main objective of the study is to improve the method of adaptive binarization for images obtained by technical vision systems by developing an automatic algorithm for detecting the required value of the image binarization window. To achieve this goal, it was decided to develop an algorithm for automatically finding the size of the scanning area in adaptive binarization for processing technological images of the SOE topology.

Keywords: Process image processing, Adaptive binarization, Otsu method, GP topology, Finding "Block size".

REDUCING THE LEVEL OF INTERFERENCE CONSIDERING THE MORPHOLOGICAL CHARACTERISTICS OF OBJECTS IN THERMAL NONDESTRUCTIVE TESTING

Oleksandr MIAHKYI, Volodymyr STOROZHENKO, Roman OREL, Sergey MESHKOV

Department of Physics, Kharkov National University of Radio Electronics, Kharkov, Ukraine

ABSTRACT

The interferences characteristic of thermal non-destructive testing that reduces the reliability of the obtained results are described. A methodology for their reduction is proposed, consisting of two interdependent stages. The first stage consists in calculating and analysing the nature and level of the expected signal according to the developed thermophysical model against the background of the experimentally obtained level of interference. According to the results of the analysis of the calculations based on the thermophysical model for the selected samples, the most influential interference was the heterogeneity of the emissivity of the sample surface. The second stage of data processing is devoted to reducing this interference. The second stage consists of processing the thermograms of temperature fields and includes morphological analysis of the surface condition, filtering, and reduction of characteristic interference. It is divided into four practical procedures. Analysis of the visual image and obtaining a map of zones with the different emissivity of the sample surface, analysis of the thermogram with an assessment of the level of discreteness of the thermogram and the position of the reference points on the image, smoothing of the thermographic image and selection of zones with the different emissivity of the surface of the object under control on the thermogram, followed by noise filtering. Since the results of thermal control are strongly influenced by the shape of the object, the capabilities and effectiveness of the proposed methodology are illustrated on a cylindrical object (Figure).

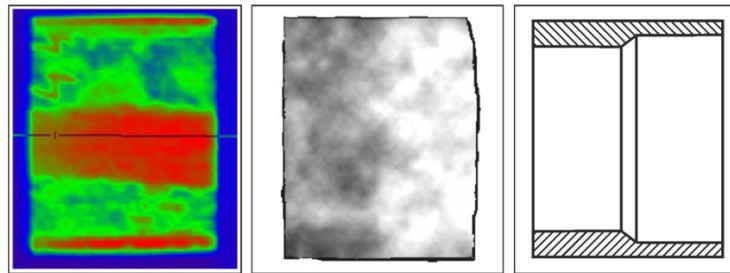


Figure - Thermogram of a sample fragment, its reconstructed temperature field and longitudinal section

The experiment confirmed the validity and correctness of the theoretical statements and allowed us to determine the internal structure of the object under study (different wall thicknesses) and reduce the level of structural interference by 3.6 °C. The research shows that the processing of experimental data, which was carried out taking into account the specifics of the thermal and structural characteristics of the objects under control, gives a significant positive result and is an important step towards automating thermal non-destructive testing procedures on the way to implementation in current production.

Keywords: thermal nondestructive testing, structural interference, thermophysical model, image processing, morphological analysis.

THE EFFECT OF HEAT TREATMENT ON THE STRUCTURE OF NIOBIUM OXIDE FILMS

Oleksandr CHUBUKIN

Applied Physics, Faculty of Automatics and Computerized Technologies, Kharkiv National University of Radio Electronics, Kharkiv, Ukraine

ABSTRACT

Niobium oxide films are used as optical coatings, sensor materials and electrochromic films. They have a high refractive index in the visible range and a high dielectric constant. However, structural heterogeneities in their working layer can be a factor in reducing the reliability of products where these films are used. This is due to the fact that the integrated electrophysical parameters of devices are determined by locally changed properties of the working layer of this dielectric, which may differ from the properties of its main part. For example, a local increase in electrical conductivity in a dielectric layer entails heating of the defective area, which, in turn, increases the local conductivity of the dielectric and leads to its thermal breakdown. One of the methods for detecting defects in dielectric films is the method of electrography, which allows visualizing these defects. Electrography is used to study the structural inhomogeneities of solids that are decorated with specially selected physical process products, followed by visualization of the decorated areas using appropriate observation techniques. The aim of this work was to investigate phase formation in thin-film structures during annealing, in the course of which the dependence of the structure and composition of oxide films on the conditions of their heat treatment was investigated. This paper presents the methods and results of an electrographic study of the conductive properties of Nb_2O_5 films of the Nb-Nb₂O₅ system by analyzing the spatial distribution of inhomogeneities on samples annealed in different modes.

Keywords: Niobium oxide films, Heat treatment, Electrography, Spatial distribution of inhomogeneities

SYNTHESIS, CHARACTERIZATION AND EVALUATION OF ANTI-TUBERCULOSIS POTENTIAL OF NOVEL HYBRID COMPOUNDS BASED ON ISONIAZID AND PYRAZINAMIDE

Lili Arabuli^{1*}, Ketevan Tavamaishvili², Tomas Macek³, Petra Lovecka³, Rudolf Jezek³, Hristo Najdenski⁴

^{1*}University of Georgia, School of Science and Technology, Tbilisi, Georgia.

²Georgian-American University, Medical school, Tbilisi, Georgia

³University of Chemistry and Technology, Department of Biochemistry and Microbiology, Prague, Czech Republic

⁴The Stephan Angeloff Institute of Microbiology, Bulgarian Academy of Sciences, Bulgaria

ABSTRACT

Tuberculosis remains one of the most dangerous infectious diseases and causes over 1 670 000 deaths annually all over the world. To treat tuberculosis, there are traditionally old drugs but several new medications like bedaquiline, delamanide, pretomanide and rifapentine were proposed which are under phase 3 clinical trials. The main problem in Tub therapy, drug-resistant and multidrug-resistant tuberculosis is considered. Therefore, the main goal in therapy and drug discovery is to shorten duration of treatment, reduce side effects of drugs and develop/discovery new effective drugs, showing less side effects. Herein, we present preparation, structural characterization (¹H, ¹³C NMR, FT-IR, UV-vis, determination of melting points) of new hybrid compounds (Fig. 1.) consisting in the molecule isoniazid, pyrazinamide, L-Dopa, 1,4,7,10-tetraazacyclododecane and small peptide fragments, as well as evaluation their anti-mycobacterial properties/activities on the strains of *M. tuberculosis* H37 (ATSS 25177 and ATSS 19274). In addition, ADME software was used for prediction of drug-likeness properties and their deviations from optimal drug-likeness rules. Among 10 novel synthesized compounds, some of them showed promising anti-tubercular activities and based on preliminary results, further structural modification and detailed anti-Tub bacterial investigation will be planned.

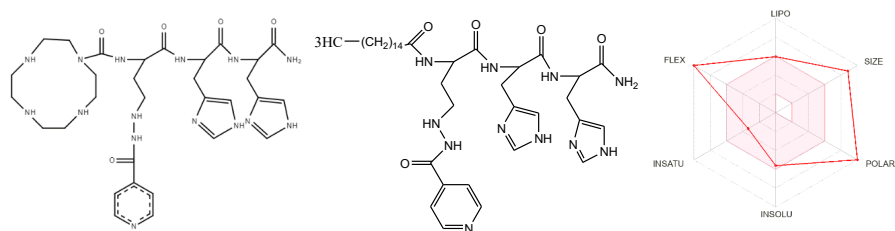


Fig. 1. Structures of synthesized hybrid compounds based isoniazid and pyrazinamide and ADME diagramme

Keywords: Tuberculosis, drug-likeness, isoniazid, pyrazinamide, L-dopa, cyclen, biological activity

THE POWER OF GREEN WALLS: A SUSTAINABLE DESIGN SOLUTION

Tugce PEKDOGAN^{1,*}

¹ Department of Architecture, Faculty of Architecture and Design, Adana Alparslan Turkes Science and Technology University, Adana, Turkey

ABSTRACT

In recent years, the climate change crisis has driven architects and urban planners towards sustainable building designs that can reduce energy demand, minimize environmental impact, and mitigate the urban heat island effect. Adding green roofs and living walls to buildings is part of an urban design approach that aims to address the existing challenges of built environments. Green roofs can cover impermeable roof areas in urban areas, thus providing numerous environmental, economic, and social benefits. Additionally, living walls located inside and outside buildings have the potential to improve air quality, reduce pollution levels, lower indoor and outdoor temperatures, decrease energy consumption, provide sound insulation, promote biodiversity, and enhance human physical and psychological health. As such, it is crucial to examine and evaluate the impact of living walls on indoor air quality, thermal performance, noise reduction, and social and visual aspects with their environmental, social, and economic dimensions in mind. In this paper, the concept of green walls is explored, including its advantages and disadvantages and its applicability.

Keywords: Green walls, sustainable design, environmental impact.

SHUTTLE-BASED STORAGE AND RETRIEVAL SYSTEM 3D MODEL IMPROVEMENT AND DEVELOPMENT

Igor Nevliudov¹, Vladyslav Yevsieiev¹, Svitlana Maksymova¹, Oleksandr Klymenko², Maksym Vzhesniewski²

¹ Department of Computer-Integrated Technologies, Automation and Mechatronics;
Kharkiv National University of Radio Electronics, Kharkiv, Ukraine
²«Kapelou» LLC, Kyiv, Ukraine

ABSTRACT

The development of new design solutions for Radioshuttle will increase the storage density of heterogeneous goods, increase the efficiency and productivity of warehouse logistics, reduce the cost of renting warehouse space and reduce the negative impact on the environment, which makes this development extremely relevant and necessary in modern logistics.

Authors proposed to improve the designs of the Radioshuttle, through the use of the Mecanum Wheel. To test this, the authors designed a 3D model of a Radioshuttle with a Mecanum Wheel using Autodesk Fusion 360 while maintaining overall dimensions and a 3D model of rack structures.

Keywords: Shattle, Storage, Retrieval System, Warehouse Management System, Warehouse 4.0.

CONTROL AUTOMATION OF ASSEMBLY OPERATIONS USING A COMPUTER VISION SYSTEM IN INTELLIGENT PRODUCTION

Igor NEVLIUDOV¹, Serhii NOVOSELOV¹, Oksana SYCHOVA¹

¹Department of Computer-Integrated Technologies, Automation and Mechatronics, Faculty of Automatics and Computerized Technologies, Kharkiv National University of Radio Electronics, Kharkiv, Ukraine

ABSTRACT

The using principles control means of assembly operations in production are described. An methods analysis for assessing the accuracy of component installation during assembly work was carried out. The scheme of the automated system operation for controlling the execution of assembly operations has been developed. The mathematical model synthesis of the proposed automated system was performed. The experimental research result is described.

Keywords: Computer vision, assembly operations, Industry 4.0, Emgu CV.

AKILLI ULAŞIM SİSTEMLERİNİN ULAŞIM AĞINDAKİ YAPISAL BOZULMALARIN TESPİTİNDEKİ ETKİNLİĞİ

Onur ŞAHİN¹

¹ İnşaat Mühendisliği Bölümü, İnşaat Fakültesi, Ulaştırma Ana Bilim Dalı, Yıldız Teknik Üniversitesi, İstanbul, Türkiye

ABSTRACT

Ulaşım sistemleri bir ülkenin gelişmişlik düzeyiyle paralel ölçüde gelişen hizmet sistemleridir. Aktif, sürdürülebilir ve tıkanmalara anlık müdahale imkânı tanıyan teknoloji odaklı sistemler ise akıllı ulaşım sistemleri olarak nitelendirilmektedir. Bu bağlamda ulaşım ağının sürekli olarak gözlemlenmesi ve karşılaşılan engellerin tespiti, ulaşım ağında teknolojinin yoğun bir biçimde kullanılması, hem uygulanabilirlik hem de zaman kazandırması açısından büyük önem taşımaktadır. Özellikle yoğun yağış alan ve zemin dolguları yeterli düzeyde bulunmayan ulaşım altyapıları sebebiyle heyelanlar meydana gelmekte ve bu büyük toprak kütlelerinin hareketleri sonucu aktif kullanılan bazı ulaşım sistemleri bozulmaktadır. Güzergâhı kullanan araç sayısına bağlı olarak bu tıkanıklığın maddi manevi sonuçları çok büyük boyutlara ulaşabilmektedir. Dolayısıyla bu tip bir durum meydana geldiğinde süratle tespiti ve müdahale ekibinin yönlendirilmesi oluşacak birçok kaybın önüne geçilmesine olanak sağlayacaktır. Akıllı ulaşım sistemleri olarak adlandırılan ve aktif olarak takip edilebilir ve anlık uyarı bildirim merkezi sayesinde çok hızlı ve etkin bir biçimde hasar alan bölgenin tespit edilmesini sağlayan sistemlerin heyelan riski bulunan bölgeleri uygulanması gereklilikten öte bir zorunluluk haline gelmiştir. Ekonomik açıdan akıllı ulaşım sistemlerinin kent ulaşım politikalarına uyarlanması ek bir yük getirirse de uzun vadede sağladığı fayda ve önüne geçebileceği kayıplar düşünüldüğünde maliyetini karşılama ve pozitif bir etki bırakması öngörülmektedir. Bu çalışmada, akıllı ulaşım sistemlerinin hangi bölgelere nasıl uygulanabileceği ve etkinliği incelenecek ve sağlanan faydaların tespiti yapılacaktır.

EXAMINATION OF THE RELATIONSHIP BETWEEN THE OCCUPATIONAL IDENTITY PERCEPTIONS OF PRIMARY SCHOOL MATHEMATICS TEACHER CANDIDATES AND TPCK

Emine Nur ÜNVEREN BİLGİÇ^{1,*}, Nazire Burçin HAMUTOĞLU², Emre ÇAM³

¹ Education Faculty, Mathematics and Science Education department, Düzce University, Düzce, Turkey

² The Centre for Teaching and Learning Excellence, Eskişehir Technical University, Eskişehir, Turkey

³ Niksar Niksar Vocational School, Tokat Gaziosmanpaşa University, Tokat, Turkey

ABSTRACT

It is important for the element of quality in education to define the factors that form or change the perceptions of teachers who are new to the profession and who gain experience over time, the reasons why teachers choose the profession or which conditions are effective over time, the way teachers perceive themselves in the region where they live or in the society in general or how the society perceives teachers, the change in the perception of the teacher after the interaction of the teacher with other teachers, students and administrators of the school. Another important context for quality in educational processes is Pedagogical Content Knowledge defined by Schulman (1987). Today, with the inclusion of the technology component in teacher knowledge, it is a very important topic to examine teacher knowledge, which was redefined as Technological Pedagogical Content Knowledge by Mishra and Koehler (2016), in this context (Vijayan & Joshith, 2018). The aim of this study is to examine the relationship between pre-service elementary mathematics teachers' perceptions of professional identity and Technological Pedagogical Content Knowledge. From this point of view, the research will be carried out in a relational survey design with a quantitative paradigm. "Teachers' Perception of Professional Identity Scale" developed by Yıldız and Çetin (2020) and "Technological Pedagogical Content Knowledge Scale (TPACK-Math)" developed by Önal (2016) will be used for the participants who will be provided from all grade levels with maximum diversity sampling.

Keywords: Professional Identity, TPCK, Mathematics Education

MATHEMATICAL MODELLING OF THE INFORMATIVE FEATURE CHOICE FOR LIFECYCLE STATE ANALYSIS OF RADIO-ELECTRONIC MEANS PROCESSES

VICTORIA NEVLYUDOVA, NIKOLAY STARODUBTSEV

Department of Computer Integrated Technologies, Automation and Mechatronics, Faculty of Automation and Computerized Technologies, Kharkiv National University of Radio Electronics, Kharkiv, Ukraine

ABSTRACT

The solution of problems of mathematical modeling of efficiency functions of radio electronic means life cycle processes (REM LC) and selection of informative attributes for REM LC monitoring, by classification of REM states and life cycle processes in attribute space, each of which has a certain significance, that allowed to find a complex criterion and to formalize selection procedures, is given. The cases of insufficient amount of a priori data for correct classification are considered; heuristic methods of selection according to criteria of basic prototypes and information priorities are proposed.

Keywords: informative features, identification of REM states, life cycle monitoring.

NUMERICAL METHODS TO SOLVE OPTIMAL CONTROL PROBLEMS FOR TECHNICAL APPLICATIONS UNDER NOVEL GLOBAL CHALLENGES

Igor NEVLIUDOV¹, Murad OMAROV¹, Yurii ROMASHOV^{1,2,*}

¹ Computer Integrated Technologies, Automation and Mechatronics, Faculty of Automatics and Computerized Technologies, Kharkiv National University of Radio Electronics, Kharkiv, Ukraine

² Applied mathematics, School of Mathematics and Computer Sciences, V.N. Karazin Kharkiv National University, Kharkiv, Ukraine

ABSTRACT

The optimal control problem formulation and the most fundamental results are associated with L. Pontryagin. Such problems are researched last decades, but we have only a lot of analytic-numerical methods suitable for particular classes of the tasks. We have no of all-conventional pure numerical methods to solve optimal control problems directly without additional dimensions restrictions and linearity requirements. The interests to improved optimal controls is the aftermaths also of decisions striving to resolve of different novel global challenges. Well-known European plans of introducing a Carbon Border Tax is the example of it, because in this reality the optimal controls providing the minimal carbon leakages will be the principal for modern automation. Engineering implementations of optimal controls with different optimality criteria requires considering of corresponded complicated optimal control problems without dimensions restrictions and linearity requirements, and only the numerical methods can do it. To use the numerical methos to solve the optimal control problem, it is proposed to reduce it to minimizing of some many variable objective function. The principal difficulty of this approach in optimal control considering will be the necessity of solving the nonlinear system of ordinary differential equations to compute the value of the objective function for its given arguments. Due to this, the significant amounts of computing will be required, and it is required the correspondent computers and programming languages providing the maximum fast executing code.

Keywords: Optimal control, numerical methods, objective function, minimization

KAOLİN KİLİ TOZU İLE ÜRETİLEN METAZEOLİT TABANLI GEOPOLİMER HARÇLARDA MAGNEZYUM SÜLFAT ETKİSİ

Yurdakul AYGÖRMEZ^{1,*}

¹ İnşaat Mühendisliği Bölümü, Davutpaşa Kampüsü, Yıldız Teknik Üniversitesi, İstanbul, Türkiye

ÖZET

Çimento esaslı malzeme dünyanın her ülkesinde yaygın olarak kullanılan bir yapı malzemesidir ve zaman geçtikçe şehirlerin daha da büyümesi ile bu ihtiyacın artması beklenmektedir. 2050 yılında beton ihtiyacının 1990 yılına göre yaklaşık dört kat daha fazla olacağı tahmin edilmektedir. Ayrıca Portland Çimentosu kullanımı ile sera gazı emisyonu önemli ölçüde artmaktadır. Bu şekilde oluşan emisyonların önümüzdeki yıllarda artacağı bir gerçektir. Küresel ısınma endeksi de bu durumdan etkilenmektedir. Bu durumda inşaat alanında betonun yoğun olarak kullanılması, gelecekte sürdürülebilirlik ile ilgili adımların atılmasını gerekli kılmaktadır. Farklı alternatif üretimler kullanılması önemli bir avantaj sağlar ve sürdürülebilirlik kavramını sağlamak için çevresel olumsuz etkileri azaltmaktadır. Geopolimer üretimi bu bakımdan büyük önem taşımaktadır.

Sülfat saldırısı, tüm dünyada beton ve harç yapılarının dayanıklılığını azaltır ve zarar görmesine neden olduğu kabul edilen sebeplerden biridir. Bu nedenle, sülfat saldırı direnci, inşaatta kullanılan malzemeler için önemli bir dayanıklılık ve hizmet verebilirlik sorunudur. Magnezyum sülfat direncini değerlendirmek için metazeolit tabanlı geopolimer harç numuneler üretilmiştir. Bu çalışmada kaolin kili tozu üç farklı oranda (%5, %15 ve %25) metazeolit tabanlı geopolimer harç numunelere agrega olarak katılmıştır. Numuneler 24 aya kadar %5 magnezyum sülfat çözeltisine daldırılmıştır. Bu çalışmada değerlendirilen özellikler, görsel inceleme, numunelerin ağırlık değişimi, basınç dayanımı, eğilme dayanımıdır. Sonuçlar, kaolin kili tozunun %5 oranında katılmasının basınç dayanımı sonuçlarını artırdığını gösterirken %15 oranında kullanımın kabul edilebilir seviyelerde dayanım sonuçları oluşturduğunu göstermiştir. %25 oranında kaolin kullanılması durumunda ise önemli dayanım azalması görülmüştür. Genel olarak, geopolimer harçlar magnezyum sülfat çözeltisine karşı önemli dirençler göstermiştir.

Anahtar Kelimeler: Geopolimer, Metazeolit, Kaolin, Magnezyum sülfat etkisi

HIGH SELECTIVE ETCHING GAAS/AL_{0.3}GA_{0.7}AS FOR PN JUNCTION SOLAR CELL USING CITRIC ACID SOLUTION

Hülya KURU MUTLU^{1,2,*}, Mustafa KULAKCI^{2,3}, Uğur SERINCAN²

¹Opticianry Program, University of Eskişehir Osmangazi, Eskişehir, Türkiye

²Nanoboyut Research Laboratory, Department of Physics, Eskişehir Technical University, Eskişehir, Türkiye

³Institute of Earth and Space Sciences, Eskişehir Technical University, Eskişehir 26470, Türkiye

⁴Advanced Technologies Application and Research Center, Eskişehir Technical University, Eskişehir, Türkiye

ABSTRACT

In this study, effects of selective citric acid solution on the surface properties of p-n junction solar cells were investigated and analyzed. Solar cell structures were grown by molecular beam epitaxy (MBE) system and cut into small pieces with a size of $0.5 \times 0.5 \text{ cm}^2$ for a detailed etch study. First of all, the samples were cleaned sequentially in acetone, isopropanol (at 80°C), and distilled water for a duration of 5 minutes and then dried with N₂ flow. Following the cleaning procedure, the native oxide on the samples was removed in HCl acid solution at a ratio of (H₂O) 5:1 (HCl) in 20-25 seconds. After oxide removal, samples surfaces were coated with a photoresist (AZ 5214E) using a spin coating system at 3000 rpm for 40 seconds and then pre-cured at 110°C on a hot plate. Mesa patterns were transferred onto the samples using a photo-lithography system. After UV exposure, mesa patterns appeared in the developer solution (AZ400K: H₂O; 1:4) and the samples were cured again at 120 °C for 5 minutes on a hot plate. The photoresist thickness of each sample was measured using a profilometer. Afterward, a mixture of citric acid and water was prepared at a ratio of 1:1, and a solution of citric acid was prepared by mixing the prepared mixture with H₂O₂ at a ratio of 1:5. The samples were kept in this prepared citric acid solution for 30, 60, 90 or 120 seconds. Etch depths were measured using a profilometer and an etching graph was formed. Surface photographs were taken before and after citric acid treatment and the effects of etching on the surface were examined.

Keywords: Citric acid, Etching, pn junction, solar cell

This study was supported by Eskişehir Osmangazi University BAPSİS project unit with the project code FBA-2021-1607.

TWO-DIMENSIONAL DATA GENERATION METHOD FROM MULTIPLE TIME SERIES FOR 2D-CNN-BASED RUL ESTIMATION OF LITHIUM-ION BATTERIES

Mehmet FIDAN¹

¹ Rail Systems Electrics and Electronics Program, Vocational School of Transportation, Eskişehir Technical University, Eskişehir, Turkey

ABSTRACT

As the use of electric vehicles increases in our age, the reliability of Lithium-Ion batteries increases their importance. One way to increase the reliability of Lithium-Ion batteries is to strongly estimate the Remaining Useful Life of these batteries. A robust RuL estimation contains important information for the control of these batteries. In this study, a new two-dimensional data generation method is proposed from multiple time series formed from the past current and voltage values measured from the terminals and chargers of Lithium-Ion batteries, as well as the simultaneously measured battery temperature data. The two-dimensional data generated by the proposed method are used in RuL estimation with pretrained 2d-CNN networks and detailed estimation performances are presented.

Keywords: Lithium-Ion batteries, 2d-CNN, Multiple time series, RuL estimation

**ANALYSIS of C–H···O INTERACTION BETWEEN ANION and CATION
of 1,3-DIMETHYLIMIDAZOLIUM METHYLSULPHATE USING
NATURAL BOND ORBITAL METHOD**

Nihal KUŞ

Department of Physics, Science Faculty, Eskisehir Technical University, 26470, Eskisehir, Turkey

ABSTRACT

It is clear that more studies should be done on ionic liquids, as the usage areas and importance of ionic liquids have increased considerably. In this study, geometry optimizations, charge density and natural bond orbital (NBO) analysis of 1,3-dimethylimidazolium and methylsulphate (DIMIM-MS) ionic liquid in cation and anion form were carried out at the Becke, 3-parameter, Lee, Yang-Parr (B3LYP) version with 6-311++G(2d,2p) basis set. Stabilization energies due to the C–H···O weak hydrogen bonds orbital interactions are calculated from the second-order perturbation approach using Fock matrix equation. Donor-acceptor interactions and hybridization for the C–H···O interaction between anion and cation orbital interactions of DIMIM-MS were analyzed and orbital electron density schemes were plotted. HOMO-LUMO, Mulliken charges and NBO charges were calculated and interpreted using DFT-B3LYP/6-311++G(2d,2p) method.

Keywords: Ionic liquid, orbital interaction, stabilization energy, 1,3-dimethylimidazolium methylsulphate, NBO.

ACKNOWLEDGMENT

This study was supported by the Eskisehir Technical University Commission of Research Project under grant no: 23ADP042.

**AN EVALUATION on INCLUSIVE EDUCATION DURING DISTANCE EDUCATION PROCESS:
CLASSROOM TEACHERS' PERCEPTIONS**

Emrah BİLGİÇ^{1*}, Emine Nur ÜNVEREN-BİLGİÇ², Nazire Burçin HAMUTOĞLU³

¹ Department of Basic Education, Faculty of Education, Sakarya University, Sakarya, Turkey

² Education Faculty, Mathematics and Science Education department, Düzce University, Düzce, Turkey

³ The Centre for Teaching and Learning Excellence, Eskisehir Technical University, Eskisehir, Turkey

ABSTRACT

The covid-19 pandemic, which has caused changes in many fields globally, and the natural disaster in our country on February 6, 2023, centered in Kahramanmaraş, have shown that various changes are necessary in the field of education. This change has manifested itself in the form of closing schools in the field of education and switching from face-to-face education to distance education. This distance education process led to many new experiences by conducting synchronous and asynchronous distance education with children with normal development as well as inclusion of student with special education needs (SEN) who need various support in face-to-face education. In this study, it is aimed to determine the perceptions of primary school teachers toward SEN at the primary school level in the distance education process. In this direction, the process that classroom teachers experiences with the inclusion of SEN in distance education (advantages and disadvantages of the process, difficulties experienced in the process, examination of the process in terms of academic disciplines, family support, etc.) are going to be revealed. The research is going to be conducted according to the qualitative method and is going to be designed with phenomenology study. The study group of the research is going to consist of 10 primary school teachers teaching in the 1st, 2nd, 3rd, and 4th grades who are going to be determined according to the convenience sampling method. The research data is going to be obtained through individual interviews with the participant teachers. In the process of collecting the data, an interview form with semi-structured interview questions prepared by the researchers and reorganized by taking expert opinion is going to be used. The data is going to be subjected to content analysis. In this process, codes, categories, and themes is going to be created. It is thought that the results to be obtained from the study is going to shed light on the inclusive education of SEN and teachers who are going to be responsible for the inclusive education of SEN.

Keywords: Distance education, inclusive education, students with special educational needs, teachers' perceptions.

THE IMPORTANCE OF THE PLANNING CYCLE FOR AN EFFECTIVE STRUCTURING OF ONLINE TEACHING PROCESSES

Ash KAYA¹, Nazire Burçin HAMUTOĞLU², Emre ÇAM³, Emine Nur ÜNVEREN-BİLGİÇ⁴

¹Department of Statistics, Faculty of Science, Anadolu University, 26470, Eskisehir, Turkey

² The Centre for Teaching and Learning Excellence, Eskisehir Technical University, Eskisehir, Turkey

³Niksar Niksar Vocational School, Tokat Gaziosmanpaşa University, Tokat, Turkey

⁴Education Faculty, Mathematics and Science Education department, Düzce University, Düzce, Turkey

ABSTRACT

The need for effective structuring of learning and teaching processes in the changing world makes itself felt more and more every day. As a matter of fact, as seen in the past Covid 19 pandemic and the Kahramanmaraş-Pazarcık-centered earthquake(s) on February 6, 2023; rapid decision-making policies regarding the transition process to online learning environments also form the basis of the need for an effective structuring of online learning environments. The ability of educational institutions to show quick reflexes to emerging problems and to provide adaptation processes; possible on the basis of effective planning carried out in advance. In all these processes, it has been seen that the primary measure taken against the emerging problems is the transition to the distance education method. However, the interruption of educational activities in institutions where there is no effective planning cycle; creates a handicap in terms of gaining learning outcomes that cannot be compromised. In this study, the importance of the planning cycle in the effective structuring of teaching processes is mentioned. The importance of the planning cycle is emphasized in the study and its reflections will be examined in terms of creating the input of the web-based system that is under development.

Keywords: Online learning, quality, planning cycle, effective structuring, teaching and learning.

DEEP LEARNING ADVANCEMENTS IN RAILWAY TRACK SEGMENTATION: PREVIOUS STUDIES AND IMPROVEMENTS

Turan TEYMURBAYLI¹, Utku KAYA²

¹ "Railway Systems Engineering Department, Eskişehir Technical University Eskişehir, Turkey

² Vocational School of Transportation, Eskişehir Technical University Eskişehir, Turkey

ABSTRACT

This article focuses on investigating the utilization of deep convolutional neural networks for segmenting railway tracks. Deep learning, which aims to simplify data processing by emulating human intelligence on computers, plays a significant role in this regard. Railway tracks are widely recognized for their importance in railway transportation. Consequently, ensuring track integrity requires thorough surface scanning. However, considering the extensive expanse of railway tracks, manual scanning proves to be a challenging and time-consuming task. Railway track segmentation serves as a fundamental step in identifying track defects, enabling easier detection by extracting tracks from surrounding images. This article discusses various studies conducted in this field and provides insights into the advantages offered by each approach.

Keywords: Deep learning, Railway track segmentation, Convolutional neural networks

INVESTIGATION OF THE EFFICIENCY OF DSSC FOR SAFFRON EXTRACT

Fehmi ASLAN¹

¹Rail Systems Machinery Technology, Yeşilyurt Vocational School, Turgut Özal University, Malatya, Turkey

ABSTRACT

This study used the soxhlet method to extract the saffron dye. TiO₂ nanoparticles were produced by hydrothermal method. The XRD peaks of the synthesized particles confirmed the mineralogical structure. Surface photographs of TiO₂ were examined with SEM images. These images showed microsphere structures in close contact with each other. When the UV analyses of the saffron dye were examined, remarkable absorption behaviors were detected in the visible region. When the photovoltaic parameters of the produced dye-sensitized solar cell were examined, the photoelectric conversion efficiency (η), open circuit voltage (V_{oc}), short circuit current (J_{sc}) and filling factor (FF) were found to be 0.007, 0.2 V, 0.081 mA/cm² and 0.46, respectively.

Keywords: Solar cell, organic dye, photovoltaic.

EVALUATION OF THE CENTRAL-METAL EFFECT ON ANTICANCER ACTIVITY AND MECHANISM OF ACTION OF ISOSTRUCTURAL Cu(II) AND Ni(II) COMPLEXES CONTAINING PYRIDINE-2,6-DICARBOXYLATE

Sara Abdolmaleki, Samad Khaksar ^{**}

School of Science and Technology, The University of Georgia, Tbilisi, Georgia

ABSTRACT

Metal ions have a significant role in the biological processes of the body as the vital activities of the cell and enzymes are organized by their inherently existent metals. Therefore, through many decades, metal-based compounds have been evaluated for the treatment of various diseases. Two Cu(II) (C1) and Ni(II) (C2) complexes were designed through the one-pot reaction of pyridine-2,6-dicarboxylic acid and 2-amino benzimidazole respectively with copper(II) nitrate hexahydrate and nickel(II) nitrate hexahydrate. Both complexes were characterized by single-crystal X-ray diffraction and the distorted octahedral geometry was recognized for them. The anticancer evaluations showed that these compounds have a different inhibition effect on the tested cell lines and it was concluded that the type of central metal could affect the inhibitory effect and action mechanism of the compounds as an anticancer drug.

The assay of apoptosis- and autophagy-related proteins indicated that bimodal death can be suggested through mitochondria-mediated apoptosis and autophagy pathways in BEL-7404 cells treated with the complexes, although each of these processes may be more prominent depending on the type of central metal in the complexes.

Keywords: Cu(II) and Ni(II) complexes, Anticancer effect, Production of ROS, Apoptosis, Autophagy

SIMULATION OF FLEXIBLE PRINTED STRUCTURES DESIGN FOR MOBILE ROBOT PLATFORM

Igor Nevliudov¹, Iryna Zharikova¹, Sergiy Novoselov¹, Dmytro Nikitin¹

¹ Department of Computer-Integrated Technologies, Automation and Mechatronics, Faculty of Automatics and Computerized Technologies, Kharkiv National University of Radioelectronics, Kharkiv, Ukraine

ABSTRACT

The mobile robot platform was designed for remote performing of special tasks for various fields. For example, these tasks can be the next: reconnaissance and surveillance, research of dangerous objects in the military sphere; surveillance, dangerous objects search and identification in the field of public safety; victims search and assistance during emergencies liquidation; and also tasks for fields of health care and agriculture.

The control system of proposed mobile platform consists of sensors, actuators and auxiliary modules such as navigation subsystem, power management subsystem and others. The conducted research made it possible to determine that the main nodes of the robot are the movement control node, the manipulator control node, the main control node, as well as navigation, sensor, technical vision, power control and communication nodes.

One of the important advantages of proposed robot platform design is replacement of rigid hardware components with flexible ones. This decision can reduce their weight and size, improve quality, functionality, reliability etc. Such structures ensure the connections stability between the platform modules, even if it is affected by destabilizing external factors, for example, vibrations and shocks during its movement.

Based on the results of stress-strain state studies for flexible boards and loops flexible-rigid the interconnections system based on copper-foiled polyimide was designed for the developed robotic platform.

Thus, the subject of research is the commutative system of a mobile robotics platform based on flexible polyimide structures.

Keywords: flexible printed structures, mobile robot platform, 3D model, polyimide.

VOICE CONTROL USING IN PHARMACEUTICAL PRODUCTS LOGISTICS SYSTEMS

Svitlana Maksymova¹, Viktoriia Nevliudova¹, Oleksandr Klymenko², Gennadii Makarenko¹

¹ Department of Computer-Integrated Technologies, Automation and Mechatronics;
Kharkiv National University of Radio Electronics, Kharkiv, Ukraine

² «Kapelou» LLC, Kyiv, Ukraine

ABSTRACT

Existing technologies development, as well as the creation of new ones, lead to the emergence of new trends in various areas of automation. Thus, in the pharmaceutical industry, logistics systems are widely used for the selection of products in automated warehouses, which significantly increase the speed and accuracy of processing requests, which leads to an increase in the efficiency of production as a whole. One of the extremely relevant directions in the development of production control, as well as individual operations, is the use of voice control at various stages of production processes. The authors suggest introducing voice control for critical operations execution on an automated logistics line. The study conducted by the authors showed that in some cases it may be appropriate. Thanks to the use of at least elements of such control, production efficiency can be increased, including by reducing the cost of logistics systems.

Keywords: Storage, Voice Control, Pharmaceutical Production, Warehouse Management System, Warehouse 4.0.

INVESTIGATION OF HYDROGEN PRODUCTION BY USING CONCENTRATED PHOTOVOLTAIC/THERMAL HYBRID COLLECTOR WITH SPECTRAL BEAM SPLITTING

Cihangir Kale

Hikmet Esen

^{1,2} Department of Energy Systems Engineering, Faculty of Technology, University of Firat, Elazığ, Turkey

ABSTRACT

Hydrogen (H₂) is an element with high heating value. In addition, it is energy efficient and does not harm the environment as it only releases water and a small amount of NO_x when burned with air. However, although hydrogen is an abundant element on earth, hydrogen is not found in nature alone as a gas. H₂ can be obtained by using primary energy sources and renewable energy sources. Using renewable energy sources to produce hydrogen is of great importance for a faster transition to a sustainable-clean environment. Solar energy is the richest renewable energy source in the world. Hydrogen can be produced with different technologies from solar energy. The most practical and widely used method among these technologies is the electrolysis of water. However, the efficiency in conventional Photovoltaic (PV)-electrolysis systems is quite low.

In this study, hydrogen production potential was investigated with a concentrated photovoltaic/thermal (SBS-CPV/T) hybrid collector with spectral beam splitters are also used instead of conventional PV-electrolysis. As a result of the study, the optical efficiency of the SBS-CPV/T collector was found to be 83.6%. While the average temperature of the multi-junction solar cell was found to be 79.7°C under 765X condensation, it was concluded that it provided 38.8% electrical efficiency at this temperature. Based on these findings, it has been seen that high temperature hydrogen production with SBS-CPV/T collector is a promising solution.

Keywords: Concentrated photovoltaics, multi-junction solar cell, spectral beam splitting, hydrogen.

BAYESIAN REGULARIZATION OF LEARNING

Murad Omarov¹, Vusala Muradova²

¹ Department of Computer-integrated technologies, automation and mechatronics, Kharkov National University of Radio Electronics, Kharkov, Ukraine

² Department of Natural Sciences, Kharkov National University of Radio Electronics, Kharkov, Ukraine
Email of corresponding author: viusalia.muradova@nure.ua

ABSTRACT

The subject of research in the article is the Bayesian approach based on the first principles of the probability theory is the most consistent paradigm of statistical learning. From practical perspective Bayesian learning offers intrinsic regularization procedure providing a viable alternative to traditional cross-validation technique. **Objective:** Machine learning aims to identify patterns in empirical data. In contrast to mathematical modeling, which studies the consequences of known laws, machine learning seeks to recreate the causes by observing the consequences generated by them are empirical data training, so thus, it belongs to the class of inverse problems and, in the general case, is a poorly defined or ill-posed problem. These tasks are different special sensitivity of some solutions to data and finding stable solutions implies a regularization procedure, which is a restriction of the class of feasible solutions. **The following tasks are solved in the article:** Bayesian regularization, the subject of this review, is an alternative technique for optimizing model complexity. It is not based on an estimate of the expected error, but on the choice of the most plausible model supported by the available data. This approach has a number of advantages. First, it proceeds from the first principles of probability theory and statistical learning theory, which guarantee a reduction in generalization error. Secondly, it implies an assessment of variations in the model parameters and, accordingly, an assessment of the accuracy of one's predictions. Thirdly, the problem posed in this way can in some cases of practical importance be solved with a minimum number of additional simplifying assumptions. And finally, as a consequence, last but not least: Bayesian regularization can be built directly into learning algorithms. Moreover, such regularized algorithms no longer imply a validation stage, uniformly using all available data both to select the optimal complexity of the model and to configure its parameters.

Keywords: Bayesian regularization, Bayesian learning, machine learning, mathematical modeling.

RESEARCH OF THE STABILITY OF THE SECURE RADIO-FREQUENCY COMMUNICATION IN THE DISTRIBUTED SYSTEMS BY USING MULTY-CHANNEL IOT LPWAN TECHNOLOGIES

Makovetskyi Sergii¹, Kauk Viktor²

¹ PhD student, Faculty of Computer Science, Kharkiv National University of Radio Electronics, Kharkiv, Ukraine

² Assistant professor of the Department of Software Engineering, Scientific supervisor of CTDL, Member of EMC, Candidate of Technical Sciences, Assistant professor, Faculty of Computer Science, Kharkiv National University of Radio Electronics, Ukraine

ABSTRACT

Nowadays, the distributed systems for processing and transmitting information are of considerable interest among the scientists. The existing methods of the information processing and transmission are not entirely efficient and in some specific cases do not work at all in the distributed systems. The distribution systems don't have a central computing module, so the usual methods of the information processing do not work in this case.

The data processing in the distributed systems is in high demand in the systems that support people's life both in critical infrastructure facilities and in military systems.

The information transfer methods occupy a special place in modern distributed systems. In some cases, people's lives and health depend on the effectiveness of the chosen methods.

This article will present the results of the practical research on the stability of radio frequency communication in distributed systems using the example of a distributed system based on LoRa technology.

The work shows the main advantages of broadband LoRa technology and the practical results of using Mesh modules.

Keywords: Cybersecurity, LPWAN, LoRaWAN, distributed systems

CO-AGGREGATION OF S100A9 PROTEIN WITH L- DOPA AND CYCLEN-BASED COMPOUNDS – EFFECT ON THE AMYLOID FIBRIL SELF-ASSEMBLY

L. Arabuli^{1,2}, I. A. Iashchishyn¹, N. V. Romanova¹, G. Musteikyte³, V. Smirnovas³, H. Chaudhary¹, Ž. M. Svedruži'c⁴, and L. A. Morozova-Roche¹

¹Department of Medical Biochemistry and Biophysics, Umeå University, SE-90781 Umeå, Sweden

²Department of Natural Sciences, School of Science and Technology, University of Georgia, 0171 Tbilisi, Georgia

³Institute of Biotechnology, Life Sciences Center, Vilnius University, LT-10257 Vilnius, Lithuania

⁴Department of Biotechnology, University of Rijeka, HR-51000 Rijeka, Croatia

E-mail: l.arabuli@ug.edu.ge

We studied the effect of cyclic compounds and their conjugates on the amyloid formation of pro-inflammatory S100A9 protein, which was found to be a common denominator in Alzheimer's and Parkinson's disease as well as in traumatic brain injury, which is considered as a pre-cursor state for neurodegenerative ailments [1,2]. Indeed, amyloid formation is commonly associated with neuroinflammation, and pro-inflammatory S100A9 protein acts both as an alarmin, inducing the production of pro-inflammatory cytokines, and as a highly amyloidogenic protein, which self-assembles into amyloids under physiological conditions.

The amyloid cascade is central for the neurodegeneration disease pathology, including Alzheimer's and Parkinson's, and remains the focus of much current research. S100A9 protein drives the amyloid-neuroinflammatory cascade in these diseases. DOPA and cyclen-based compounds were used as amyloid modifiers and inhibitors previously, and DOPA is also used as a precursor of dopamine in Parkinson's treatment. Here, by using

fluorescence titration experiments we showed that five selected ligands: DOPA-D-H-DOPA, DOPA-H-H-DOPA, DOPA-D-H, DOPA-cyclen, and H-E-cyclen, bind to S100A9 with apparent K_d in the sub-micromolar range. Ligand docking and molecular dynamic simulation showed (Fig.1) that all compounds bind to S100A9 in more than one binding site and with different ligand mobility and H-bonds involved in each site, which all together is consistent with the apparent binding determined in fluorescence experiments. By using amyloid kinetic analysis, monitored by thioflavin-T fluorescence, and AFM imaging, we found that S100A9 co-aggregation with these compounds does not hinder amyloid formation but leads to morphological changes in the amyloid fibrils, manifested in fibril thickening. Thicker fibrils were not observed upon fibrillation of S100A9 alone and may influence the amyloid tissue propagation and modulate S100A9 amyloid assembly as part of the amyloid-neuroinflammatory cascade in neurodegenerative diseases.

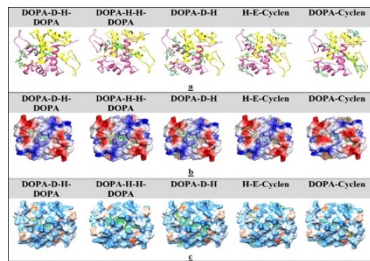


Figure 1. Binding sites on S100A9 homo-dimer for different DOPA and Cyclen-based compounds.

[1] Wang, C.; Klechikov, A.G.; Gharibyan, A.L.; Wärmländer, S.K.T.S.; Jarvet, J.; Zhao, L.; Jia, X.; Narayana, V.K.; Shankar, S.K.; Olofsson, A.; et al. *Acta Neuropathol.* 2014, 127, 507–522.

[2] Horvath, I.; Iashchishyn, I.A.; Wang, C.; Moskalenko, R.A.; Wärmländer, S.K.T.S.; Wallin, C.; Gräslund, A.; Kovacs, G.G.; Morozova-Roche, L.A. *J. Neuroimmun.* 2018, 15, 172.

30

3,5-BIS(TRIFLUOROMETHYL) PHENYLAMMONIUM TRIFLATE: A NEW AND GREEN ORGANOCATALYST FOR THE SYNTHESIS OF INDENO[1,2-B]PYRIDINES

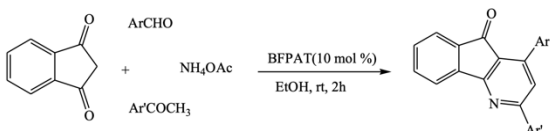
Peyman Salahshour, Samad Khaksar *

School of Science and Technology, The University of Georgia, Tbilisi, Georgia

ABSTRACT

In the past 20 years, organocatalysis has emerged as an important area of research. Organocatalysts are easy and inexpensive to assemble, generate no waste, have simple purification, and have aspects of the high atomic economy thus encompassing the principles of green chemistry. Recently, aryl ammonium triflate has gotten impressive consideration for numerous organic reactions, giving the corresponding products in high yields with great selectivity.

In this study, we have demonstrated an efficient and practical process for the synthesis of indeno[1,2-b]pyridine compound derivatives



by four-component condensation of aldehyde, aromatic ketones, 1,3-indanedione, and ammonium acetate using BFPAT as a green, inexpensive, and powerful organocatalyst in ethanol.

The advantages offered by this method are simple reaction conditions, operational simplicity, a green and cost-effective catalyst, easy purification, and excellent yields.

Keywords: Organocatalyst, Green, Pyridine, Reusable, Heterocycle

31

PECULIARITIES OF Cs_{1-x}Rb_xCu₂Cl₃ SOLID SOLUTIONS ABSORPTION SPECTRA

Olena KOVALENKO¹, Olga YUNAKOVA², Mykola YUNAKOV³

¹Department of Physics, Faculty ACT, Kharkiv National University of Radio Electronics, Kharkiv, Ukraine

²Physical optics Department, Faculty of Physics, V. N. Karazin Kharkiv National University, Kharkiv, Ukraine

³Department of Materials for Reactor Constructing and Physical Technologies, Education and Research Institute "School of Physics and Technology", V. N. Karazin Kharkiv National University, Kharkiv, Ukraine

ABSTRACT

Peculiarities and characteristics of absorption spectra Cs_{1-x}Rb_xCu₂Cl₃ solid solutions have been studied in this work. Many complex compounds related to this system have high ionic conductivity and are classified as solid electrolytes [1,2], some of them can be decent luminophores [3] and can be used in light-emitting devices. The absorption spectra of thin films of CsCu₂Cl₃ and RbCu₂Cl₃ are isostructural and are close by spectral position of the bands [1]. The exciton spectrum of both compounds is interpreted on the basis of transitions in the Cu⁺ ion.

Thin films for investigation were prepared by vacuum evaporation of a melt mixture of pure CuCl, CsCl and RbCl. Then the films were annealed for an hour at 100°C.

In the concentration range 0 ≤ x ≤ 0.6, the absorption spectra of Cs_{1-x}Rb_xCu₂Cl₃ thin films are similar in the structure of the spectrum and close in the spectral position of the absorption bands (Fig. 1a). As x increases, the A and B exciton bands slightly linearly shift to the short-wavelength region of the spectrum with dE_m/dx = 0.03 eV and 0.045 eV, respectively. In the range 0.6 < x ≤ 1, on the contrary, a noticeable linear long-wavelength shift of the A and B exciton bands is observed with increasing x with dE_m/dx = -0.43 eV and -0.59 eV. The half-width Γ(x) of the exciton bands A and B (Fig. 1b) slightly linearly increases in the range 0 ≤ x ≤ 0.6 with dΓ_A/dx = 0.05 eV and dΓ_B/dx = 0.049 eV. In the interval 0.6 < x ≤ 1, the half-width Γ(x) increases with dΓ_A/dx = 0.19 eV and dΓ_B/dx = 0.185 eV.

We assume that the presence of two concentration intervals with different concentration behavior of E_m(x) and Γ(x) of the exciton A and B bands is due to the different crystal structure of the Cs_{1-x}Rb_xCu₂Cl₃ compounds in the intervals 0 ≤ x ≤ 0.6 and 0.6 < x ≤ 1. In the first concentration range, apparently, the Cs_{1-x}Rb_xCu₂Cl₃ solid solutions are isostructural with CsCu₂Cl₃, since their exciton spectra are similar by structure and close in the spectral position of the bands. A slight short-wavelength shift of the A and B bands in the

range $0 \leq x \leq 0.6$ indicates a slight increase in the ionicity of the compounds and the bandgap width E_g . In this concentration range $E_g(x)$ grows linearly (Fig. 1c) according to equation $E_g(x) = E_g(0) + ax$, where $E_g(0) = 4.605 \pm 0.001$ eV, $a = dE_g/dx = 0.03 \pm 0.003$ eV.

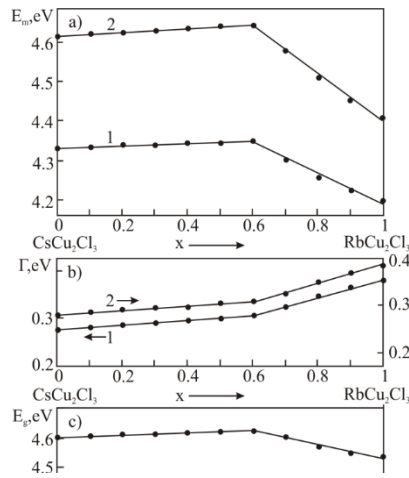


Fig. 1. The concentration dependences of the spectral position $E_m(x)$ (a), half-width $\Gamma(x)$ (b) of the long-wavelength exciton bands A(1) and B(2) and the bandgap width $E_g(x)$ (c).

In the range $0.6 < x \leq 1$ solid solutions $Cs_{1-x}Rb_xCu_2Cl_3$ are isostructural with $RbCu_2Cl_3$. A significant long-wavelength shift of the spectral position $E_m(x)$ of the A and B exciton bands in this concentration range indicates a decrease in the ionicity of the $Cs_{1-x}Rb_xCu_2Cl_3$ solid solutions. In this concentration range, the bandgap width $E_g(x)$ decreases linearly (Fig. 1c) from $dE_g/dx = -0.23$ eV. The linear concentration dependences of the bandgap width $E_g(x)$, spectral position $E_m(x)$ and half-width $\Gamma(x)$ of exciton bands in $Cs_{1-x}Rb_xCu_2Cl_3$ solid solutions confirm the localization of excitons in the sublattice of compounds that contains Cu^+ ions.

Keywords: solid solutions, thin films, absorption spectra, excitons

REFERENCES

- [1] S. Hull, P. Berastegui, Crystal structures and ionic conductivities of ternary derivatives of the silver and copper monohalides-II: ordered phases within the $(AgX)_x(MX)_{1-x}$ and $(CuX)_x(MX)_{1-x}$ ($M=K, Rb$ and Cs ; $X=Cl, Br$ and I) systems. *J. Solid State Chem.* 2004; 177(9): 3156- 3173.
- [2] A.K. Ivanov-Shits, I.V. Murin, *Ionics of the Solid State*, vol. 1. 2000; 616 p.
- [3] R. Rocanova, A. Yangui, H. Nhalil, H. Shi, M.-H. Du, B. Saporov. Rb_2CuX_3 ($X = Cl, Br$): 1D All-Inorganic Copper Halides with Ultrabright Blue Emission and Up-Conversion Photoluminescence. *ACS Appl. Electron. Mater.* 2019; 1 (3): 269.

32

FACTOR ANALYSIS OF PHOTOPOLYMER RESINS FOR 3D PRINTING

Igor Nevludov, Dmytro Nikitin, Roman Strelets, Yegor Korotun

Department of Computer-Integrated Technologies, Automation and Mechatronics;
Kharkiv National University of Radio Electronics, Kharkiv, Ukraine

ABSTRACT

3D printing is one of the key elements of Industry 4.0, which is the fourth industrial revolution. This technology allows you to create objects with three-dimensional shapes from various materials, including metals, plastics, ceramics and others. It is used in many industries, including medicine, aviation, automotive and engineering. The main advantage of 3D printing is the ability to create objects without a large amount of production and tooling costs. Instead, 3D printing allows you to create objects directly from digital models, which reduces production time and costs. In Industry 4.0, 3D printing is used to create customised products, reduce prototype development and production time, and produce parts for complex systems and machines where precision and quality are essential. Applications of 3D printing in Industry 4.0 can include processes such as prototyping, manufacturing, repair and maintenance of equipment, as well as the setup and optimisation of production processes. One of the most important advantages of 3D printing is the ability to reduce the time required to develop and manufacture new products. The technology also helps to reduce production costs and increase productivity by optimising production processes and reducing prototype development time. The development of additive manufacturing technologies is becoming increasingly common in industry and everyday life. 3D printing is one of the most versatile and affordable means of producing three-dimensional parts of complex shapes. Currently, 3D printers can produce parts made of plastic (FDM printing), metal (SLS/SLM printing) and photopolymer (SLA, DLP and LCD printing). Photopolymer 3D printing has a number of advantages, such as affordability, high precision of manufacturing parts, simplicity of technology and a large number of free software. Due to these advantages and features of the technology, this manufacturing method can be used in many areas, such as jewellery production (creation of master models for casting), dentists (creation of dentures), creation of decorative models for interior design.

Keywords: additive technologies, photopolymer 3D printing, resins, factor analysis, production, technical quality control.

EXAMINING THE SYMMETRY OPERATIONS OF THE DNA MOLECULE WITH CLIFFORD ALGEBRA

Hatice Güney¹ Abidin KILIÇ¹
¹Eskişehir Technical University

ABSTRACT

The DNA Molecule has a structure similar to the Platonic Solids Dodecahedron in terms of its properties. The physical properties of this molecule can be studied with Clifford Algebra. The Clifford Algebra was used to establish a general and practical method for obtaining operators of the kinetic energy of molecular vibrational-rotation of polyatomic molecules and symmetric molecules. Whereas, the vibration and rotation measurement vectors appearing in the metric tensor for any geometrically defined coordinate of the shape and frame of the molecules were easily determined using geometric algebra. The present method (Clifford algebra) generates molecular vibrational-rotational kinetic energy operators that are in excellent agreement with previous work. In this study, the symmetry operations of the DNA molecule were investigated by Clifford Algebra.

Keywords: Clifford Algebra, Symmetric Molecules, Symmetry Operations

This study was supported by the Eskişehir Technical University Commission of Research Project under grant no: 23ADP043.

INVESTIGATION OF TRANSFORMATION' SYMMETRIC MOLECULES WITH CLIFFORD ALGEBRA

Abidin KILIÇ¹
¹Eskişehir Technical University

ABSTRACT

Clifford Algebra was used to create a general and practical method for obtaining the operators of the kinetic energy of the molecular vibration-rotation of polyatomic molecules and symmetric molecules. On the other hand, these polyatomic molecules' precise intrinsic kinetic energy operators include a metric tensor. The elements of this metric tensor were expressed as the mass-weighted sum of measuring vector inner product vectors compatible with the molecule's nucleus. Whereas, the vibrational and rotational measuring vectors that appear in the metric tensor for any geometrically defined coordinates of the shape and frames of the body were easily determined using geometric algebra. The current method (Clifford algebra) generates molecular vibration- rotation kinetic energy operators that are in perfect agreement with earlier studies. In this study The symmetric molecule's symmetry operations was investigated by Clifford Algebra.

Keywords: Clifford Algebra, Symmetric Molecules, Transformation Matrices

This study was supported by the Eskişehir Technical University Commission of Research Project under grant no: 23ADP043.

ENSURING THE ROBOT SNAKE'S MOVEMENT ON SLIPPERY SURFACES

Murad Omarov, Vladyslav Korobskiy, Viktoriia Nevliudova

Department of Computer-Integrated Technologies, Automation and Mechatronics, Faculty of Automation and Computerized Technologies, Kharkiv National University of Radio Electronics, Kharkiv, Ukraine

ABSTRACT

A relevant issue today is the ability of a robot snake to move on different surfaces due to friction forces. In nature, when a robot snake moves over loose sands, its movement differs from that of a snake moving over a rough surface. A living snake crawls not forward, but sideways ("laterally"), pulling the back of its body forward, it flips it over without touching the surface forward, and then, leaning on the entire side of the body, pulls the front part up. The support with this type of movement is more stable to fix the snake's position. This type of movement is asymmetrical, so the load on the muscles is uneven; to equalize it, the snake has to periodically change the "working side" of its body - crawl forward with its left or right side.

The problem with modern snake robots is that if the surface of movement is slippery or loose, such as smooth glass, or smooth ice, or loose dust, then the movement of the snake robot is almost impossible. Since the snake-like movement uses a support - the surface of movement, the efficiency of movement depends on the roughness of the support.

Keywords: Snake robot, lateral movement, support, slippery surface.

A GEOTECHNICAL EXAMINATION OF KAHRAMANMARAS (TURKEY) PAZARCIK & EKINOZU 6 FEBRUARY 2023 EARTHQUAKES

Emre Aytuğ ÖZSOY^{1,*}

¹ Building Inspection Program, Porsuk Vocational School, Eskisehir Technical University, Eskisehir, TURKEY

As it is known, Turkey is located on the geologically active fault zones. On 6 February 2023, 2 major destructive earthquakes occurred within the borders of Kahramanmaraş province on some fault segments forming the East Anatolian Fault (EAF) Zone, one of the most important active faults of our country. The first of these earthquakes, which occurred at 04:17, is 7.7 (Mw) according to Boğaziçi Kandilli Observatory and 7.8 (Mw) (later corrected as 7.7) according to AFAD, and the focal depth of this earthquake, which is called Pazarcık Earthquake, is still in focus. 10 km and 8.6 km respectively according to the same organizations. (KOERI, 2023; AFAD, 2023). The epicenter of the second earthquake, which occurred at 13:24 on the same day, was near the Ekinözü district in the south of Elbistan district, its magnitude was Mw7.6 according to KOERI and AFAD, and its focal depth was 10 km and 7 km, respectively, according to these two institutions. It was named Ekinözü after the earthquake.

In the earthquakes total of 11 provinces, including Hatay, Kahramanmaraş, Adıyaman, Malatya, Gaziantep, Osmaniye, Adana, Şanlıurfa, Kilis and Diyarbakır were affected to varying degrees. According to official records; The number of our citizens who lost their lives has exceeded 50,000 and 107,204 citizens have been injured, and according to official statements, 304.000 buildings have completely collapsed and severely damaged.

In addition to the destruction and damage in the buildings, transportation structures (highway, railway, bridge), industrial facilities, power lines, infrastructure elements etc. in these earthquakes. is also damaged. In addition, mass movements such as landslides, rockfalls, soil liquefaction and lateral spreading, which adversely affect the surface structures and buried structures, were observed.

In this study, the field studies, reports and all published studies after the 6 February 2023 Kahramanmaraş earthquakes were examined, how much of the local soil properties and geoscience data were used correctly at the right time.

Keywords: Earthquake, Kahramanmaraş, Geotechnics, Soil Properties.

NUMERICAL ANALYSIS OF A NEW THERMOSYPHON HEAT PIPE

Çetin YAVUZ 1 , Ali TAROKH 2 , Aydın DİKİCİ 3

1 Department of Electrical and Energy, Tatvan Vocational School, Bitlis Eren University, Bitlis, Turkey

2 Department of Mechanical Engineering, Lakehead University, Thunder Bay, Canada

3 Department of Energy System Engineering, Fırat University, Elazığ, Turkey

ABSTRACT

In this study, an experimental and 3-dimensional numerical analysis of a thermosiphon heat pipe (THP) using two-phase fluid cycling was performed to model the heat transfer process by evaporation and condensation. R404A refrigerant was chosen as the working fluid for the THP and 50% of the evaporator section was filled with the working fluid. Numerical analysis was performed using ANSYS FLUENT program and VOF method. In the meantime, in order to model the evaporation and condensation process successfully, a UDF code written in C was used and introduced to the fluent program. As a result of the study, it was seen that the temperature values obtained from the experimental and numerical analysis for the evaporator and condenser parts of the THP were in good agreement. As a result of the numerical analyzes carried out in 3D, the contours of the evaporation and condensation process and the heat transfer process are presented visually. The analysis took a total of 200 seconds.

Keywords: Thermosiphon heat pipe, Evaporation and condensation, ANSYS, VOF

STUDY OF MANUFACTURING DEFECTS IN THE TECHNOLOGY OF MANUFACTURING MOEMS SEMICONDUCTOR SUBSTRATES FOR TECHNICAL AUTOMATION MEANS

Igor NEVLIUDOV¹, Shakhin OMAROV, Olena CHALA, Serhii TESLIUK

¹Department of Computer-Integrated Technologies, Automation and Mechatronics, Kharkiv National University of Radio Electronics, Kharkiv, Ukraine

ABSTRACT

Today, in the context of the widespread use of digital, network and intelligent technologies, and the continuous development of integrated production innovations, major and profound changes are taking place in the philosophy of modern industry development. Such changes set manufacturers the task of automating production process control in real time, which involves creating a single enterprise information space that links together the technological and business levels of enterprise management, while solving many of the most important tasks for an industrial enterprise.

Integration of the cyber component allows automating the management of production processes through the use of intelligent mechatronic modules, expert systems and large data sets for production forecasting. In this context, a person controls processes at the physical level through a cybernetic system. At the same time, this system with minimal human involvement allows: automatic control of the vehicle at the physical level, analysis and decision-making in real time. Systems of this type are multilevel. At the lower level, accurate and reliable systems such as microelectromechanical and micro-optomechanical are used. They collect, process, and transmit information in the control of technological systems. The accuracy and durability of MEMS and MOEMS depends on the technology of their manufacture.

The aim of this work is to increase the efficiency of control by using proximity sensors based on MEMS and MOEMS as part of technical automation means.

Keywords: technical automation means, defect, technological process, MEMS, MOEMS, substrate, diffusion, defect engineering.

39

INTELLIGENT ENERGY SUPPLY MANAGEMENT SYSTEM IN THE MUNICIPAL SECTOR

Igor NEVLUDOV¹, Andriy SLUSAR¹, Kyrlyo KRUSTALOV¹, Sofia KRUSTALOVA¹, Shakhin OMAROV¹

¹ Department of Computer-Integrated Technologies, Automation and Mechatronics, Faculty of Automation and Computerized Technologies, Kharkiv National University of Radio Electronics, Kharkiv, Ukraine

ABSTRACT

The subject of this study is the methods, tools and intelligent systems for managing energy supply in the public utilities sector. The object of the study is the process of energy management in the municipal sector. The purpose of the study is to develop an intelligent energy management system in the public utilities sector. To achieve this goal, the following tasks were solved: the main problems of energy efficiency in the housing and communal services sector were analyzed and ways to solve them using modern technologies were proposed; the methodology for developing an intelligent system (SmartGrid) was chosen; the architecture of an intelligent energy management system was proposed; the algorithm of the intelligent energy saving management component was presented; to determine the electricity consumption in the system, a methodology was used that involves the collection and analysis of data from the Machine learning algorithms, such as the support vector method, neural networks, and decision trees, are used to determine the optimal mode of energy consumption.

Conclusions: the use of the proposed system will reduce the cost of energy supply in the municipal sector and increase its energy efficiency, the possibility of integration with other municipal management systems.

Keywords: intelligent system, energy supply management, utilities, machine learning, energy efficiency, optimization, data analysis.

P1

THE STIMULATING EFFECT OF THE *CUPRESSUS SEMPERVIRENS* MAJOR ALLERGEN (CUP S1) ON BRONCHIAL EPITHELIAL CELLS (BEAS -2B)

Imane BOUGUENOUN^{1,*}, Widad BOUGUENOUN², Dalila BENDJEDDOU³, Marie-Claire DE PAUW-GILLET⁴, Edwin DE PAUW⁵

1 Department of Biology, Faculty of Biologic Sciences and Agronomic Sciences, University of Mouloud Mammeri, Algeria.
 2 Department of Nature and Life Sciences, Faculty of Exact Nature and Life Sciences, University of Mohamed Khider, Algeria.
 3 Department of Biology, Faculty of Nature and Life Sciences, Earth and Universe Sciences, University of 8 May 1945, Algeria.
 4 Laboratory of mammals cells culture, Institute of chemistry, University of Liège, Belgium
 5 University of Liège, Faculty of Sciences, Belgium.

ABSTRACT

Allergic diseases have a central place in chronic pathologies. For over 20 years, their frequency has been increasing. Allergies to pollen, at present, are a major public health problem because of pollen diversity. However, all the pollens are not allergenic, their nature and quantity vary significantly depending on the region and climatic conditions. *Cupressus sempervirens* is one of the most widespread species in Algeria with very high allergenic capacity. The aim of this work is to evaluate the stimulatory effect of the major allergen of this species

The present study was carried out on human bronchial epithelial cells (BEAS-2B) transformed by an adenovirus 12 SV40 hybrid. In this context we are interested in the stimulation, in vitro, of those cells by different doses of the major allergen Cup s1 to test the viability and the release of IL-8 and IL-6. After a series of culture, the cells were exposed for 24 hours at a concentration of 0.02µg/µl, 0.06µg/µl, 0.1 µg/µl, 0.3 µg/µl and 0.9µg/µl of allergen Cup s1. The viability was assessed by the MTS assay and the assay of cytokine was carried out in the supernatant using the technology Luminex100. The MTS test showed that cells exposed to different doses were all viable. The release of IL-8 by the cells exposed to different concentrations of Cup s1 showed a highly significant increase with cells exposed to 0.1 µg/µl, 0.3µg/µl and 0.9µg/µl of the major allergen. However, cell culture with 0.1 µg/µl, 0.3 µg/µl and 0.9µg/µl stimulated significant release of IL-6. Our experiments showed that the allergen Cup s1 represents no risk vitality of the cells and had the potential to stimulate the release of IL-8 and IL-6 in a dose-dependent manner.

Keywords: Allergy, Pollen, *Cupressus sempervirens*, BEAS-2B, IL-8, IL-6.

P2

SYNTHESIS AND STUDY OF NEW SURFACE-ACTIVE POLYMER COMPLEX WITH CATIONIC SALT

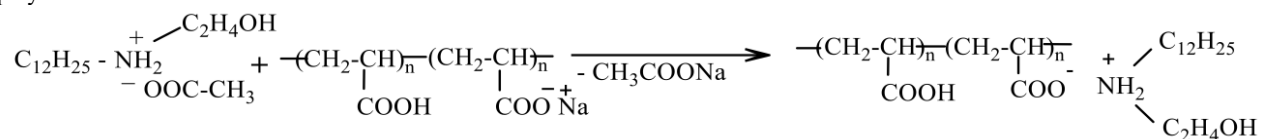
Poladova Tarana Ali

Y. H. Mamedaliyev's Institute of Petrochemical Processes
 of the Ministry of Science and Education

ABSTRACT

The extensive carrying of crude oil and its products across the oceans has increased concerns about the effects of accidental spillage of petroleum hydrocarbons in the marine environment. Major marine oil spills highlight the need for cost-effective and environmentally responsible ways for their liquidation. Similar oil spill incidents worldwide indicate that the 'first-minute response' principle plays a key role as an environmentally safe and cost-effective response to marine oil spills. Polymer surfactants find applications in different operations of petroleum production. They are essentially used to improve the total recovery of petroleum as well as in environment protection.

The main aim of the presented work was to produce a new, ecologically safe and efficient oil slick-collecting agent based on a new polymer-complex surfactant. It was synthesized by interaction of dodecylmonoethylolammonium ethanoate with neutralized polyacrylic acid:



It is a yellow wax, well-soluble in water accompanied with intensive foam formation. Composition and structure of this reagent have been identified by IR- spectroscopy. Surface tension at the water-air interface in the presence of the synthesized surfactants was

determined by a Du Nouy ring tensiometer. A high surface activity of aqueous solutions of the synthesized product was revealed (at 0.2% -50.8 mN/m; 0.5%-46.8 mN/m; 0.7%-40.9 mN/m; without surfactant 72.0 mN/m).

The specific electroconductivity of the surfactant solutions was measured using a conductometer. By the electroconductometric method it was found that the specific electrical conductivity (κ , in $\mu\text{S}/\text{cm}$) of aqueous solutions of this surfactant increases as the concentration (% by weight) of the solution increases (19°C): 0.025% 139.4; 0.075% 369.1; 0.1% 524.2; 0.5% 2516.4; 0.7% 4060.4.

The petrocollecting effectiveness of the surfactant was studied using an unthinned reagent and its 5 wt.% aqueous solution (or dispersion). The tests were carried out in three types of water having various degrees of mineralization (fresh, Caspian sea and distilled waters) using thin (thickness: 0.17 mm) layers of Pirallahy petroleum (from the oil field near Baku, Azerbaijan). This surfactant has a high petrocollecting capacity. When it is applied in unthinned form and used as a 5% aqueous dispersion, this polymer complex demonstrates high values of petrocollecting coefficient (K) which characterizes a ratio of surface areas of initial petroleum slick and petroleum spot formed by a surfactant action. Maximum value of K equals 80.2, the time of the reagent action exceeding 192 hours.

Keywords: petroleum production, surfactant , electroconductivity, petrocollecting

P3

SYNTHESIS OF SODIUM TITANATES USING CHITOSAN IN THE ENVIRONMENT

A.N. Mammadov, U.N. Sharifova, F.S. Ibrahimova, A.M. Qasimova , Mustafayeva A.N.

Nagiyev Institute of Catalysis and Inorganic Chemistry ANAS, H.Javid Avn.,113, AZ 1134, Baku

ABSTRACT

The method of hydrothermal synthesis was used to obtain titanates with the general formula $\text{Na}_2\text{Ti}_n\text{O}_{2n+1}$ in the environment. Polytitanates $\text{TiO}_2 \cdot n\text{H}_2\text{O}$ obtained from titanium concentrate were treated with concentrated aqueous NaOH solution.

From Fig.1 It follows that the production of single-phase $\text{Na}_4\text{Ti}_6\text{O}_{14}$ from Na_2TiO_3 , anatase and rutile modifications of TiO_2 is possible at temperatures above 950K. In the dissertation work, titanates $\text{Na}_4\text{Ti}_6\text{O}_{14}$, $\text{Na}_2\text{Ti}_3\text{O}_7$ and $\text{Na}_2\text{Ti}_6\text{O}_{13}$ were also obtained by hydrothermal method, the compositions of which are in accordance with the phase diagram of the $\text{Na}_2\text{O} - \text{TiO}_2$ system.

To desilicate titanium dioxide, the mixture was treated with a weak solution of sodium hydroxide at the boiling point of the solution. Polytitanic acid powder $x\text{TiO}_2 \cdot y\text{H}_2\text{O}$ was mixed with pure chitosan powder in a mass ratio of 20:1 and calcined in a temperature range of 850-900°C to obtain technical titanium dioxide in the form of a mixture of 94.5% anatase and 4.5% rutile. When calcining polytitanic acid powders $x\text{TiO}_2 \cdot y\text{H}_2\text{O}$ in the absence of chitosan, technical titanium dioxide mainly consisted of rutile.

The use of chitosan as a modifier is not accidental. We have revealed the influence of a bioactive natural polymer – chitosan as an organic reagent on the formation of the texture morphology and phase composition of products during hydrothermal treatment of TiO_2 powders.

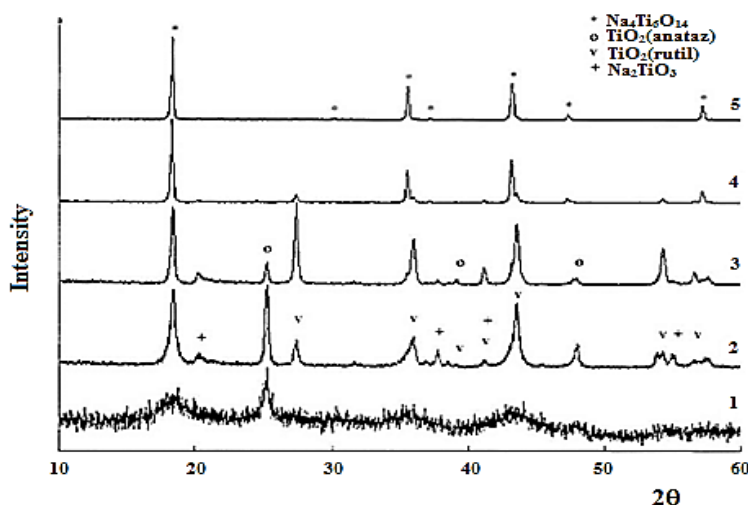


Figure 1. Fragments of anatase, rutile, Na_2TiO_3 and $\text{Na}_4\text{Ti}_6\text{O}_{14}$ diffractograms annealed for 6 hours at 650 (1). 750 (2). 850 (3). 950 (4). 1050K (5).

Keywords: chitosan, sodium titanates, polytitanates $\text{TiO}_2 \cdot n\text{H}_2\text{O}$

P4

STUDY OF ACTIVITY AND SELECTIVITY OF OXIDE CATALYSTS IN HYDROCARBON OXIDATION REACTIONS

Ulkar Shrahiyeva, Elmira Huseynova, Aida Rzayeva, Zarifa Mammadova, Saida Nadjafova, Nurana Mardanova

Scientific Research Institute "Geotechnological Problems of Oil, Gas and Chemistry", ASOIU, 20, Baku, Azerbaijan

ABSTRACT

The selectivity of complex reactions is one of the main problems of heterogeneous catalysis. Thus, it is known that the oxidation of hydrocarbons can proceed with the formation of soft and deep oxidation products. Finding the factors that determine one or the other direction of the reaction means obtaining a method for controlling the selectivity of the process. For a few catalytic oxidation reactions, there is reliable information about their mechanism.

Keywords: deep oxidation; C₃-C₄-olefins; the selectivity; catalytic reactions; re-oxidation.

P5

THE IMPORTANCE OF EARTHQUAKE EDUCATION IN SCIENCE CENTER

Nur ULUHAN¹, Abidin KILIÇ¹

¹Eskisehir Technical University, Faculty of Science, Physics Department

ABSTRACT

Turkey is an earthquake country on fault lines region from its east to west boundaries. Therefore, earthquake awareness training is important in our country. As AFAD, The Ministry of Education, AKUT, non-governmental organizations organize educations about earthquakes. This article describes both earthquake and earthquake education importance. It is mentioned that science centers' importance, earthquake education in the world and in science centers. Furthermore, the earthquake education in Eskisehir Science Center is mentioned in the article too. The search about the effects of earthquake education is mentioned in the results and conclusion.

Keywords: Earthquake Education, Science Center, Non-Formal Education

P6

AN APPROACH TO THE REPRESENTATION OF PLATONIC SOLIDS WITH GEOMETRIC ALGEBRA

Almila Selcen Uray¹

Abidin KILIÇ¹

¹Eskisehir Technical University, Faculty of Science, Physics Department

Geometric algebras known as a generalization of Grassmann algebras complex numbers and quaternions are presented by Clifford and this algebra describing the geometric symmetries of both physical space and spacetime is a strong language for physics. Groups generated from 'Clifford numbers' is firstly defined by Lipschitz (1886). They are used for defining rotations in a Euclidean space. In this work, Clifford algebra are identified. Energy of classic particles with Clifford algebra are defined. This calculations are applied to some Archimedean solids. Also, the vertices of Archimedean solids presented in the Cartesian coordinates are calculated.

Platonic Solids can also be represented by Geometric Algebra, which provides advantages mathematically and physically. These advantages have been demonstrated in many studies. But maybe as a new perspective, can a platonic solid's volume decrease or increase in 3-dimensional space be defined directionally by Geometric Algebra? This recommendation is discussed in this study.

FULL TEXTS

DOI: [10.5281/zenodo.810528310](https://doi.org/10.5281/zenodo.810528310)

INVESTIGATION OF HYDROGEN PRODUCTION BY USING CONCENTRATED PHOTOVOLTAIC/THERMAL HYBRID COLLECTOR WITH SPECTRAL BEAM SPLITTING

Cihangir KALE^{1*}, Hikmet ESEN¹

¹ Department of Energy Systems Engineering, Faculty of Technology, University of Firat, Elazığ, Turkey

ABSTRACT

Hydrogen (H₂) is an element with high heating value. In addition, it is energy efficient and does not harm the environment as it only releases water and a small amount of NO_x when burned with air. However, although hydrogen is an abundant element on earth, hydrogen is not found in nature alone as a gas. H₂ can be obtained by using primary energy sources and renewable energy sources. Using renewable energy sources to produce hydrogen is of great importance for a faster transition to a sustainable-clean environment. Solar energy is the richest renewable energy source in the world. Hydrogen can be produced with different technologies from solar energy. The most practical and widely used method among these technologies is the electrolysis of water. However, the efficiency in conventional Photovoltaic (PV)-electrolysis systems is quite low.

In this study, hydrogen production potential was investigated with a concentrated photovoltaic/thermal (SBS-CPV/T) hybrid collector with spectral beam splitter is also used instead of conventional PV-electrolysis.

As a result of the study, the optical efficiency of the SBS-CPV/T collector was found to be 81.28%. While the average temperature of the multi-junction solar cell was found to be 82°C under 765X concentration, it was concluded that it provided 32.39% electrical efficiency at this temperature. The total hydrogen conversion efficiency of the SBS-CPV/T hybrid collector was calculated as 33.3%. Based on these findings, it has been seen that high temperature hydrogen production with SBS-CPV/T collector is a promising solution.

Keywords: Concentrated photovoltaics, multi-junction solar cell, spectral beam splitting, hydrogen.

1. INTRODUCTION

Multi-junction solar cells can achieve higher efficiencies, ranging from 30% to 46% [1], which are approximately 2.5 times higher than the efficiencies of traditional crystalline silicon cells, due to their ability to utilize a wider part of the solar spectrum between 350 nm and 1850 nm [2,3]. . . However, these cells, also known as III-V group cells, are more costly in terms of materials and production technology. Nevertheless, the use of optical materials such as Fresnel lenses, parabolic mirrors, and lenses to concentrate the incident sunlight on these cells can lead to an increase in their electrical efficiency [4]. Furthermore, employing these optical materials allows for the development of more cost-effective systems by avoiding the use of expensive III-V group cells in large areas. Systems that concentrate sunlight using optical materials and generate electricity with PV cells are referred to as Concentrated Photovoltaic (CPV) systems [5].

Although III-V group cells can harness sunlight within the wavelength range of 350-1850 nm, they are unable to convert the ultraviolet (UV) part below 350 nm and the infrared (IR) part above 1850 nm into electrical energy. This limitation leads to heating of the cell [6]. Additionally, the excessive current generated in the Ge cell used in the subcell of these cells cannot be utilized as electrical energy, contributing to overheating of the cell [7].

Dielectric coatings applied to the surfaces of lenses used in CPV systems allow desired wavelengths of light to pass through while reflecting unwanted wavelengths. By using spectral beam splitting (SBS) lenses, which are spectral beam separators, the part of light within the wavelength range that cannot be converted into electrical energy is prevented from reaching the solar cell, thereby avoiding excessive heating of the cell. Moreover, the light within this wavelength range can be utilized as thermal energy in other applications. These types of systems are referred to as spectral beam splitting concentrated photovoltaic/thermal (SBS-CPV/T) hybrid systems [8].

In this study, the potential for hydrogen production using a spectral beam splitting concentrated photovoltaic/thermal (SBS-CPV/T) hybrid collector and solid oxide electrolyzer (SOE) has been numerically evaluated.

2. MATERIALS AND METHODS

In this study, a cassegrain type SBS-CPV/T hybrid collector was designed and its hydrogen production potential was evaluated. Optical System consists of primary mirror, spectral beam splitter (SBS), homogenizer, light guide, CPV solar cell and heat sink. The collector is designed using ZEMAX Optic Studio software under 765X concentration for the 3C44C model GaInP/GaInAs/Ge triple-junction CPV solar cell with 7x7 mm² active area from Azur Space. Concentration ratio can be calculated using Equation 1:

$$CR = \frac{A_{in}}{A_{out}} \quad (1)$$

where, A_{in} and A_{out} stand for the optical system input and output areas, respectively.

In this study, VIS-NIR coating N-BK7 glass lens, which is a commercial product by Edmund optics, was used as SBS lens. VIS-NIR coated and uncoated lens transmission graph is given in Figure 1.

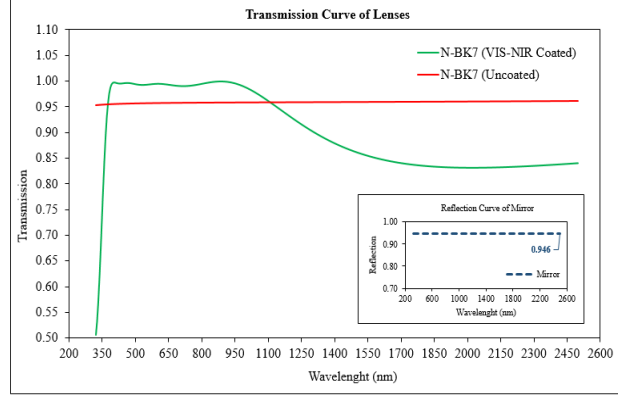


Figure 1. VIS-NIR coated and uncoated N-BK7 glass lens transmission graph.

The single diode model is considered the most convenient way to describe triple-junction solar cells [9,10]. In this study, numerical analysis was performed using a single diode model for CPV solar cell using the MATLAB software. The short-circuit current density of the sub-cells can be calculated as in Equation 2 [11]:

$$I_{sc,i} = A_c \cdot CR \cdot \int_{\lambda_1}^{\lambda_2} SR_{i,(\lambda)} \cdot \eta_{opt,(\lambda)} \cdot G_{(\lambda)} \cdot d\lambda \quad (2)$$

where, SR is the spectral response, η_{opt} is the optical efficiency, G is the incident radiation, A_c is the CPV cell area and λ refer to photon wavelength. The “ i ” subscripts used in the equation represents the sub-cell where the calculation is made. The spectral response is expressed as in Equation 3:

$$SR = \frac{q\lambda}{hc} EQE \quad (3)$$

where, q is the electron charge, h is the Plank's constant, c is the speed of light and EQE indicates the external quantum efficiency In Equation 4, the current-voltage characteristic produced by the solar cell can be found according to the Shockley diode equation [9]:

$$I = I_{ph} - I_0 \left(\exp \frac{q(V + I.R_s)}{n.K_b.T_c} - 1 \right) - \frac{V + I.R_s}{R_{sh}} \quad (4)$$

where, V is the cell voltage, R_s is the series resistance, R_{sh} is the shunt resistance, I_0 is the reverse saturation current and I_{ph} stands for photocurrent. The photocurrent is equal to the short-circuit current under ideal conditions ($I_{ph} = I_{sc}$).

The reverse saturation current as shown in Equation 5 [12]:

$$I_{0,i} = A_c \cdot k \cdot T_c^{(3+\frac{\gamma}{2})} \exp \frac{-E_g}{n.K_b.T_c} \quad (5)$$

where, K_b is the Boltzmann constant, n is the ideality factor, E_g is the energy band gap, T_c is the cell temperature, k and γ refer to the material constants.

The total short-circuit current and open-circuit voltage of the CPV solar cell are expressed as given in Equations 6 and 7:

$$I_{sc,tot} = \min(I_1, I_2, I_3) \quad (6)$$

$$V_{oc,tot} = \sum_{i=1}^3 V_{oc,i} \quad (7)$$

The unknown parameters used in the model are given in Table 1 in detail.

Table 1. Unknown parameters used in the model.			
	GaInP	GaInAs	Ge
n	1	1	1
γ	2	2	2
k (A/cm ² .K ⁴)	1.999E-05	4.958E-07	1.972E-05
R_s (Ω /cm ²)	0.209	0.209	0.209
R_{sh} (Ω /cm ²)	6600	6600	6600

CPV solar cell temperature has an important parameter on solar cell efficiency. It is also a parameter that must be kept under control in order not to damage the cell under high concentration. Therefore, in this study, a finned heat sink was designed for passive cooling and the temperature analysis of the CPV solar cell was numerically modelled using COMSOL Multiphysics software according to the outdoor conditions of Elazig province.

The heat transferred by conduction between the solid components in the receiver can be explained by the Fourier law shown in Equation 8 [10]:

$$q_{cond} = -k.A \frac{dT}{dx} \quad (8)$$

where, q_{cond} is the heat conduction rate (W/m²), k is the thermal conductivity coefficient (W/m.K) and A represents the heat conduction area (m²). Heat transfer by convection from the receiving solid body to the environment is expressed according to Newton's cooling law shown in Equation 9 [10]:

$$q_{conv} = h.A.\Delta T \quad (9)$$

where, h is the convection heat transfer coefficient (W/m².K) and ΔT indicates the temperature difference between the object. Heat transfer, which occurs through radiation, is explained by the Stefan-Boltzmann law as in Equation 10 [10]:

$$q_{rad} = \varepsilon.\sigma.(T_s - T_a^4) \quad (10)$$

where, ε is the emissivity of the surface, σ is the Stefan-Boltzmann constant, T_s and T_a refers to the temperature of the object and the ambient temperature, respectively.

When calculating the mixed (natural and forced) convection heat transfer for outdoor application, the convection heat transfer coefficient can be determined as in Equation 11[13]:

$$h_{mixed} = 15 + 1.5WS \quad (11)$$

where, h_{mixed} represents the mixed heat transfer coefficient and WS is the air speed.

Thermophysical and geometric properties of the components used in the model are given in Table 2.

In this study, a solid oxide electrolyzer (SOE) operating at high temperature (800 °C) was modelled using COMSOL Multiphysics software to evaluate the hydrogen production potential of the collector. The reactions taking place in the SOE anode region, in the cathode region and in total are given in Equation 12, 13 and 14.



Table 1. Thermophysical and geometric properties of the components used in the model.

Component	Thermal Conductivity k (W/m.K)	Specific Heat Capacity C_p (J/g-°C)	Emissivity	Width (mm)	Area (mm ²)
Homogenizer	1.40	0.858	0.84	22	7x7
Silicone Adhesive	0.15	0.7		0.2	7x9
Cell	60	0.32		0.19	7x7
Soldering	65	0.22		0.05	7x9
Top Copper	400	0.385		0.3	25x25
Alumina	24	0.800		0.38	26x26
Bottom Copper	400	0.385		0.3	25x25
Thermal Interface Rubber	3.3	0.83		0.5	30x30
AL base	138	0.880		4	40x40
Oil Compound	0.7	1		0.2	40x40
Heat Sink	200	0.9	0.8	4	200x200

It was modelled as a three-dimension small size (active area= 0.1 cm²) single-cell and single-channel SOE and optimum sizing was carried out according to CPV values. The geometric and physical parameters used in the model are given in Table 3.

Table 2. The geometric and physical parameters used in the model.

Parameters	Value [Unit]	Descriptions
l_c	0.01 [m]	Cell length
w_c	1 [mm]	Cell width
$d_{cathode}$	0.4 [mm]	Cathode thickness
$d_{electrolyte}$	0.03 [mm]	Electrolyte thickness
d_{anode}	0.04 [mm]	Anode thickness
$l_{channel}$	0.01 [m]	Cathode channel length
$w_{channel}$	0.5 [mm]	Cathode channel width
$d_{channel}$	0.5 [mm]	Cathode channel thickness
T	800 [°C]	Cell temperature
$i_{0,c}$	0.1 [A/m ²]	Cathode exchange current density
$i_{0,a}$	1 [A/m ²]	Anode exchange current density
ε	0.4	Porosity
ξ	0.3	Volumetric fraction of ion conductor
$\sigma_{e,cathode}$	$9.5 \cdot 10^7 \exp(-1150/T)/T$ [S/m]	Electronic conductivity, cathode
$\sigma_{e,anode}$	$4.2 \cdot 10^7 \exp(-1200/T)/T$ [S/m]	Electronic conductivity, anode
$\sigma_{i,electrolyte}$	$33.4 \cdot 10^3 \exp(-10300/T)$ [S/m]	Electrolyte conductivity
A_v	10^9 [m ⁻¹]	Volumetric reactive surface area

The layers and isometric view of single-cell and single-channel SOE modelled by COMSOL Multiphysics software are shown in Figure 2.

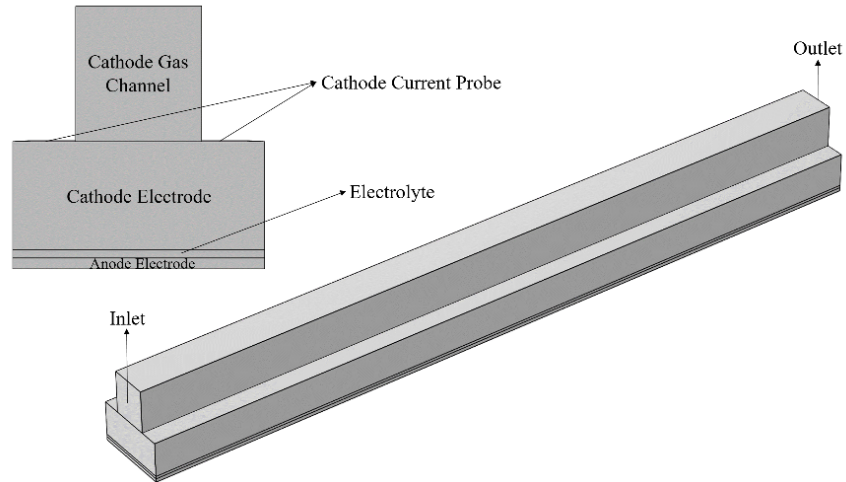


Figure 2. The layers and isometric view of single-cell and single-channel SOE

3. RESULTS AND DISCUSSIONS

For the SBS-CPV/T hybrid collector designed with Zemax Optic Studio, CPV, light guide detector and the total radiated power amount was measured as 31.358 W, 1.145 W and 32.503 W, respectively. CPV and light guide detector images are shown in Figure 3. According to the results obtained, the thermal efficiency of the SBS-CPV/T hybrid collector was 2.86%, while the total optical efficiency was calculated as 81.28%.

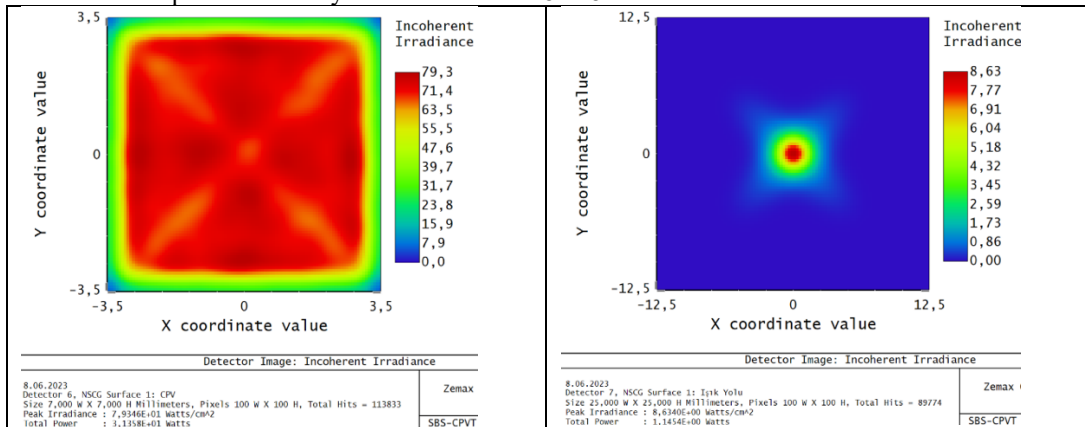


Figure 3. CPV and light guide detector.

For the CPV solar cell with 7x7 mm² active area used in the study, the cell performance was examined under 25 °C, 1000W/m² direct normal irradiation (DNI), the total cell V_{oc} value under 765X concentration was 3.12 V, while the I_{sc} value is calculated as 5.03 A.

The maximum generating power of the total cell was found to be 14.09 W. The electrical energy conversion efficiency value of SBS-CPV/T hybrid collector was calculated as 35.27% as seen in Figure 4.

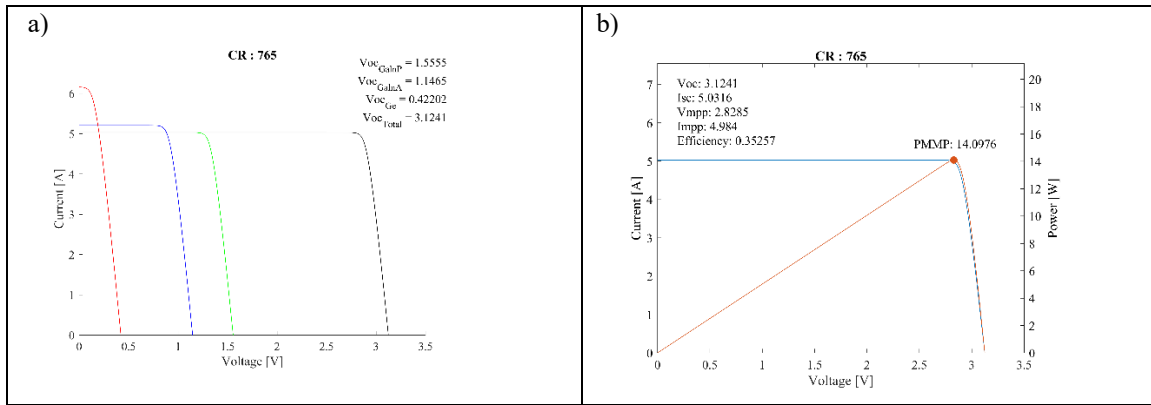


Figure 4. 765X CR and 25 °C temperature a) I-V curves of sub-cells b) I-V and power curves of total cell.

CPV solar cell thermal analysis was carried out according to the climatic conditions of Elazig province. Thermal analysis was carried out for the CPV solar cell using the COMSOL Multiphysics and it was concluded that the cell temperature reached 82 °C in the outdoor weather conditions of Elazig province as seen in Figure 5.

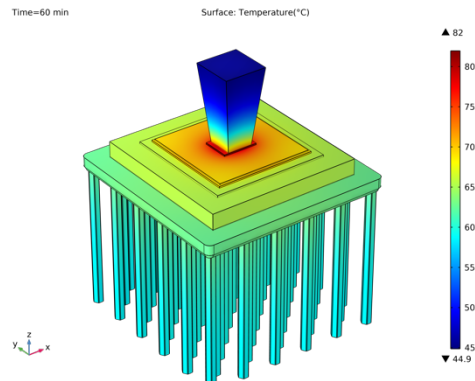


Figure 5. Surface temperatures of the receiver part in outdoor conditions in Elazig province.

The analyzes of the solar cell and SBS-CPV/T hybrid collector were carried out under 1000 W/m² direct irradiation value at 82 °C. While the open circuit voltage of the cell was calculated as 2.763 V under outdoor conditions, the short circuit current was found as 5.391 A. It was concluded that the electrical conversion efficiency of the SBS-CPV/T hybrid collector was 32.39%. The Matlab results are given in Figure 6.

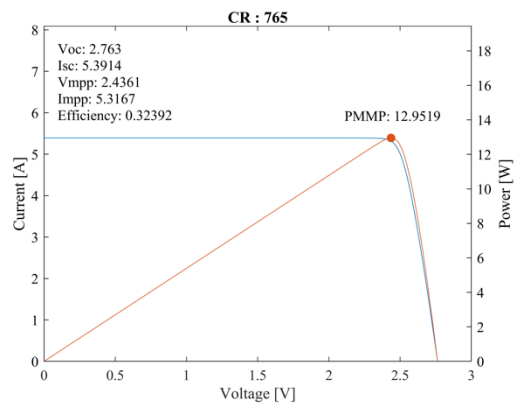


Figure 6. I-V and power curves of total cell at 765 CR and 82 °C.

As seen in Figure 7, cell current values are 1047, 2115, 3752, 8300, 10966 and 13843 A/m², respectively, according to 0.1V intervals and 1V-1.6V potential differences. Since the voltage value is 2.43 V at the maximum power point at 82 °C by the CPV solar cell, the operating voltage for SOE was chosen as 1.2 V and evaluated as 2 cells connected in series in order not to use converter.

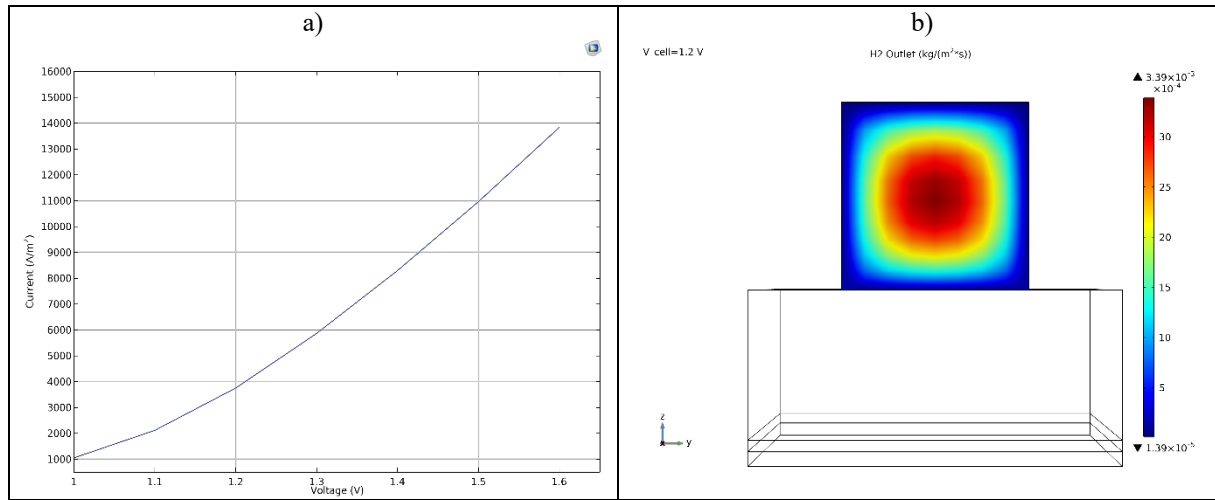


Figure 7. a) I-V curves of SOE cell b) H₂ production by SOE

For SOE electrolyzer, the amount of H₂ production at 1.2 V potential difference was calculated as 3.998×10^{-10} kg/s as seen Figure 7. The electrolyzer efficiency value, which was realized in accordance with Faraday's law, was calculated as 102.81%. Here, it is seen that the efficiency value is above 100%. The reason for this is that the SOE electrolyzer operates at a temperature of 800 °C.

3. CONCLUSION

In this study, a cassegrain type SBS-CPV/T hybrid collector was designed using a multi-junction solar cell with high electrical conversion efficiencies. While the total optical efficiency of the designed hybrid system was calculated as 81.28%, it was observed that the thermal efficiency of the system was 2.86%. The total system electrical conversion efficiency was found to be 32.39% with the CPV solar cell, which was observed to rise to 82 °C in the outdoor conditions of Elazig province. In the case of using SOE operating at high temperatures, the total hydrogen conversion efficiency of the SBS-CPV/T hybrid collector was calculated as 33.3%. According to the results obtained, it has been seen that hydrogen production with SBS-CPV/T hybrid collector is promising between hydrogen production methods by using renewable energy sources.

Acknowledgments: This paper is a part of the PhD. thesis of candidate Cihangir Kale in Firat University, Department of Energy Systems Engineering, Elazig, Turkey. Within the scope of his thesis, we would like to thank the Department of Scientific Support (BİDEB) of TÜBİTAK, which gave Cihangir Kale a scholarship within the scope of priority fields. The authors also would like to thank Rafael Cervantes and BSQ solar company for providing helpful insights and supports for this thesis.

REFERENCES

- [1] M. Wiesenfarth, S.P. Philipps, A.W. Bett, K. Horowitz, S. Kurtz, Current Status Of Concentrator Photovoltaic (CPV) Technology Version 1.3, 2017. <https://www.ise.fraunhofer.de/content/dam/ise/de/documents/publications/studies/cpv-report-ise-nrel.pdf>.
- [2] S.L. Diedenhofen, G. Grzela, E. Haverkamp, G. Bauhuis, J. Schermer, J.G. Rivas, Broadband and omnidirectional anti-reflection layer for III/V multi-junction solar cells, Sol. Energy Mater. Sol. Cells. 101 (2012) 308–314. <https://doi.org/10.1016/J.SOLMAT.2012.02.022>.
- [3] P.M. Kaminski, F. Lisco, J.M. Walls, Multilayer broadband antireflective coatings for more efficient thin film CdTe solar cells, IEEE J. Photovoltaics. 4 (2014) 452–456. <https://doi.org/10.1109/JPHOTOV.2013.2284064>.
- [4] A. Bajju, M. Yarema, Status and challenges of multi-junction solar cell technology, Front. Energy Res. 10

- (2022) 1453. <https://doi.org/10.3389/FENRG.2022.971918/BIBTEX>.
- [5] A. Kribus, D. Kaftori, G. Mittelman, A. Hirshfeld, Y. Flitsanov, A. Dayan, A miniature concentrating photovoltaic and thermal system, *Energy Convers. Manag.* 47 (2006) 3582–3590. <https://doi.org/10.1016/J.ENCONMAN.2006.01.013>.
- [6] N. Ahmad, K. Hatakeyama, Y. Ota, K. Nishioka, Designing of long wavelength cut thin film filter for temperature reduction of concentrator photovoltaic, *MATEC Web Conf.* 65 (2016) 1–4. <https://doi.org/10.1051/mateconf/20166504002>.
- [7] S. Bernardes, R.A. Marques Lameirinhas, J.P.N. Torres, C.A.F. Fernandes, Characterization and design of photovoltaic solar cells that absorb ultraviolet, visible and infrared light, *Nanomaterials.* 11 (2021) 1–16. <https://doi.org/10.3390/nano11010078>.
- [8] X. Ju, C. Xu, Z. Liao, X. Du, G. Wei, Z. Wang, Y. Yang, A review of concentrated photovoltaic-thermal (CPVT) hybrid solar systems with waste heat recovery (WHR), *Sci. Bull.* 62 (2017) 1388–1426. <https://doi.org/10.1016/j.scib.2017.10.002>.
- [9] G. Segev, G. Mittelman, A. Kribus, Equivalent circuit models for triple-junction concentrator solar cells, *Sol. Energy Mater. Sol. Cells.* 98 (2012) 57–65. <https://doi.org/10.1016/J.SOLMAT.2011.10.013>.
- [10] M. Theristis, T.S. O’Donovan, Electrical-thermal analysis of III–V triple-junction solar cells under variable spectra and ambient temperatures, *Sol. Energy.* 118 (2015) 533–546. <https://doi.org/10.1016/J.SOLENER.2015.06.003>.
- [11] G. Peharz, G. Siefer, A.W. Bett, A simple method for quantifying spectral impacts on multi-junction solar cells, *Sol. Energy.* 83 (2009) 1588–1598. <https://doi.org/10.1016/J.SOLENER.2009.05.009>.
- [12] M.A. Steiner, J.F. Geisz, D.J. Friedman, W.J. Olavarria, A. Duda, T.E. Moriarty, Temperature-dependent measurements of an inverted metamorphic multijunction (IMM) solar cell, *Conf. Rec. IEEE Photovolt. Spec. Conf.* (2011) 002527–002532. <https://doi.org/10.1109/PVSC.2011.6186461>.
- [13] M. Theristis, Development of a spectral dependent electrical & thermal model for High Concentrating Photovoltaic (HCPV) receivers, Heriot-Watt University, 2016.

INVESTIGATION OF THE EFFICIENCY OF DSSC FOR SAFFRON EXTRACT

Fehmi ASLAN¹

¹Rail Systems Machinery Technology, Yeşilyurt Vocational School, Turgut Özal University, Malatya, Turkey

ABSTRACT

This study used the soxhlet method to extract the saffron dye. TiO₂ nanoparticles were produced by hydrothermal method. The XRD peaks of the synthesized particles confirmed the mineralogical structure. Surface photographs of TiO₂ were examined with SEM images. These images showed microsphere structures in close contact with each other. When the UV analyses of the saffron dye were examined, remarkable absorption behaviors were detected in the visible region. When the photovoltaic parameters of the produced dye-sensitized solar cell were examined, the photoelectric conversion efficiency (η), open circuit voltage (V_{oc}), short circuit current (J_{sc}) and filling factor (FF) were found to be 0.007, 0.2 V, 0.081 mA/cm² and 0.46, respectively.

Keywords: Solar cell, organic dye, photovoltaic.

1. INTRODUCTION

The high costs and environmental risks of silicon-based solar cells have focused research on alternative cell studies. Ease of manufacture, relatively low cost, dye-sensitized solar cells (DSSC) have come to the fore in terms of technology [1]. DSSCs were first produced by Grazel et al using TiO₂-based photoanodes. Efficiency values of approximately 7% have been reached in the experiments performed in the laboratory environment [2]. In subsequent studies on DSSCs, efficiency values were improved by up to 15%. Efficiencies of up to 15% hold hope for the commercialization of DSSCs. DSSCs consist of a porous nanocrystalline TiO₂-coated glass electrode, TiO₂ surface sensitized with dye molecules, redox electrolyte, and counter electrode [3].

It is known that some natural dyes obtained from plants exhibit high absorption in the visible and near-infrared regions (NIR). These dyes can significantly affect the performance of DSSCs. The highest efficiency values in DSSCs were generally observed when ruthenium (Ru) based dyes were used. But Ru-based dyes are both costly and not recyclable. These undesirable reasons for Ru-based dyes have shifted studies on DSSCs to natural paints that are both cheap and environmentally friendly [4,5]. Saffron is a member of the Iridaceae family. It is sessile and has an onion. Dried style or stigmas contain many chemicals. These include crocin, which belongs to a natural group of carotenoids. Its color is dark red and is responsible for the color [6]. The presence of crocin in saffron gives it the potential to be a sensitizer in DSSC [7]. This study investigated how the saffron dye obtained using the Soxhlet method affects the performance of DSSC.

2. METHODOLOGY

2.1. Materials

The procured materials were used without further purification. Titanium IV isopropoxide (TTIP, $\geq 97.0\%$, Sigma-Aldrich), ethyl alcohol ($\geq 99.5\%$, Sigma-Aldrich) and Urea (Chemsolid) were used for the synthesis of nanoparticles. Ethyl cellulose (Sigma-Aldrich) and alpha-terpinol (Sigma-Aldrich) were used as binders in TiO₂ paste production. Fluorine doped tin oxide coated glass (FTO, surface resistivity about 13 Ω /sq), Iodolyte AN-50 (Solaronix) and Platinum (Solaronix) were used as conductive glass, electrolyte solution and counter electrode.

2.2. Production of Titanium Dioxide (TiO₂) nanoparticles

TiO₂ nanoparticles were prepared by hydrothermal method. 40 ml of deionized water and 1.6 g of urea were mixed for 1 hour until a homogeneous structure was formed. While the mixing process was continuing, 3.5 ml of TTIP was added dropwise and mixed for another half hour. The resulting solution was ultrasonically treated for half an hour and then placed in a hydrothermal device with Teflon autoclave integrated for 24 hours at 120 °C. After the Teflon autoclave was cooled to room temperature, the collected particles were washed several times with deionized water and alcohol to remove unwanted residues. These particles were dried in an oven at 50 °C for 12 hours and then calcined in a muffle furnace at 450 °C. The resulting TiO₂ particles were pounded in a mortar and made ready for cake making.

2.3. Production of dye

The Soxhlet method was used to obtain dye extracts from previously collected and dried saffron onion rings. 10 g of dried saffron was placed in the extraction cartridge and then dye extraction was obtained by siphoning 3 times in ethyl alcohol environment. The dyes produced and their dried forms are shown in Fig. 1.

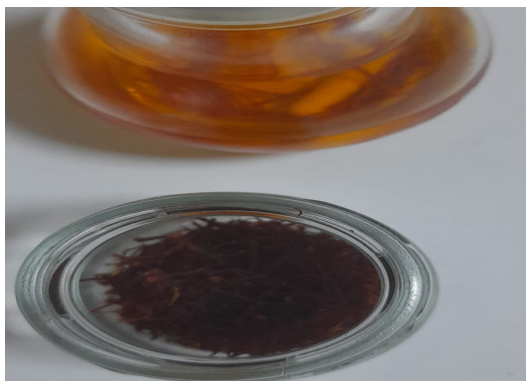


Figure 1. Saffron dye and dry form of the plant.

2.4. Preparation of dye-sensitized solar cell (DSSC)

For the production of cake, 1 gram TiO_2 , 0.45 gram ethyl cellulose and 3 ml terpinol were mixed in a mortar until the appropriate paste consistency was achieved. The prepared pastes were covered with a doctor-blade technique on the conductive surface of the FTO with the help of a mask. The produced photoanode was calcined at $450\text{ }^\circ\text{C}$ for 45 minutes. After the photoanode was cooled at room temperature, it was placed in the dye obtained from the saffron plant and kept in a dark environment for 24 hours. The dye-immersed state of the photoanode is given in Fig. 2. The photoanode, which absorbed the dye, was washed several times with alcohol and quickly dried. A few drops of electrolyte solution were dropped on the part where TiO_2 was located on the photoanode layer and combined with the Pt counter electrode. After this procedure, a sample was placed in the holder for DSSC measurement.



Figure 2. Photoanode layer dipped saffron dye.

3. DISCUSSION AND RESULTS

In this study, the crystal phases of TiO_2 were investigated by XRD analysis. It has been observed that the values of the peaks and the angles are compatible with each other. XRD analyzes confirmed the peaks of anatase TiO_2 . XRD analyzes of the produced TiO_2 nanoparticles are given in Fig. 3.

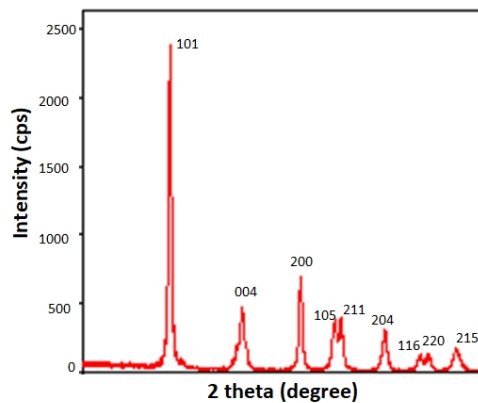


Figure 3. XRD peaks of TiO₂.

The surface images of the produced TiO₂ were examined by SEM analysis. As can be seen from the images, the presence of spherical structures in close contact with each other has been detected. It is known that such a structure improves electron transport. SEM photographs of the produced TiO₂ nanoparticles are given in Fig. 4.

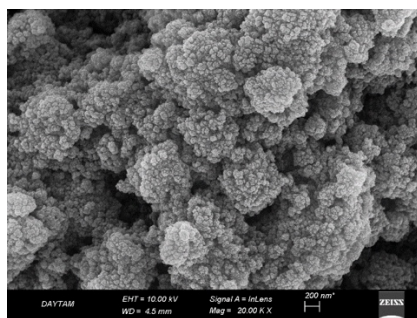


Figure 4. SEM image of TiO₂ powders.

The UV-vis analyzes of the dye extracted from the saffron plant are shown in Fig. 5. From the analysis, it was understood that the saffron dye exhibits high absorption at wavelengths of 400-500 nm. High absorptions in the visible region play an important role in improving the performance of DSSCs.

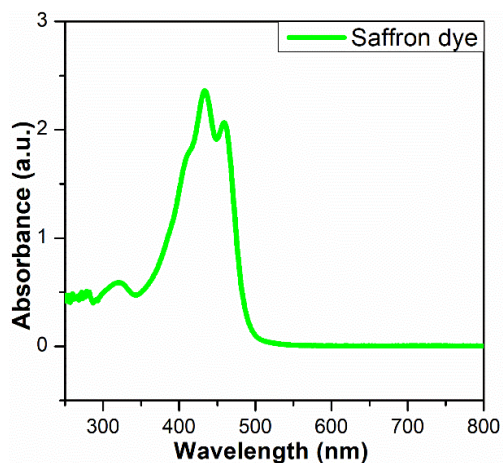


Figure 5. Absorption curves of the extracted dye.

Table 1. Photovoltaic parameters of DSSC.

Sample	J _{sc} (mAcm ⁻²)	V _{oc} (V)	FF	η (%)
DSSC sensitized with saffron dye	0.083	0.20	0.46	0.007

Electrical parameter measurements of the previously prepared DSSC have performed with the LSS 9000 Fytronix Solar Simulator device under 100 mW/cm^2 light intensity (AM1.5G). Fig. 6 shows the J_{sc} -V curves of saffron dye sensitized DSSC. The obtained photovoltaic parameters are summarized in Table 1. According to this table, the filling factor (FF), Open circuit voltage (V_{oc}), short circuit current density (J_{sc}) and efficiency (η) of DSSC were found to be 0.46, 0.20 V, 0.083 mA/cm^2 and 0.007, respectively. Although these values are meaningful for DSSCs produced with many organic dye derivatives, higher performance solar cells can be produced by improving the V_{oc} and J_{sc} values.

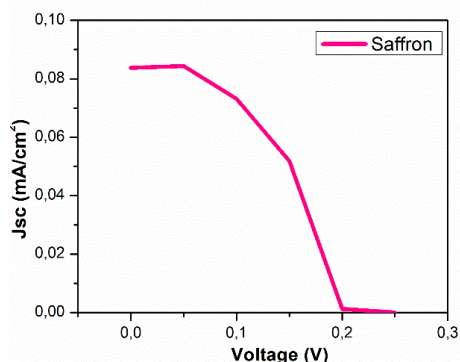


Figure 6. J_{sc} -V curves of the produced DSSC.

3. CONCLUSION

In this study, the soxhlet method was used to extract the dye from the saffron plant. TiO_2 nanopowders were produced by hydrothermal method. XRD analyzes confirmed the mineralogical analysis of anatase TiO_2 . SEM images showed microsphere structures in close contact with each other. It was determined by UV-vis analysis that saffron dye exhibited remarkable absorption behavior in the visible region. It was concluded that the J_{sc} and V_{oc} values of the produced DSSC were significant for organic dyes.

REFERENCES

- [1] M.L. Parisi, S. Maranghi, R. Basosi, The evolution of the dye sensitized solar cells from Grätzel prototype to up-scaled solar applications: A life cycle assessment approach, *Renewable and Sustainable Energy Reviews*. 39 (2014) 124–138. <https://doi.org/10.1016/j.rser.2014.07.079>.
- [2] H. Li, B. Zheng, Y. Xue, S. Liu, C. Gao, X. Liu, Spray deposited lanthanum doped TiO_2 compact layers as electron selective contact for perovskite solar cells, *Solar Energy Materials and Solar Cells*. 168 (2017) 85–90. <https://doi.org/10.1016/j.solmat.2017.04.027>.
- [3] A.K. Arof, N.A. Mat Nor, N.R. Ramli, N. Aziz, I.M. Noor, R.M. Taha, Utilization of saffron (*Crocus sativus* L.) as sensitizer in dye-sensitized solar cells (DSSCs), *Optical and Quantum Electronics*. 49 (2017) 1–8. <https://doi.org/10.1007/s11082-016-0882-6>.
- [4] N.A. Ludin, A.M. Al-Alwani Mahmoud, A. Bakar Mohamad, A.A.H. Kadhum, K. Sopian, N.S. Abdul Karim, Review on the development of natural dye photosensitizer for dye-sensitized solar cells, *Renewable and Sustainable Energy Reviews*. 31 (2014) 386–396. <https://doi.org/10.1016/j.rser.2013.12.001>.
- [5] S. Shalini, R. Balasundara Prabhu, S. Prasanna, T.K. Mallick, S. Senthilarasu, Review on natural dye sensitized solar cells: Operation, materials and methods, *Renewable and Sustainable Energy Reviews*. 51 (2015) 1306–1325. <https://doi.org/10.1016/j.rser.2015.07.052>.
- [6] Y.K. Syu, Y. Tingare, S.Y. Lin, C.Y. Yeh, J.J. Wu, Porphyrin dye-sensitized zinc oxide aggregated anodes for use in solar cells, *Molecules*. 21 (2016). <https://doi.org/10.3390/molecules21081025>.
- [7] M. Grätzel, Solar energy conversion by dye-sensitized photovoltaic cells, *Inorganic Chemistry*. 44 (2005) 6841–6851. <https://doi.org/10.1021/ic0508371>.

MATHEMATICAL MODELLING OF THE INFORMATIVE FEATURE CHOICE FOR LIFECYCLE STATE ANALYSIS OF RADIO-ELECTRONIC MEANS PROCESSES

VICTORIA NEVLYUDOVA, NIKOLAY STARODUBTSEV

Department of Computer Integrated Technologies, Automation and Mechatronics, Faculty of Automation and Computerized Technologies, Kharkiv National University of Radio Electronics, Kharkiv, Ukraine

ABSTRACT

The solution of problems of mathematical modeling of efficiency functions of radio electronic means life cycle processes (REM LC) and selection of informative attributes for REM LC monitoring, by classification of REM states and life cycle processes in attribute space, each of which has a certain significance, that allowed to find a complex criterion and to formalize selection procedures, is given. The cases of insufficient amount of a priori data for correct classification are considered; heuristic methods of selection according to criteria of basic prototypes and information priorities are proposed.

Keywords: informative features, identification of REM states, life cycle monitoring.

1. INTRODUCTION

A distinctive feature of radio electronic means (REMs) is the presence of a large number of monitored parameters. Monitoring, which provides the ability to measure and record the values and rates of change of REM parameters, may have the additional capability to provide insight into the state of the REM under a multitude of parameters as a statistical ensemble. In science the technique is known when the description of behaviour of a micro ensemble of particle parameters gives the possibility to define macro parameters of systems, consisting of them, to create the phenomenological theory and to use for estimation and control of such systems' state. A physical medium consisting of atoms and molecules is an example, microparameters here are coordinates and impulses of these particles, phenomenological theory is thermodynamics, macroparameters are volume, pressure, temperature etc. The observation, in the field of view of which the phase plane on which one can observe decay and mixing of statistical ensemble of REM parameters, gives additional possibilities for monitoring of life cycle of radio electronic means (LC REM). The functional problem of selecting informative features for LC REM monitoring, as well as reducing their list, and reducing uncertainty can be solved within the methodology of developing a dictionary of features in systems of classification and recognition of the state of objects [1-3]. Here, the goal of selection is to provide optimal recognition.

2. STUDY PROBLEM STATEMENT

In a working dictionary, only the attributes that are, on the one hand, most informative and, on the other hand, affordable (e.g. in terms of costs) for measurement should be used. The definition of a feature dictionary in the context of constraints on the cost of observational hardware has peculiarities.

If the attributes of objects are denoted by δ_j , $j = 1, 2, \dots, N$, then each object in the N -dimensional feature space can be represented as a vector $x = (x_1, x_2, \dots, x_N)$, with coordinates characterizing the properties of objects.

The metrics for the determination of a measure of proximity or similarity of objects in the N -dimensional feature vector space are introduced. It is possible to use the Euclidean metric

$$d^2(w_{pk}, w_{ql}) = \sum_{j=1}^N (x_{pk}^j - x_{ql}^j)^2, \quad (1)$$

$$p, q = 1, 2, \dots, m; \quad k = 1, 2, \dots, k_p; \quad l = 1, 2, \dots, k_q,$$

where x_{pk}^j are the values of the j -th attribute of the k -th object of the p -th class, i.e. object of the q -th class, i.e. object w_{ql} .

As a measure of proximity between objects of a given class Ω_p , $p = 1, 2, \dots, m$, we will use the value

$$S(\Omega_p) = \sqrt{\frac{2}{k_p} \frac{1}{k_{p-1}} \sum_{k=1}^{k_p} \sum_{l=1}^{k_p} d^2(w_{pk}, w_{pl})}, \quad (2)$$

which has the meaning of root mean square scatter of the class or mean square dispersion of objects within the class Ω_p , as a measure of proximity between objects of a given pair of classes Ω_p and Ω_q , $p, q = 1, \dots, m$, the value

$$R(\Omega_p, \Omega_q) = \sqrt{\frac{1}{k_p k_q} \sum_{k=1}^{k_p} \sum_{l=1}^{k_q} d^2(w_{pk}, w_{ql})}, \quad (3)$$

which has the meaning of the root mean square scatter of objects of classes Ω_p and Ω_q .

The set of features of the objects used in the working dictionary can be described by an N -dimensional vector $A = (\alpha_1, \alpha_2, \dots, \alpha_N)$ the components of which take values 1 or 0, depending on whether the corresponding feature of the object is available or not.

Taking into account the α square of the distance between the two objects w_{pk} and w_{ql}

$$d^2(w_{pk}, w_{ql}) = \sum_{j=1}^N \alpha_j (x^{(j)}_{pk} - x^{(j)}_{ql})^2. \quad (4)$$

Consequently, root mean square scatter of Ω_p class and objects of the classes Ω_p and Ω_q can be written as

$$S(\Omega_p) = \sqrt{\frac{2}{k_p} \frac{1}{k_{p-1}} \sum_{k=1}^{k_p} \sum_{l=1}^{k_p} \sum_{j=1}^N \alpha_j (x^{(j)}_{pk} - x^{(j)}_{pl})^2}, \quad (5)$$

$$R(\Omega_p, \Omega_q) = \sqrt{\frac{1}{k_p k_q} \sum_{k=1}^{k_p} \sum_{l=1}^{k_q} \sum_{j=1}^N \alpha_j (x^{(j)}_{pk} - x^{(j)}_{ql})^2}. \quad (6)$$

It can be assumed that the cost of using a feature is proportional to its informativeness, i.e. the number of features of the objects that can be identified using it. This assumption (leaving aside the issue of the accuracy of the observing instruments) is quite general.

Thus, the costs of using the features

$$C = C(\alpha_1, \dots, \alpha_N) = \sum_{j=1}^N C_j \alpha_j, \quad (7)$$

where C_j are the costs of determining the j -th feature.

As an indicator of the quality or efficiency of the designed recognition system we consider a functional, which in general depends on the function $S(\Omega_p)$, $R(\Omega_p, \Omega_q)$ of the decisive rule $L(w, \{w_g\})$

$$I = F[S(\Omega_p); R(\Omega_p, \Omega_q); L(w, \{w_g\})]. \quad (8)$$

Let the value $L(w, \{w_g\})$ be a measure of proximity between a recognizable object w and a class Ω_g , $g = 1, 2, \dots, m$, given by its objects $\{w_g\}$. As this proximity measure, consider the quantity

$$L(w, \{w_g\}) = \sqrt{\frac{1}{k_g} \sum_{g=1}^{k_g} d^2(w, w_g)}, \quad (9)$$

which is the root mean square distance between the object w and the objects of the class Ω_p .

The decisive rule is as follows $w \in \Omega_g$, if

$$L(w, \{w_g\}) = \text{extr } L(w, \{w_i\}). \quad (10)$$

It is important to note that decreasing the value $S(\Omega_p)$, "shrinking" the objects belonging to each given class, while increasing $R(\Omega_p, \Omega_q)$, i.e. "diluting" the objects belonging to different classes provides, ultimately, an improvement in the quality of the recognition system. Therefore, improving the performance of the system will be associated with the achievement of the extremum of the functional I .

The statement of the research problem can be formulated as follows.

Let the set of objects is subdivided into classes $\Omega_i, i=1, \dots, m$, all classes are a priori described in the language of attributes $x_j, j=1, \dots, N$, and funds are allocated to create technical means of observation, the value of which is equal to C_0 . It is required, not exceeding the allocated amount of money, to construct a working dictionary of features, which provides the highest possible efficiency of the system.

Thus, the problem is reduced to the finding of conditional extremum of the functional of the form (8), i.e. to the definition of A implementing $\text{extr}_\alpha I = \text{extr}_\alpha F [S(\Omega_p); R(\Omega_p, \Omega_q); L(w, \{w_g\})]$

$$C = \sum_{j=1}^N C_j \alpha_j \leq C_0. \quad (11)$$

Possible types of the functional. Let us consider some particular kinds of functional (11). If the required efficiency of the recognition system can be achieved by a more compact arrangement of objects of each class under some conditions with respect to the value of $R(\Omega_p, \Omega_q)$, then the problem is reduced to finding

$$\min_\alpha \max_{i=1, \dots, m} [S(\Omega_i)] \quad (12)$$

at

$$\sum_{j=1}^N C_j \alpha_j \leq C_0 \text{ and } R(\Omega_p, \Omega_q) \geq R_0^{(pq)}. \quad (13)$$

If the required system efficiency can be achieved by "removing" objects belonging to different classes from each other, subject to certain conditions regarding the value of $S(\Omega_i), i=1, \dots, m$, then the problem is reduced to finding

$$\max_\alpha \min_{p, q=1, \dots, m} [R(\Omega_p, \Omega_q)] \quad (14)$$

at

$$\sum_{j=1}^N C_j \alpha_j \leq C_0 \text{ and } S(\Omega_i) \leq S_0^i. \quad (15)$$

If the proper efficiency of the system can only be achieved by increasing the ratio of distances between classes to the rms scatter of objects within the classes, then the problem is reduced to finding

$$\max_\alpha \min_{p, q=1, \dots, m} \left[\frac{R^2(\Omega_p, \Omega_q)}{S(\Omega_p)S(\Omega_q)} \right] \quad (16)$$

at

$$\sum_{j=1}^N C_j \alpha_j \leq C_0. \quad (17)$$

3. SOLVING THE PROBLEM OF SELECTING INFORMATIVE ATTRIBUTES CHARACTERISING THE STATE OF THE LC REM PROCESSES

The problem considered above is a generalization of the nonlinear programming problem. The optimality conditions for it can be formulated as follows: for vector C^0 to be an optimal strategy, it is necessary that there exist a scalar $\beta \geq 0$ and a vector $\mu = \{\mu_1, \dots, \mu_n\}$ such that

$$\left. \begin{aligned} \left[\sum_{r=1}^n \mu_r \rho_r^j \right] \frac{dP_j(C_j^0)}{dC_j} &= \beta, \quad j = 1, \dots, N_p; \\ \sum_{j=1}^{N_p} C_j^0 &= C_0; \\ \sum_{r=1}^n \mu_r &= 1, \mu_r = 0, \text{ if } \mu = \{\mu_1, \dots, \mu_n\} \sum_{j=1}^{N_p} \rho_r^j P_j(C_j^0) > W(C^0). \end{aligned} \right\} \quad (18)$$

The introduction of a scalar β and a vector μ increases the number of unknowns C_j^0 , μ_r and β to the value $N_p + n + 1$. However, the number of equations equals the number of unknowns, since for any r either $\mu_r = 0$, or

$$\sum_{j=1}^{N_p} \rho_r^j P_j(C_j^0) = W(C^0). \quad (19)$$

Thus, the solution of the system of equations (18) makes it possible to determine the composition of the features of the working dictionary and the optimal allocation of the costs of the observational means of the recognition system, under the assumption of dependency $P_j = P_j(C_j)$ and limitations on the total cost of these means.

With the constraints of being able to use the entire feature vocabulary, the task arises of selecting a limited list (up to 2-3 features). Here we can focus on the location of individual components of the feature vector with respect to the boundaries of the serviceability area of the monitoring objects.

Since at the boundary value of the parameter y_{bd}^j , the end of the vector X must be located at the boundary of the serviceability area, the following equation must be fulfilled

$$x_{zp}^i = a_{ij}^i y_{bd}^j. \quad (20)$$

In statistical estimation, an additional criterion for selection can be the correlation coefficient r_{ij} between the parameters. As the maximum correlation coefficient provides the maximum amount of information

$$J(y^j) = H(y^i) - H\left(\frac{y^j}{y^i}\right), \quad (21)$$

contained in the parameter y^i . Here $H(y^i)$ – initial entropy; $H\left(\frac{y^j}{y^i}\right)$ – conditional entropy of the object after measurement of the parameter y^i .

The use of binary correlation algorithms makes it possible to formalise and automate the input, processing and recognition of the resulting image with the participation of the decision maker (DM).

4. IDENTIFICATION OF LC REM PROCESSES STATUS

Identification of LC REM implies the existence of rules defining the states of the REM. The attributes to distinguish the states of the monitored object are the performance indicators, which for the allocated state will have a given or extreme value. In order to identify REM states in the monitoring process, it is necessary to check whether the observed parameters are those that provide performance criteria, whether they belong to the set on which the value of performance indicators will have set or extreme values. Functional analysis methods can be used to solve state estimation problems [4, 5].

Objects of observation are REM parameters and characteristics can be considered as points of vector and function spaces. For all possible pairs of points on the set Q , there exists a binary relation of comparative efficiency: a point x is

more efficient than y if and only if $(x, y \in \Phi)$ or in another notation $x \Phi y$. In providing LC REM, the problem of selecting the kernel, the set of maximal elements from X by the binary relation $\Phi : X^* = \text{Max}(Q, \Phi)$. It is assumed that a solution to the problem exists, i.e. the set X^* is not empty. In many problems, it can be assumed that the solution - the set X^* - consists of a single element, and the relationship between the elements is established using functionals $\Lambda(x)$. For example, a point x is more efficient than y when $\Lambda(x) < \Lambda(y)$ or $\Lambda(x) > \Lambda(y)$. It can be shown that in the problems of determining effective points $x_0 \in X^*$ in the presence of constraints $x \in Q_1$, the functional $f = \lambda \Lambda'(x_0)$, where $\Lambda'(x_0)$ is the Frechette derivative at the point x_0 , is a reference functional to Q_1 , at the point x_0 (i.e. $(f, x_0) < (f, x)$ for all $x \in Q_1$).

Thus, the task of analysing the observation results during monitoring comes down to determining the reference functionals at the observation points, which makes it possible to assess the deviation of the observed points from the effective ones.

In terms of functional analysis: let Q be a set in a linear topological space E , E' - a conjugate space, $x_0 \in Q$ - an outermost point of Q , K_b - a cone of possible directions in Q at the point x_0 , K_k - a cone of tangent directions for Q at x_0 . If the set of linear functionals supported to Q at the point x_0 denote by Q^* , then $Q^* = \{f \in E', f(x) \geq f(x_0)\}$ for all $x \in Q$, i.e., the support functional and the boundary point $x_0 \in Q$ allow us to distinguish the set Q . It can be shown that if Q is a closed convex set, then $Q^* = K_k^*$, i.e. forms cones formed by the set of linear functionals supported by Q at x_0 . The cone of tangent directions can be defined by the Frechette derivatives of the operators (convex functions) that bind the sets of parameters and performance measures.

Let us consider methods of finding K^* for ways of setting K with different functionals.

Variant 1: For a cone of decreasing directions K_0 . A functional $\Lambda(x)$ in linear space E has a derivative $\Lambda'(x_0, g)$ at a point x_0 in the direction g , i.e. there exists

$$\lim_{\varepsilon \rightarrow +0} \frac{\Lambda(x_0 + \varepsilon g) - \Lambda(x_0)}{\varepsilon} = f(x_0, g). \quad (22)$$

$\Lambda(x)$ satisfies the Lipschitz condition in the region x_0 (for a certain $\varepsilon_0 > 0$ it will be $|\Lambda(x_1) - \Lambda(x_2)| \leq \beta \|x_1 - x_2\|$ at all $\|x_1 - x_0\| \leq \varepsilon_0$, $\|x_2 - x_0\| \leq \varepsilon_0$) and $\Lambda'(x_0, g) < 0$, then $\Lambda(x)$ - properly descending in x_0 , and

$$K = \{g : \Lambda'(x_0, g) < 0\}.$$

Variant 2. For a cone of possible directions. In the case of a set which is not defined by a functional. If Q is a convex set, then the set of decreasing directions K_b at a point x_0 has the form

$$K_b = \{\lambda(Q - x_0), \lambda > 0\},$$

(i.e. $K_b = \{g : g = \lambda(x - x_0), x \in Q, \lambda > 0\}$).

Variant 3. For a cone of possible directions. In the case of definition Q by means of affine sets: $E = E_1 \times E_2$, E_1, E_2 are linear topological spaces, the set of efficiency features is defined in E_2 , D is a linear operator from E_1 to E_2 ,

$K = \{x \in E, x = (x_1, x_2) : Dx_1 = x_2\}$, $K^* = \{f \in E', f = (f_1, f_2) : f_1 = -D^* f_2\}$, and as a reference separating function one can use

$$f(x) = (-D^* f_2, x_1) + (f_2, x_2) = -(f_2, D^* x_1 - x_2).$$

The application of this function to partition the sets in the parameter space and to formulate rules that establish a correspondence between the parameter sets and the values of the performance indicators can provide state identification in the LC REM monitoring process.

Variant 4. For a cone of tangent directions. $P(x)$ - operator from E_1 to E_2 , differentiable in the neighborhood of a point x_0 , $P'(x)$ is continuous in the neighborhood of x_0 , and $P'(x_0)$ maps E_1 to all E_2 (i.e. a linear equation

$P'(x_0)g = b$ has a solution g for every $b \in E_2$, the set of tangent directions K to the set $Q = \{x : P(x) = 0\}$ at a point x_0 is a subspace $K = \{g : P'(x_0)g = 0\}$.

Variation 5. For a tangent direction cone is a typical case. Let $x \in R^m$, $Q = \{x : G_i(x) = 0, i = 1, \dots, n\}$, where $G_i(x)$ – functions continuously differentiable in the vicinity of a point x_0 , $G_i(x_0) = 0, i = 1, \dots, n$, and vectors $G_i'(x_0)$, are linearly independent. Then $K = \{g \in R^m : (G_i'(x_0), g) = 0, i = 1, \dots, n\}$. Here $E_1 = R^m, E_2 = R^n, P(x) = (C_1(x), \dots, G_n(x))$, $P'(x_0)$ is a matrix $m \times n$, the i -th column of which is equal to $G_i'(x_0)$.

Variation 6. In the process of monitoring, it is necessary to determine whether the effective value of the function characteristic REM $w(z)$, in the simplest case the extreme value of the differentiable target function of one variable, is ensured by checking whether the derivative is equal to zero at the observed value of the parameter. For multivariate target functions and their arguments, this problem can be considered within the framework of set theory and functional analysis.

The formalization in the problem of optimal tuning observation, as one of the LC REM processes, is that it is necessary to evaluate the optimality of the tuning process function $v(z) \in M$ where z is the parameter defining the numerical value of the required characteristic $w(z)$ of the tuning object to provide such a phase trajectory which provides equality

$w(0) = c, w(Z) = d$, and the extremal value of the integral functional $\int_0^Z \Phi(w(z), v(z), z) dz$, in the presence of the

relation given by the differential equation $\frac{dw(z)}{dz} = \varphi(w(z), v(z), z)$.

In problems requiring a maximum fit between the optimised characteristic and some desired one, the criterion of minimum standard deviation is used

$$W_2(X) = \overline{(Y(X) - Y^*)^2}, \quad (23)$$

where Y^* – the desired or required specification value of the characteristic.

For a characteristic defined by a discrete set of points, the target function

$$W_2(X) = \frac{1}{N} \sum_{i=1}^N \gamma_i (Y(X, p_i) - Y_i^*)^2, \quad (24)$$

where N – number of sampling points of the independent variable p ;

$Y(X, p_i)$ – value of the optimised characteristic at the i -th point of the sampling interval;

γ_i – the weighting coefficient of the i -th value of the optimised characteristic, reflecting the importance of the i -th point compared to the others (as a rule, $0 < \gamma_i < 1$).

In some optimization problems, it is necessary to ensure that the characteristic to be optimized does or does not exceed some given level. These optimality criteria are implemented by the following functions:

- to ensure that a given level is exceeded

$$W_3(X) = \begin{cases} 0 & \text{at } Y(X) \geq Y_L^*, \\ (Y - Y(X))^2 & \text{at } Y(X) < Y_L^*; \end{cases} \quad (25)$$

- to ensure that the set level is not exceeded

$$W_4(X) = \begin{cases} 0 & \text{at } Y(X) \leq Y_U^*, \\ (Y(X) - Y_U^*)^2 & \text{at } Y(X) > Y_U^*, \end{cases} \quad (26)$$

where Y_L^*, Y_U^* – lower and upper limits of the permissible area for the characteristic $Y(X)$.

If it is necessary that the characteristic to be optimised lies within a tolerance zone (corridor), a combination of the two previous optimality criteria is used

$$W(X) = \begin{cases} 0 & \text{at } Y_L^* \leq Y(X) \leq Y_U^*, \\ (Y(X) - Y_U^*)^2 & \text{at } Y(X) > Y_U^*, \\ (Y_L^* - Y(X))^2 & \text{at } Y(X) < Y_L^*. \end{cases} \quad (27)$$

Where only the shape of the curve needs to be realised, while ignoring the constant vertical displacement, the shift criterion is used

$$W_6(X) = \sum_{i=1}^N \gamma_i (Y_i^* - Y(X, p_i) - Y_{av})^2, \quad (28)$$

where $Y_{av} = \frac{1}{N} \sum_{i=1}^N (Y_i^* - Y(X, p_i))$.

Important characteristics of the computational process and, first of all, the convergence of the optimization process depend on the type of the target function. Signs of target function's derivatives on controllable parameters do not remain constant in the whole admissible domain, the latter circumstance leads to their ravine character (e.g. circuit design problems), which leads to high computational costs and requires special attention to the choice of optimization method. Another peculiarity of the target functions is that they are usually multi-extreme and along with the global minimum there are local minima.

Multicriteria optimization problems constitute the general class of problems of identification of the set of efficient solutions. They are characterized by the fact that a binary relation on the set of alternatives from which a choice is to be made is connected with a set of indices - criteria forming a vector efficiency criterion. This binary relation can be generated in various ways. Thus, if

$$W(x) = (W^1(x), \dots, W^m(x)) \quad (29)$$

vector criterion on set X , then the binary relation may be a Pareto relation or a Slater relation. In other cases, the binary relation on X is given by the DM preference system. It is assumed that the primary source of information is a person who has sufficient information to make a (single) decision. Identification of the DM preference system is one of the major problems in multicriteria problems. Typically, DM preference elicitation procedures are constructed in the language of vector evaluation of alternatives, i.e., based on vector criterion values.

Decision making by DM is facilitated by finding a Pareto set or a Slater set using criterion (29), here methodological problems are largely lost as the notion of solving a multicriteria problem is already well defined. What remains are the computational difficulties typical of extreme problems.

Techniques for solving the task of searching for effective (Pareto-optimal) and weakly effective (Slater-optimal) alternatives are being intensively developed [6-8], and there are programs, software packages and software systems that have been implemented on computers.

The algorithms based on scalarization - reduction to the parametric family of scalar optimization problems - are of great "clarity".

From the convex analysis it follows that if $x_* \in P(X, W)$ - is an effective point in a linear multicriteria problem (with linear criteria in the polyhedron X), then there exists a vector Λ

$$\lambda \in \Lambda = \left\{ \lambda \in E^m / \lambda_i > 0, i = 1, \dots, m; \sum_{i=1}^m \lambda_i = 1 \right\},$$

such that x_* is a solution to a linear and non-linear programming problem

$$\sum_{i=1}^m \lambda_i W^i(x) \rightarrow \max_{x \in X}. \quad (30)$$

Inversely, for any $\lambda \in \Lambda$ solution of problem (30) is an effective point.

It follows that well-developed linear and nonlinear programming methods can be used to find $P(X,W)$ and use the result as an effective set in the process of mapping the situation related to the location of the set of real values of the feature parameters, relative to the set of their effective values in the implementation of LC REM monitoring.

5. CONCLUSIONS

Methods for solving problems of selecting informative features for monitoring LC REM, by classifying the REM states and LC processes in the feature space, each of which has a certain significance, which allowed to find a comprehensive criterion and formalize the selection procedures.

The methods of identification of REM states that interpret them as elements of conjugate linear spaces and set initial sets by linear and non-linear functionals have been improved, making it possible to formulate rules for separation of sets in the space of states and the rules that establish correspondences between the sets of parameters and values of LC REM performance. Application of these rules makes it possible to construct algorithms for optimisation of LC REM performance indicators.

REFERENCES

- [1] Biryukov S. I. Optimisation. Elements of theory. Moscow: MH-Press, 2003. 246 p.
- [2] Vasiliev V. I. Recognizing systems: Handbook. Kyiv: Naukova Dumka, 1983. 422 p.
- [3] Nevlyudov I. Sh., Andrushevich A.A., Donskov A.N. Development and application of methods of monitoring of design processes, production and operation of LC REM. Scientific and Technical Journal "ACS and Automation Devices". 2011. Vyp. 156. P. 82 - 89.
- [4] Alexandrov P. S. Introduction to set theory and general topology. Moscow: Nauka, 1977. 368 p.
- [5] Kantorovich L. V., Akilov G. P. Functional analysis in normed spaces. Moscow: Nauka, 1984. 368 p.
- [6] Podinovsky V. V., Nogin V. D. Pareto-optimal solutions of multicriteria problems: a monograph. Moscow: Fizmatlit, 2007. 255 p.
- [7] Vishnekov A. V., Ivanova E. M., Safonova I. E. Decision-making methods in distributed CAD/CAM/CAE systems. Methods of complex estimation of variants in conditions of certainty of initial information. Quality and CALS-technologies. 2006. N 3 (11). P. 35-40.
- [8] Kozhevnikov A.M. CALS-technology methods for optimization of electrical and thermal modes selection of electro radio products. ITPP. 2000. N 3. P.23-26.

THE IMPORTANCE OF THE PLANNING CYCLE FOR AN EFFECTIVE STRUCTURING OF ONLINE TEACHING PROCESSES¹

Ash KAYA¹, Nazire Burçin HAMUTOĞLU^{2,*}, Emre ÇAM³, Emine Nur ÜNVEREN-BİLGİÇ⁴

¹Department of Statistics, Faculty of Science, Anadolu University, 26470, Eskisehir, Turkey

²The Centre for Teaching and Learning Excellence, Eskisehir Technical University, Eskisehir, Turkey

³Niksar Niksar Vocational School, Tokat Gaziosmanpaşa University, Tokat, Turkey

⁴Education Faculty, Mathematics and Science Education Department, Düzce University, Düzce, Turkey

ABSTRACT

The need for effective structuring of learning and teaching processes in the changing world makes itself felt more and more every day. As a matter of fact, as seen in the past Covid 19 pandemic and the Kahramanmaraş-Pazarcık-centered earthquake(s) on February 6, 2023; rapid decision-making policies regarding the transition process to online learning environments also form the basis of the need for an effective structuring of online learning environments. The ability of educational institutions to show quick reflexes to emerging problems and to provide adaptation processes; possible on the basis of effective planning carried out in advance. In all these processes, it has been seen that the primary measure taken against the emerging problems is the transition to the distance education method. However, the interruption of educational activities in institutions where there is no effective planning cycle; creates a handicap in terms of gaining learning outcomes that cannot be compromised. In this study, the importance of the planning cycle in the effective structuring of teaching processes is mentioned. The importance of the planning cycle is emphasized in the study and its reflections will be examined in terms of creating the input of the web-based system that is under development.

Keywords: Online learning, quality, planning cycle, effective structuring, teaching and learning.

“perfection is the enemy of quality assurance”

“never stop for improving and developing”

INTRODUCTION

The utilitarian value of an effective structuring teaching and learning processes planning cycle is an important pivot in the development of technology has placed it at an advantage position for sustainable development in the 21st century. The need for effective structuring of learning and teaching processes in the changing world makes itself felt more and more every day. The ability of educational institutions to show quick reflexes to emerging problems and to provide adaptation processes; possible on the basis of effective planning carried out in advance.

One of the areas most affected by the Covid 19 pandemic and Kahramanmaraş centered earthquake(s) is undoubtedly education. Even though educational institutions at almost all levels have updated their existing systems in line with the dynamics of our age, it is an undeniable fact that there is a serious adaptation problem in the management of these systems. A successful technology integration study is an important indicator in dealing with adaptation problems. One of the most important steps forming this indicator is the “Planning” phase of the PDCA cycle, which is based on providing internal quality assurance. An effective planning process is by thoroughly observing possible variables. It is the preparatory phase of a successful implementation process.

With this project, it is aimed to develop a web-based task, performance and documentation system for the management of education standards that assist the internal quality assurance system in accordance with the education standards of

¹ This study is supported by the Eskisehir Technical University Scientific Research Project Unit with the 23ADP032 project number.

*Corresponding

higher education institutions within the framework of the Planning cycle of the PDCA cycle. By managing the plans and practices of the web-based system aimed to be developed in the field of education, which is the main responsibility of the academic staff; Evaluation and improvement processes and effective feedback processes regarding students' learning performances are planned. In addition, it will be possible to serve the understanding of institutional agility by keeping the institutional memory alive and dynamic with the documentation module to create evidence for supporting the quality assurance system, which is very important for higher education institutions. Hence, the research problems are stated as follows:

- (1) What is the importance of the planning cycle in the effective structuring of teaching processes?
- (2) How the web-based system could be important for an effective planning cycle in terms of providing input for the quality assurance?

Based on all these expressions; Within the stated framework, the related study is aimed at providing internal quality assurance in accordance with the education standards of higher education institutions;

- in terms of integrating the web-based environment to be developed to support the functional structuralization of teaching processes, the study is *up-to-date*,
- in terms of designing the web-based environment to be developed in order to be able to dominate general education and learning situations in particular in the integration process, it will be designed to operate the Planning step of the PDCA cycle *original*,
- for the web-based environment to be developed for structuring processes to support change management, the study is *necessary*,
- in terms of planning the teaching processes through the web-based environment to be developed and including supervision regarding the planning processes, it can be said that it is *functional*.

METHOD

The method to be used in the study is based on the observance of national and international standards regarding quality assurance. In this context, the variables that will form the basis of the "Institutional Internal Evaluation Report", which institutions are expected to report every year by the higher education quality board, and the standards of the institution standards and the standards of the accreditation bodies to which the units are related. In line with the strategic plan of the institution, the web-based system to be developed in relation to the purpose, target, performance indicator and fields of activity.

(1) At the planning stage, the entry will be made by the relevant academic staff (a) the program outcomes, unit learning outcomes, institution learning outcomes related to the course learning outcomes, and the relationship between the Turkish Higher Education Qualifications Framework and the UN Sustainable Development Goals will be entered; (b) specify the method, technique and strategy on which the course learning outcomes will be achieved, and the weeks they are associated with; (c) by determining the types of assessments to be made and the weeks to which they are related; its equivalent in the system (eg Visa) will be marked.

(2) Completion of the planning cycle will culminate with a structured feedback process. In this process, the participants will have knowledge and awareness about the application, control and precaution cycles by taking individual supervision of the teaching processes.

(3) Although the system to be developed is limited to the Planning cycle; In future studies, it will be possible to integrate the Implementation, Control and Prevention cycles into the system. The documentation module of the system will also include a module that will keep the institutional memory alive and create evidence when necessary.

According to Tripp and Bichelmeyer (1990), this model has been successfully used in software engineering and, given the similarities between software design and instructional design, it is argued that rapid prototyping is a particularly suitable model for computer-based/web-based instructional and instructional design. The most important feature of the model is the continuous improvement of design tests in the process of creating the final product. The advantage of this method over other design models is that it saves time, effort and cost without sacrificing quality (Desrosier, 2011). The application process of the rapid prototyping model, which will be based on the project, is given in Figure 1 below.

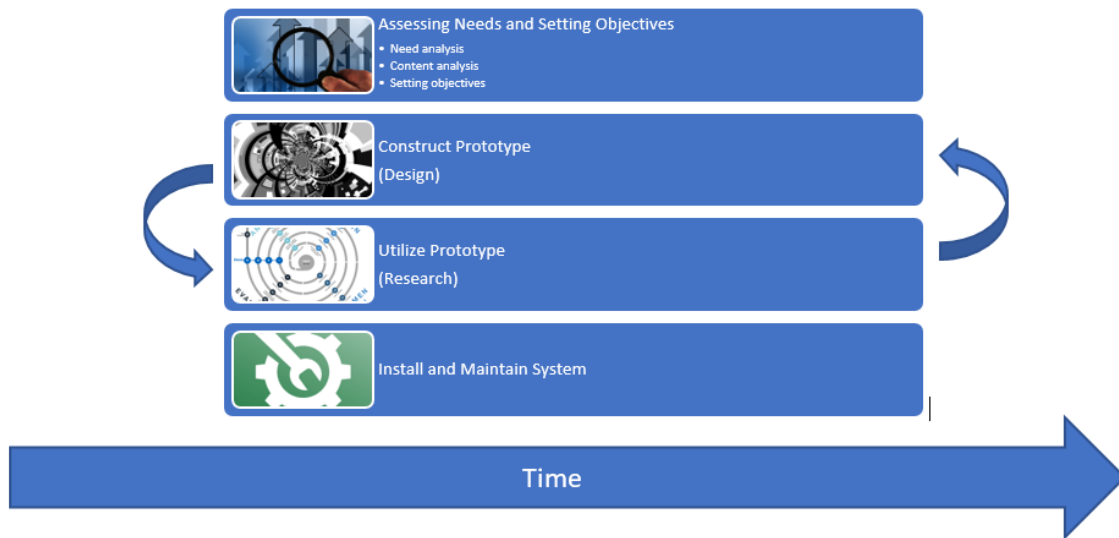


Figure 1. Rapid Prototyping Model

The development of the system within the specified framework will proceed on the basis of the "Rapid Prototyping Model". During the implementation of the said model within the scope of the proposed project; We will work with small groups representing the academic structure of our university. This is important in that faculties have their own specific practices. In order for the system to be developed to serve the purpose with its flexible and user-friendly interface, sub-teams will be formed to sample the departments/programs within each Faculty/Vocational School/Institute. Creation of teams together on a voluntary basis; Our university will be based on the basic principles of "inclusiveness" and "to achieve together". The web-based system, which will be developed to be interactive with the groups, will be updated and tested. The flow chart for the operation of the Planning step of the PDCA cycle is presented in Figure 2.

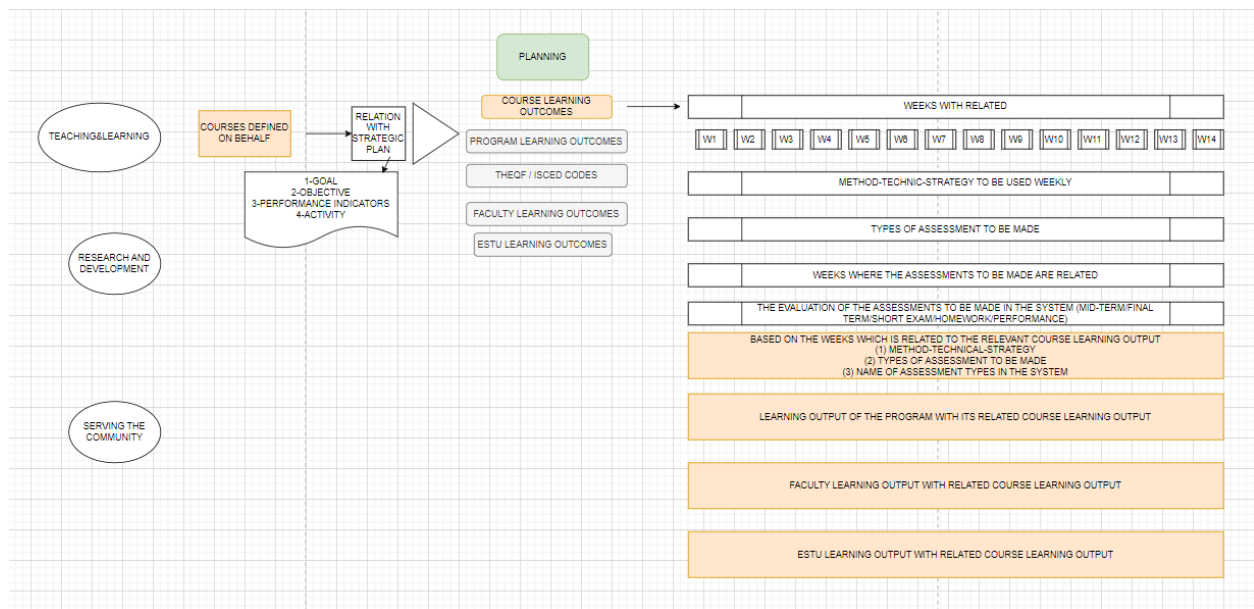


Figure 2. Proposed Web-Based System for Planning Step

CONCLUSION AND SUGGESTIONS

Educational standards play an important role in providing the internal quality assurance system in a higher education institution. In this regard, starting from the education standards of a higher education institution; being able to dominate education in general and learning situations in particular; by developing a web-based technology for the functional structuralization of teaching processes. In the integration of learning-teaching processes, it is important that the "Planning" phase is meticulously structured first and foremost. In demonstrating the effectiveness of the structuring processes the "Check" and "Action" steps, which are the next stages of the "Implementation" step, are important. Implemented applications; evaluation and improvement, closing the aforementioned PDCA cycle. It is important in terms of creating an input for the next cycle. "1-Where do we want to go?", the answer is sought for the effective structuring of the teaching processes in accordance with the education and training standards. In the process, the question of "2-How do we get there?" followed by the question "3-Did we really reach the place where we wanted to go?" In this study, which ends with the question, it is aimed to provide structured support for the planning processes to the instructors who want to structure their teaching processes effectively. It can be said that the evaluation of the developed web-based structured support platform and the opinions about this platform is important for future studies and updating the system. In sum, it is possible to assert that there is a lack of awareness of the importance of the planning cycle that will reveal the relationship between learning outcomes and learning outcomes. Addition to this, students and instructors need to develop an awareness of the level of technology they will use. They also need to be supported in using interactive digital environments. At that point, it is also necessary to underline the importance PDCA cycle online learning environments for all stakeholders. The necessity of an effective structuring for the teaching and learning process that will deal with emergency distance education in all programs should be taken into consideration as well. Finally, there is a huge need for the employment in the field of computer education and instructional technology in terms of having the competency of the instructional design.

REFERENCES

- Desrosier, J. (2011). Rapid prototyping reconsidered. *The Journal of continuing higher education*, 59(3), 135-145. <https://doi.org/10.1080/07377363.2011.614881>
- Tripp, S. D., & Bichelmeyer, B. (1990). Rapid prototyping: An alternative instructional design strategy. *Educational technology research and development*, 38(1), 31-44. <https://doi.org/10.1007/BF02298246>

EXAMINATION OF THE RELATIONSHIP BETWEEN THE OCCUPATIONAL IDENTITY PERCEPTIONS OF PRIMARY SCHOOL MATHEMATICS TEACHER CANDIDATES AND TPCK

Emine Nur ÜNVEREN BİLGİÇ¹, Nazire Burçin HAMUTOĞLU^{2,*}, Emre ÇAM³

¹ Education Faculty, Mathematics and Science Education Department, Düzce University, Düzce, Turkey

² The Centre for Teaching and Learning Excellence, Eskisehir Technical University, Eskisehir, Turkey

³ Nıksar Nıksar Vocational School, Tokat Gaziosmanpaşa University, Tokat, Turkey

ABSTRACT

It is important for the element of quality in education to define the factors that form or change the perceptions of teachers who are new to the profession and who gain experience over time, the reasons why teachers choose the profession or which conditions are effective over time, the way teachers perceive themselves in the region where they live or in the society in general or how the society perceives teachers, the change in the perception of the teacher after the interaction of the teacher with other teachers, students and administrators of the school. Another important context for quality in educational processes is Pedagogical Content Knowledge Today, with the inclusion of the technology component in teacher knowledge, it is a very important topic to examine teacher knowledge, which was redefined as Technological Pedagogical Content Knowledge. The aim of this study is to examine the relationship between pre-service elementary mathematics teachers' perceptions of professional identity and Technological Pedagogical Content Knowledge. From this point of view, the research will be carried out in a relational survey design with a quantitative paradigm. The participants who will be provided from all grade levels with maximum diversity sampling. It was found that there was no difference according to gender and moderately relation between the subscales.

Keywords: Professional Identity, TPCK, Mathematics Education

*A good teacher is like a candle – it consumes itself to light the way for others.”
- Mustafa Kemal Atatürk*

The quality of teacher education has long been a matter of concern. Many tools and measures have been taken from time to time to improve the quality of teacher education. Nowadays, several changes are taking place around the world. Among them, the prevalence of ICT/Digital technology stands out. These changes are manifested in various forms leading to changes in the curriculum structure of teacher education. Before the digital age, more emphasis was placed on content knowledge and less attention was paid to pedagogical theories. The integration of pedagogy with content processing was theoretically discussed by Schulman (1986) and this is now taken as the Pedagogical Content Knowledge (PCK) framework in teacher education. Pedagogy plays an important role in the transmission of content, but in PCK technology has been ignored in the educational activity. As almost no sphere of life today is devoid of technology, so is the field of education. Therefore, the need for technology integration in education becomes the key factors of quality education. Computer Assisted learning/Teaching/Teaching/Assessment, e-learning, e-assessment, online/virtual learning environment, educational applications and artificial intelligence in education have gradually emerged. Knowledge of content, pedagogy and technology in quantum style is not enough for effective teaching, but it is necessary to bring all these components together and to have knowledge in a system style. PCK based on Shulman (1986), Koehler and Mishra (2006) expanded the idea of teacher's knowledge by emphasising the integration of technology into education and gave a Technological Pedagogical Content Knowledge (TPK) framework. As in this digital age, there are several changes that are converging in education due to the use of technology in human activities outside education. The quality of education delivered by an institution is now compared to one of the parameters of how it is effectively integrated. Now

technology integration is gaining importance and vital importance not only in teacher education but in all kinds of education. TPACK has many implications in teacher education, so this paper focuses on these implications.

METHODOLOGY

The research was carried out in a relational survey design with a quantitative paradigm. "Teachers' Perception of Professional Identity Scale" developed by Yıldız and Çetin (2020) and "Technological Pedagogical Content Knowledge Scale (TPACK-Math)" developed by Önal (2016) were used for the participants who were from all grade levels with maximum diversity sampling.

Occupational Attitude Perception Scale

The perception of occupational identity scale has become a five-dimensional scale consisting of 17 items with proven validity and reliability. The dimensions of the scale are professional role, educational and instructional interaction, professional status/respect, professional motivation and experiential pedagogy.

TPCK Math Scale

TPCK_Math Scale is consist of 59-item, 9-dimensional which are; technological knowledge (TK), content knowledge (CK), pedagogy knowledge (PK), pedagogical content knowledge (PCK), technological content knowledge (TCK), online technological pedagogical knowledge (TPK online), offline technological pedagogical knowledge (TPK offline), technological pedagogical content knowledge (TPCK) and contexts knowledge.

The current study aims to determine the relationship between pre-service elementary mathematics teachers' technological pedagogical content knowledge and their mathematics teaching anxiety. Data analysis in the research was carried out in five primary stages. In these stages:

(i) The collected data were preprocessed for the statistical procedure. The normal distribution of data was tested with skewness and kurtosis in SPSS.

(ii) At the outset, the study had included 120 pre-service teachers; 9 showing extreme data values in the box plot chart created in the SPSS program were excluded from the evaluation. The research data included 111 pre-service teachers.

(iii) Mean and standard deviation (SD) scores were calculated for all subscale scores through the determining frequency and percent (%) values of the participant demographic characteristics.

(iv) Before testing the occupational identity perception scale and the technological pedagogical content knowledge scale according to various demographic variables, the assumption of normal data distribution was tested with the Kolmogorov-Smirnov test. The normal distribution value was less than the statistical significance level ($p < .05$). Therefore, kurtosis-skewness measures were used to describe the normal distribution. The kurtosis and skewness values showed that the distribution was linear. In this respect, parametric tests were used in the study. The statistical significance level was taken as 0.05 in the SPSS software analysis.

In this context:

- Independent groups t-test was used to determine whether the subscale scores of the students in the sample group differed according to the "Gender" variable.

- ANOVA was used to determine whether the subscale scores of the students in the sample group differed according to the "Class" variable.

- Scheffe test and LSD test were used to determine between which groups the statistical difference occurs after ANOVA.

(v) Pearson's Product Moments Correlation Analysis was employed to determine the relationships between the Occupational Identity Scale and the subscales of the Technological Pedagogical Content Knowledge Scale and subscales.

FINDINGS

Table 1 shows that the distribution of mathematics teacher candidates by gender.

Table 1. The distribution of mathematics teacher candidates by Gender

Gender	Frequency	Percentage
Female	81	73
Male	30	27
Total	111	100

Table 2 shows that the distribution of mathematics teacher candidates by class

Table 2. The distribution of mathematics teacher candidates by Class

Class	Frequency	Percentage
1st Grade	24	21,6
2nd Grade	31	27,9
3rd Grade	31	27,9
4th Grade	25	22,5
Total	111	100,0

Table 3 shows that t-test results according to the "Gender" variable

Table 3. Comparison of prospective teachers' mathematics occupational identity perceptions according to the "Class" variable

Occupational Identity Perception	Gender	n	Mean	Sd	T	P
EII	Female	81	12,34	1,44	,33	,05
	Male	30	12,23	1,86		
PR	Female	81	13,45	1,28	,87	,02*
	Male	30	13,16	1,64		
PSP	Female	81	10,43	1,79	-2,47	,19
	Male	30	11,46	2,34		
PM	Female	81	15,06	3,07	-2,06	,40
	Male	30	15,2	3,29		
EP	Female	81	17,49	2,34	-1,47	,91
	Male	30	17,56	2,26		
OIP_Total	Female	81	68,79	6,6	-4,45	,01*
	Male	30	69,63	9,21		

The participants' gender and class information distributions were determined using descriptive statistics, such as frequency (f) and percentage (%). Kolmogorov-Smirnov Normality test was used to determine which tests would be applied in data analysis. The test result has shown that the "Mathematics Teaching Anxiety Scale sub-dimensions" and the "TPCK Scale sub-dimensions" p values were less than the significance level of 0.05, and the dataset was not normally distributed. However, considering that the skewness and kurtosis values between -1.5 and +1.5 (Tabachnick and Fidell, 2013) or -2.0 and +2.0 (George and Mallery, 2010) indicate a normal distribution, the data which did not show a normal distribution in the Kolmogorov-Smirnov test, were re-evaluated with the skewness and kurtosis criteria of George and Mallery (2010).

Table 4 shows that comparison of prospective teachers' mathematics occupational identity perceptions according to the "class" variable

Table 4. Comparison of prospective teachers' mathematics occupational identity perceptions according to the "Class" variable

	Class	n	Mean	sd	F	p	Scheffe	LSD
EII	1st grade	24	12,93	1,63	1,1	,35	-	
	2nd grade	31	11,9	1,59				
	3rd grade	31	12,51	1,45				
	4th grade	25	12,56	1,55				
PR	1st grade	24	13,75	1,29	2,47	,06	-	
	2nd grade	31	12,83	1,48				

	3rd grade	31	13,45	1,28				Between 1st and 2nd grades
	4th grade	25	13,6	1,35				Between 2nd and 4th grades
PSP	1st grade	24	10,45	2,24	,84	,47	-	
	2nd grade	31	10,77	2,14				
	3rd grade	31	11,12	1,64				
	4th grade	25	10,36	1,99				
PM	1st grade	24	14,41	3,5	,73	,53	-	
	2nd grade	31	15,0	3,08				
	3rd grade	31	15,22	3,27				
	4th grade	25	15,72	2,6				
EP	1st grade	24	17,91	2,14	2,11	,10	-	Between 2nd and 4th grades
	2nd grade	31	16,74	2,92				
	3rd grade	31	17,45	2,11				
	4th grade	25	18,16	1,57				
OIP_Total	1st grade	24	66,87	8,06	,99	,39	-	
	2nd grade	31	67,25	8,41				
	3rd grade	31	69,77	6,69				
	4th grade	25	70,4	5,95				
	1st grade	24						
	2nd grade	31						
	3rd grade	31						
	4th grade	25						
	2nd grade	31						
	3rd grade	31						
	4th grade	25						

Table 5 shows that comparison of prospective teachers' mathematics TPCK according to the "Class" variable

Table 5. Comparison of prospective teachers' mathematics TPCK according to the "Class" variable

Occupational Identity Perception	Class	n	Mean	Sd	F	p	Scheffe	LSD
TK	1st grade	24	23,58	4,15	2,92	,03*	Between 2nd and 4th grades	Between 2nd and 4th grades
	2nd grade	31	22,29	5,28				
	3rd grade	31	23,96	4,31				
	4th grade	25	25,76	3,29				
PK	1st grade	24	42,87	6,74	2,97	,03*	Between 2nd and 4th grades	Between 1st and 2nd grades
	2nd grade	31	39,32	6,4				
	3rd grade	31	41,09	6,9				
	4th grade	25	43,44	4,55				
CK	1st grade	24	35,5	5,76	3,07	,03*	Between 2nd and 4th grades	Between 1st and 2nd grades
	2nd grade	31	32,74	5,48				
	3rd grade	31	34,41	4,71				
	4th grade	25	36,64	3,77				
TPK_offline	1st grade	24	11,58	1,69	5,48	,002**	Between 1st and 2nd grades	Between 1st and 2nd grades
	2nd grade	31	10,22	1,94				
	3rd grade	31	11,48	1,58				
	4th grade	25	11,96	1,67				
TPK_online	1st grade	24	10,62	1,99	2,71	,04*	Between 2nd and 3rd grades	Between 2nd and 3rd grades
	2nd grade	31	10,41	2,47				
	3rd grade	31	10,96	1,72				
	4th grade	25	11,84	1,34				

TCK	1st grade	24	18,75	2,8	2,48	,06											Between 2nd and 4th grades
	2nd grade	31	17,77	3,42													Between 2nd and 4th grades
	3rd grade	31	19,12	2,92													
	4th grade	25	19,84	2,17													
PCK	1st grade	24	26,58	4,48	1,69	,17											Between 2nd and 4th grades
	2nd grade	31	25,06	4,41													
	3rd grade	31	26,89	3,44													
	4th grade	25	27,32	3,83													
TPCK	1st grade	24	32,87	4,91	2,44	,06											Between 2nd and 3rd grades
	2nd grade	31	30,58	6,62													Between 2nd and 4th grades
	3rd grade	31	33,48	5,07													
	4th grade	25	34,32	5,13													
ContentK	1st grade	24	20,2	2,85	1,97	,12											Between 1st and 2nd grades
	2nd grade	31	18,16	3,86													
	3rd grade	31	19,16	2,93													
	4th grade	25	19,28	2,45													
TPCK_total	1st grade	24	222,58	30,16	3,27	,02*										Between 2nd and 4th grades	Between 1st and 2nd grades
	2nd grade	31	206,58	34,39													Between 2nd and 4th grades
	3rd grade	31	220,54	27,45													
	4th grade	25	230,4	22,81													

Table 5 shows that the correlation values showing the relationship between TPCK and occupational identity perceptions.

Table 5. The correlation values showing the relationship between TPCK and occupational identity perceptions

	EII	PR	PSP	PM	EP	OIP_Tot al	T K	PK	CK	TPK _offl _ine	TPK _onl _ine	TCK	PCK	TPCK	Context K	TPCK _Total
EII	1	,48**	,45**	,33**	,5**	,72**	,29*	,47**	,47**	,42**	,3**	,42**	,46**	,38**	,38**	,48**
PR	,48**	1	,2**	,23**	,57**	,62**	,19*	,38**	,33**	,3**	,2**	,27**	,36**	,23**	,5**	,36**
PSP	,45**	,2**	1	,32**	,25**	,62**	,37*	,35**	,37**	,3**	,34**	,37**	,3**	,31**	,34**	,4**
PM	,33**	,23**	,32**	1	,39**	,75**	,35*	,47**	,49**	,38**	,39**	,43**	,49**	,44**	,41**	,51**
EP	,5**	,25**	,25**	,39**	1	,76**	,33*	,49**	,48**	,52**	,4**	,49**	,47**	,38**	,57**	,53**
OIP_Tot al	,72**	,67**	,62**	,75**	,76**	1	,45*	,62**	,62**	,55**	,5**	,58**	,6**	,51**	,62**	,66**
TK	,29**	,19**	,37**	,35**	,33**	,45**	1	,65**	,65**	,6**	,6**	,73**	,54**	,71**	,43**	,78**
PK	,47**	,38**	,35**	,47**	,49**	,62**	,65**	1	,88**	,7**	,63**	,65**	,83**	,73**	,65**	,91**
CK	,47**	,33**	,37**	,49**	,48**	,62**	,63**	,88**	1	,75**	,69**	,64**	,83**	,76**	,63**	,91**
TPK _offl _ine	,42**	,3**	,3**	,38**	,52**	,55**	,6**	,7**	,75**	1	,66**	,7**	,71**	,68**	,55**	,81**
TPK _onl _ine	,3**	,23**	,34**	,39**	,4**	,5**	,6**	,63**	,69**	,66**	1	,69**	,65**	,66**	,55**	,77**

TC K	,42 **	,27 **	,37* *	,43 **	,49 **	,58**	,7 3*	,65 **	,64 **	,7**	,69* *	1	,65* *	,69**	,58**	,81**
PCK	,46 **	,36 **	,3** **	,49 **	,47 **	,6**	,5 4*	,83 **	,83 **	,71* *	,65* *	,65* *	1	,82**	,66**	,89**
TPC K	,38 **	,23 **	,31* *	,44 **	,38 **	,51**	,7 1*	,73 **	,76 **	,68* *	,66* *	,69* *	,82* *	1	,61**	,89**
Cont extK	,38 **	,5* *	,34* *	,41 **	,57 **	,62**	,4 3*	,65 **	,63 **	,55* *	,55* *	,58* *	,66* *	,61**	1	,73**
TPC K_T otal	,48 **	,36 **	,4** **	,51 **	,53 **	,66**	,7 8*	,91 **	,91 **	,81* *	,77* *	,81* *	,89* *	,89**	,73**	1

According to the t-test results, it was determined that there was a significant difference in favour of female pre-service teachers in the professional role sub-dimension of professional identity perception according to gender, while there was a significant difference in favour of male pre-service teachers in the total scores of the scale. No significant difference was found for this scale according to the class variable.

While a significant difference was found in favour of male pre-service teachers in TK, PK, TPK_offline, TPK_offline, TCK sub-scales and TPCK_Total according to gender, a significant difference was found in favour of female pre-service teachers in ContextK sub-scale. A significant difference was found between the second and fourth grades in favour of the fourth grades in the TK subdimension. A significant difference was found between first and second grades in favour of first grades in TPK_offline subdimension. In the same subdimension, a significant difference was found between the second and fourth grades in favour of the fourth grades. In TPCK_Total, a significant difference was found between the second and fourth grades in favour of the fourth grades.

Finally, it was determined that the scales were highly and very highly correlated with their sub-dimensions. In addition, a moderate relationship was found between pre-service teachers' perceptions of professional identity and TPCK self-assessments, and it was determined that all sub-dimensions of the perception of professional identity scale were moderately related to TPCK_Total. In addition to this, PR subdimension is moderately related to ContxtK subdimension and EP subdimension is moderately related to TPK_offline and ContextK subdimension.

CONCLUSION AND SUGGESTIONS

Accordingly, although a significant difference was found in favour of female teachers in the professional role subdimension, a significant difference was found in favour of male teachers in the total score.

According to this, it was determined that the self-evaluations of the fourth grades were higher in terms of TPCK_math total scores of the pre-service teachers according to their grade levels. This may be thought to be due to the fact that the field education courses are almost completed. In addition, the fact that field teaching and field courses are more in the third grade compared to other grades may indicate that pre-service teachers have a lower self-evaluation at this level.

Based on the results of this research, strengthening pre-service teachers' perceptions of professional identity is very important for their TPCK-Math self-evaluations.

Accordingly, it is recommended to emphasise the importance of educational and instructional interaction, professional role, professional status, professional motive and experiential pedagogy perception in teacher training programmes and that these interactions are related to TPCK-Math.

Practical activities for the development of professional identity perception in pre-service teachers are suggested.

It is thought that the implementation of field education courses in teacher training programmes in real school environment will feed this relationship positively and make teacher training effective. In this context, it is suggested that the teacher education period should be restructured in a way similar to other fields such as medical discipline (the process that can create a perception of professional identity in individuals).

REFERENCES

- George, D., & Mallery, P. (2010). SPSS for Windows step by step: A simple guide and reference, 16.0 update. (No Title).
- Mishra, P., & Koehler, M. J. (2006). Technological pedagogical content knowledge: A framework for teacher knowledge. *Teachers college record*, 108(6), 1017-1054.
- Önal, N. (2016). Development, Validity and Reliability of TPACK Scale with Pre-Service Mathematics Teachers. *International Online Journal of Educational Sciences*.
- Shulman, L. S. (1986). Those who understand: Knowledge growth in teaching. *Educational researcher*, 15(2), 4-14.
- Tabachnick, B. G., & Fidell, L. S. (2013). *Using multivariate statistics* (6th ed.). Boston, MA: Pearson.
- Yıldız, V., & Çetin, M. (2020). Development of Occupational Identity Perception Scale. [Mesleki Kimlik Algısı Ölçeğinin Geliştirilmesi]. *Journal of Social Sciences*, (48), 364-399.

NUMERICAL ANALYSIS OF A NEW THERMOSYPHON HEAT PIPE

Çetin YAVUZ¹, Ali TAROKH², Aydın DİKİCİ³

¹Department of Electrical and Energy, Tatvan Vocational School, Bitlis Eren University, Bitlis, Turkey

²Department of Mechanical Engineering, Lakehead University, Thunder Bay, Canada

³Department of Energy System Engineering, Firat University, Elazığ, Turkey

ABSTRACT

In this study, an experimental and 3-dimensional numerical analysis of a thermosiphon heat pipe (THP) using two-phase fluid cycling was performed to model the heat transfer process by evaporation and condensation. R404A refrigerant was chosen as the working fluid for the THP and 50% of the evaporator section was filled with the working fluid. Numerical analysis was performed using ANSYS FLUENT program and VOF method. In the meantime, in order to model the evaporation and condensation process successfully, a UDF code written in C was used and introduced to the fluent program. As a result of the study, it was seen that the temperature values obtained from the experimental and numerical analysis for the evaporator and condenser parts of the THP were in good agreement. As a result of the numerical analyzes carried out in 3D, the contours of the evaporation and condensation process and the heat transfer process are presented visually. The analysis took a total of 200 seconds.

Keywords: Thermosiphon heat pipe, Evaporation and condensation, ANSYS, VOF

1. INTRODUCTION

Heat pipes and/or thermosiphons are heat transfer devices that perform the fluid cycle in two phases in a vacuumed closed tube. A thermosiphon consists of 3 main parts, known as the evaporator, where the heat is given to the working fluid, adiabatic, and the condenser, where the condensation event is carried out. In the evaporator section, the working fluid is heated and evaporation is carried out. The resulting steam then reaches the adiabatic section and then the condenser section. Here, the steam coming into contact with the surface of the condenser section below the saturation temperature condenses and returns to the evaporator section again. This cycle continues throughout the operation of the THP [1]. THP's are used in many areas [2-7]. As a result of the literature research, it has been seen that many 2D numerical analyzes have been carried out for thermosiphons. However, there is no comprehensive 3D numerical analysis that reaches steady state. Therefore, this study is extremely important in this respect. As it is known, CFD analysis, which is used in the solutions and visualization of complex flow events occurring in the interior of thermosiphons, is effectively used in engineering fields due to its visualization possibilities and extremely efficient.

Kamburova et al. [8] carried out a numerical analysis in which they modeled the simultaneous evaporation and condensation event in a thermosiphon in 2D. They used the VOF technique and distilled water as the working fluid in their work. As a result of their studies, they reported that they successfully realized the complex flow events occurring in the thermosiphon. At the same time, they stated that it was in good agreement with the experimental results.

Yang et al. [9] carried out an experimental and numerical analysis of the thermal properties of a heat pipe. Researchers using UDF and VOF techniques in their studies stated that evaporation and condensation phenomena can be simulated with these methods. At the same time, they stated that the axial velocity fluctuation in most areas of the heat pipe was very small, and they reported that the velocity magnitudes changed from 0 to the maximum value from the end of the evaporator and condenser sections, and the maximum value was maintained in the adiabatic section.

Tarokh et al. [10] carried out a numerical analysis to improve the heat transfer performance of a thermosiphon with a vortex-forming barrier placed in its body. The researchers stated that the positioning of the barrier in the adiabatic and condenser sections had a very good effect on the overall thermal resistance and average wall temperature distribution.

Fadhl et al. investigated a thermosiphon heat pipe in two different studies. They used water, R134a and R404a as working fluid. The researchers, who evaluated the thermosiphon heat pipe using different heat inputs, stated that the average temperature values obtained from the numerical and experimental analyzes were in good agreement as a result of their studies. At the same time, they have successfully visualized the evaporation and condensation phenomenon using VOF and UDF techniques [11, 12].

Kim et al. [13] conducted a study examining the effects of mass transfer time relaxation parameters on a thermosiphon heat pipe. Using the mass transfer relaxation parameter as 0.1 for evaporation and 4 different values for condensation, they stated that the most appropriate β_c value was $0.1 \times (\rho_L/\rho_V)$. Using water as the working fluid, researchers simulated

evaporation and condensation using VOF and UDF techniques in their numerical analysis. Wang et al. [14] reported that the β_e value should be approximately 10-1000 times greater than the β_c value. This is also an indication that the mass transfer time relaxation parameters can be selected in accordance with the experimental results.

In this context, experimental and 3-dimensional numerical analyzes of a Thermosiphon heat pipe with a finned structure were carried out in the presented study. In the meantime, it is of great importance to choose the appropriate mass transfer time relaxation parameters for successful evaporation and condensation analysis. The mentioned values were determined as 0.1 for evaporation and 20 for condensation in this study. In addition, the numerical analyzes performed in this study were carried out using ANSYS FLUENT 2022R1 using high-performance computing (HPC) systems from the Digital Research Alliance of Canada.

2. MATERIAL AND METHOD

As mentioned before, complex flow events occurring inside the thermosiphon heat pipes are carried out by numerical analysis. However, the numerical analyzes in question are based on the finite volume method and the analyzes performed with two phases are much more difficult than those with single phase. Because the interfaces between the phases are movable in the analyzes carried out as two-phases. This situation brings with it a more intense computational effort [15, 16, 17]. As a result of the literature research, it has been seen that the VOF method is the most suitable method in terms of its convenience in monitoring the interface, and this method has been used in many studies in this field. With the VOF method, surface tracking of two or more fluids that do not mix with each other is carried out. Therefore, the VOF method was used in the numerical analysis in this study [15, 16, 17]. In this method, the volume fractions in both phases are added to the calculations and the sum of the volume fractions of both phases in any control volume is equal to one. This situation is expressed in the equation below.

$$\alpha_l + \alpha_v = 1 \quad (1)$$

If $\alpha_v=1$, the cell is completely filled with vapor.

If $0 < \alpha_l < 1$, both liquid phase and vapor phase are present in the cell [18].

At the same time, since the analysis performed in this study was performed in two phases, the continuity, momentum, and energy equations given below are expressed as vapor and liquid phases. The equations used for numerical analysis of the thermosiphon heat pipe are given below.

Continuity equation

$$\frac{\partial}{\partial t}(\alpha_L \rho_L) + \nabla \cdot (\alpha_L \rho_L \vec{u}) = S_M \quad (2)$$

The terms α_L , ρ_L , \vec{u} , t , and S_M in this equation represent the volume fraction for the liquid phase, density for the liquid phase, velocity, time, and the source term for mass, respectively.

Energy equation

$$\frac{\partial}{\partial t}(\rho e) + \nabla \cdot [\vec{u}(\rho e + \rho)] = \nabla \cdot (k \cdot \nabla T) + S_E \quad (3)$$

The terms T , ρ , \vec{u} , k , t , and S_E in the energy equation are the mass-averaged temperature shared by the phases, density, velocity, thermal conductivity, time, and source terms, respectively. The term e given in the equation represents the specific internal energy and is expressed by the equation below.

$$e = \frac{\rho_L \alpha_L e_L + \rho_V \alpha_V e_V}{\rho_L \alpha_L + \rho_V \alpha_V} \quad (4)$$

When Equation 4 is examined, it is seen that the terms e_L and e_V exist. These stand for the specific internal energy of the liquid and vapor phases, respectively, and these terms defined by the caloric equation of state [19] are expressed in equations 5 and 6.

$$e_L = C_{pL}(T - T_{sat}) \quad (5)$$

$$e_V = C_{pV}(T - T_{sat}) \quad (6)$$

Also, the terms ρ and k given in the energy equation are volume-averaged parameters and are expressed as follows.

$$\rho = \alpha_V \rho_V + (1 - \alpha_V) \rho_L \quad (7)$$

$$k = \alpha_V k_V + (1 - \alpha_V) k_L \quad (8)$$

Momentum equation

$$\frac{\partial}{\partial t}(\rho \vec{u}) + \nabla \cdot (\rho \vec{u} \vec{u}^T) = -\nabla p + \nabla \cdot [\mu(\nabla \vec{u} + \nabla \vec{u}^T)] + \rho \vec{g} + \vec{F}_{CSF} \quad (9)$$

The terms p , \vec{g} , μ , and \vec{F}_{CSF} in the momentum equation are local pressure, gravity, viscosity, and volumetric surface tension force, respectively. Here, the viscosity is volume-averaged and is expressed as follows. However, the volumetric surface tension force is expressed by equation 11 [20].

$$\mu = \alpha_V \mu_V + (1 - \alpha_V) \mu_L \quad (10)$$

$$\vec{F}_{CSF} = 2\sigma_{lv} \left(\frac{\alpha_L \rho_L C_V \nabla \alpha_V + \alpha_V \rho_V C_L \nabla \alpha_L}{\rho_V + \rho_L} \right) \quad (11)$$

The terms σ_{lv} , C_V , and C_L given in Equation 11 are surface tension and surface curvetures for vapor and liquid, respectively.

The expressions suggested by Lee and De schepper et al [21, 15] were used to calculate the mass and energy transfer in the numerical analysis of thermosiphon working in two phases. These expressions are given below:

For the mass transfer process;

Evaporation: $T_{mix} > T_{sat}$

$$S_M = -\beta_e \alpha_l \rho_l \left| \frac{T_{mix} - T_{sat}}{T_{sat}} \right| \quad (12)$$

$$S_M = \beta_e \alpha_l \rho_l \left| \frac{T_{mix} - T_{sat}}{T_{sat}} \right| \quad (13)$$

Condensation: $T_{mix} < T_{sat}$

$$S_M = \beta_c \alpha_V \rho_V \left| \frac{T_{mix} - T_{sat}}{T_{sat}} \right| \quad (14)$$

$$S_M = -\beta_c \alpha_V \rho_V \left| \frac{T_{mix} - T_{sat}}{T_{sat}} \right| \quad (15)$$

For the heat transfer process;

Evaporation: $T_{mix} > T_{sat}$

$$S_E = -\beta_e \alpha_l \rho_l \left| \frac{T_{mix} - T_{sat}}{T_{sat}} \right| \cdot LH \quad (16)$$

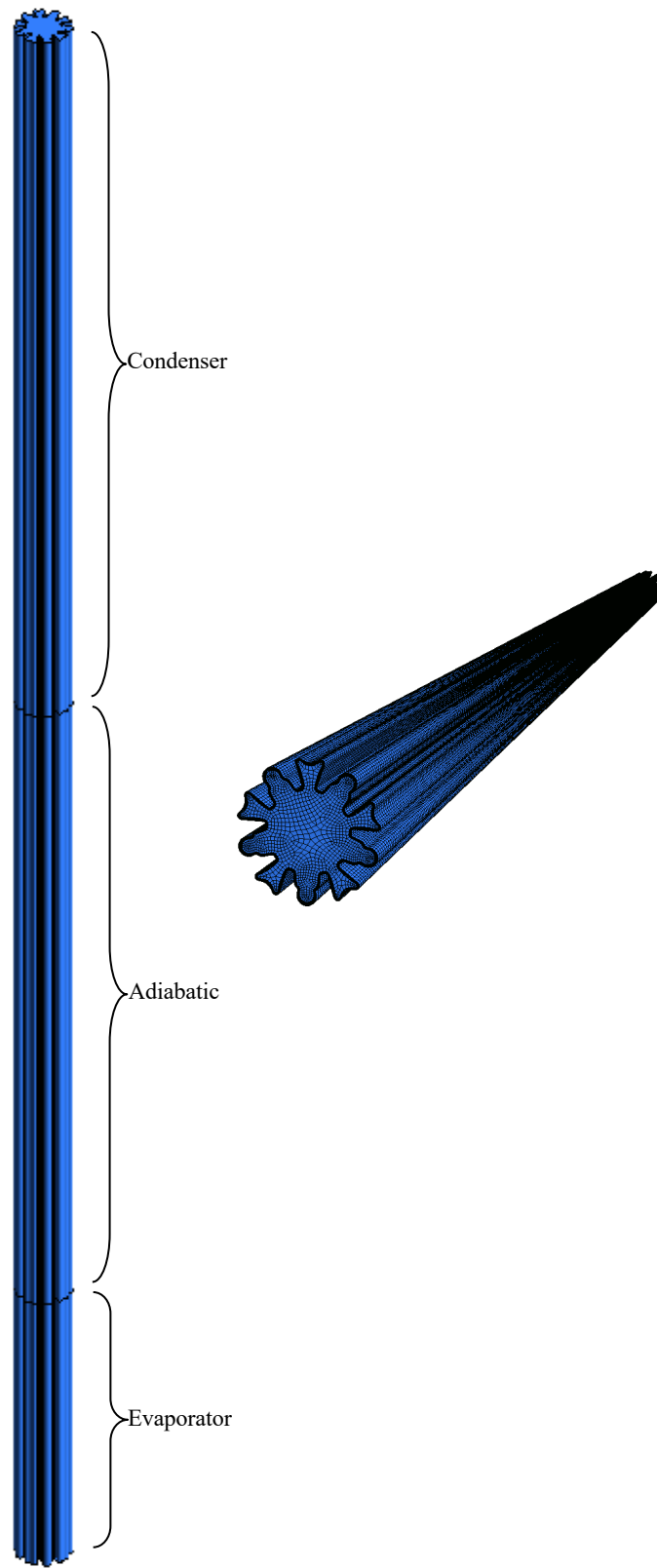
Condensation: $T_{mix} < T_{sat}$

$$S_E = \beta_c \alpha_V \rho_V \left| \frac{T_{mix} - T_{sat}}{T_{sat}} \right| \cdot LH \quad (17)$$

The terms T_{mix} , T_{sat} , LH , β_e and β_c in the equations given for the mass and heat transfer process, the mixture temperature, saturation temperature, latent heat, the mass transfer time relaxation parameters for evaporation and condensation, respectively. As mentioned before, these values should be chosen in accordance with the experimental results in order to perform the evaporation and condensation analyzes successfully and to match the experimental and numerical results. In this study, β_e and β_c parameters were determined as 0.1 and 20, respectively. At the same time, the equations given above for mass and heat transfer were written in UDF using the C programming language and introduced to the fluent program.

Mesh and boundary conditions applied in numerical analysis

The thermosiphon heat pipe presented in this study has an outer diameter of 25 mm and a total length of 700 mm. The material from which THP is produced is aluminum. The lengths of the evaporator, adiabatic and condenser sections are 120, 270 and 310 mm, respectively, and are shown in Fig. 1a. The thermosiphon heat pipe consists of 3556874 nodes and 3430000 elements, and the mesh structure in question is indicated in Fig. 1b. The boundary condition for the inner walls of the thermosiphon heat pipe is chosen as no-slip. The gravitational acceleration is taken as -9.81 m/s². A constant temperature boundary condition has been applied for the evaporator and condenser section, and these temperature values are 323.15 and 283.15 K, respectively. The zero-flux boundary condition was chosen for the adiabatic section. The operating pressure value was determined as 1084400 Pascal in accordance with the saturation temperature taken as 293.15 K. The initialization process was carried out at the saturation temperature after the patch process was performed in such a way that 50% of the evaporator section was the working fluid and the remaining section was steam. The working fluid was used as R404A. The analysis was carried out at 20 C saturation temperature and the properties of the fluid were determined in accordance with this temperature value and given in Table 1.



a- THP Sections

b- Mesh

Figure 1. THP sections and mesh structure

Table 1. Properties of working fluid

Properties	Primary phase	Secondary phase
ρ [kg/m ³]	56.306	1067.3
μ [kg/m.s]	0.011849	0.00013748
k [W/m.K]	0.015178	0.065499
σ_{lv} [11]	$\sigma_{lv} = 0.09805856 - 1.845 \times 10^{-5}T - 2.3 \times 10^{-7}T^2$ (18)	
C_p [J/kg.K]	1163.6	1502
LH [kJ/kg]	374.74	228.75

The time step size used in the numerical analysis was chosen as 0.0005 and thus the courant number remained below 2 throughout the analysis. The SIMPLE algorithm has been chosen for pressure-velocity coupling. First-order upwind discretization, Geo-Reconstruct and Presto discretization were chosen for momentum and energy equations, volume fraction and pressure interpolation, respectively. Explicit formulation was used in the numerical analysis performed within the scope of the study. Residuals are determined as 10^{-4} for volume fraction and velocity, and 10^{-6} for energy. The saturation temperature and enthalpy value of the working fluid are specified in the UDF code.

3. RESULTS AND DISCUSSION

The numerical analyzes carried out within the scope of this study took a total of 200 seconds. The said numerical analysis became steady state after 200 seconds. As a result of the constant temperature boundary condition applied to the walls of the evaporator section, the working fluid in this section is heated and nucleate boiling occurs. The steam that emerges later reaches the adiabatic and then the condenser section over time. The steam, which comes into contact with the walls of the condenser section below the saturation temperature, condenses here and reaches the evaporator section again. This process was continued until the system reached the steady state and at the end of 200 seconds, when the system reached the steady state, the analysis was completed. Images of the above-mentioned process are given later in this section.

The average temperature values obtained from the experimental and numerical results of the evaporator and condenser section are given in Table 2.

Table 2. Average temperature values obtained from experiment and numerical analysis and Relative error

Section	$T_{EXP,ave}$ (K)	$T_{CFD,ave}$ (K)	R_e(%)
Evaporator	320.97003	313.3941618	2,36
Condenser	297.4961	299.16323895	0.56

When the table above is examined, it is seen that the average temperature values obtained from the experimental and numerical analyzes are in perfect harmony with each other. Especially when the relative error values are looked at, it can be clearly seen that the condenser and evaporator sections fit very well.

Fig. 2 shows the contours of the evaporation and condensation event occurring in the THP. When these contours are examined, it can be seen that the pool boiling event occurs in the form of nucleate boiling and the condensation takes place in the first times when the analysis starts. As a result of heating the evaporator section, the temperature value of the working fluid increased over time and evaporation started with the formation of bubbles at the points where it reached the boiling point. These bubbles that emerged later moved upwards in the pool and came to the upper part of the pool. Here, the steam in the bubbles reached the upper part and was released and started to rise towards the condenser part with the effect of the pressure difference. Here, the vapor condensed in the form of droplets came back to the evaporator section with the effect of gravity. As a result of this event, which took place during the numerical analysis process, after a small decrease in the amount of liquid occurred, it remained stable after 200 seconds, and thus the system reached a stable structure.



Figure 2. Evaporation and condensation contours of THP in 0.1-0.2-5-15-50-100-150 and 200 seconds, respectively

Fig. 3 shows the temperature contours that occur inside the THP. Between 0.1 and 15th seconds, the temperature increased in seconds and after 15th seconds, the average temperature value of THP no longer changed and became uniform. When Fig. 3 is examined, it can be easily seen that the temperature of the THP no longer changes after 15th seconds.

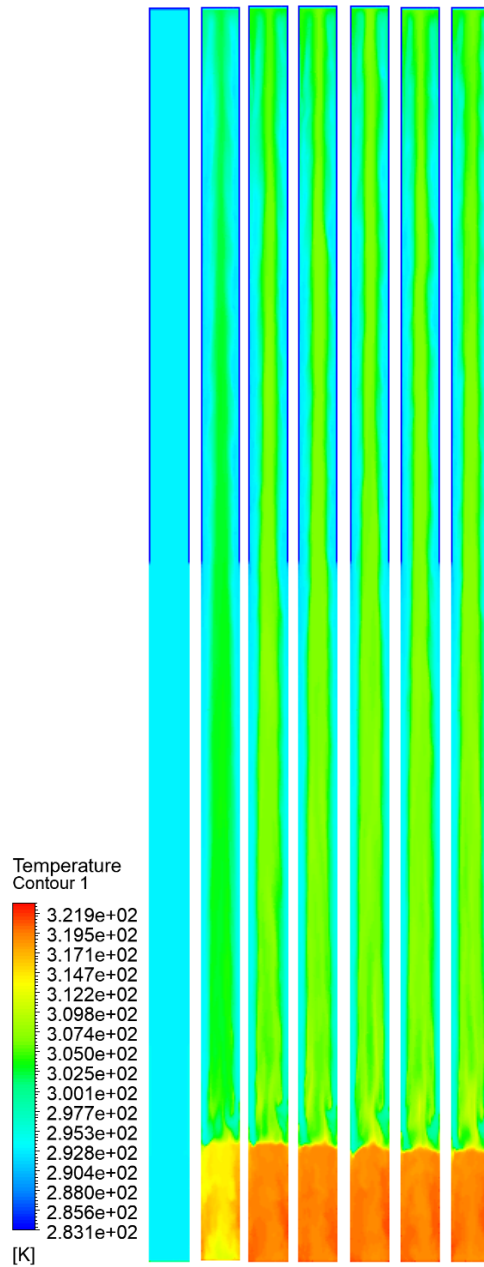


Figure 3. Temperature contours of THP in 0.1-5-15-50-100-150 and 200 seconds, respectively

4. CONCLUSION

In this study, an experimental and 3D numerical analysis of a thermosiphon was carried out. The average temperature values obtained from the experiments for the condenser and evaporator sections were compared with the values obtained from the CFD analysis. It has been seen that the results are in very good agreement. especially the average temperature values of the condenser section were found to be very close to the experimentally obtained values. As a result of the CFD analysis performed, the evaporation and condensation event was successfully modeled and visualized.

ACKNOWLEDGEMENT

The authors are deeply grateful to Mert GÜRTÜRK, Beşir KOK, and Cihangir KALE for allowing the use of experimental setups.

The authors thank Compute Canada for giving them access to the computational resources.

This publication was produced from the PHD Thesis named Realization of experimental and numerical analysis of a new thermosiphon heat pipe that will realize the thermal energy transfer from liquid to gas.

REFERENCES

- [1] J. Legierski, B. Wie, G. De Mey, et al., Measurements and simulations of transient characteristics of heat pipes, *Microelectron. Reliab.* 46 (1) (2006) 109–115.
- [2] Y.-C. Weng, H.-P. Cho, C.-C. Chang, S.-L. Chen, Heat pipe with {PCM} for electronic cooling, *Appl. Energy* 88 (5) (2011) 1825–1833, <http://dx.doi.org/10.1016/j.apenergy.2010.12.004>, URL <<http://www.sciencedirect.com/science/article/pii/S0306261910005118>>
- [3] D. Jafari, A. Franco, S. Filippeschi, P. Di Marco, Two-phase closed thermosyphons: a review of studies and solar applications, *Renew. Sustain. Energy Rev.* 53 (2016) 575–593.
- [4] H. Shabgard, M.J. Allen, N. Sharifi, S.P. Benn, A. Faghri, T.L. Bergman, Heat pipe heat exchangers and heat sinks: opportunities, challenges, applications, analysis, and state of the art, *Int. J. Heat Mass Transfer* 89 (2015) 138–158.
- [5] L.L. Vasiliev, S. Kakaç, *Heat Pipes and Solid Sorption Transformations Fundamentals and Practical Applications*, Ed. CRC Press- Taylor & Francis Group, 2013.
- [6] T. He, C. Mei, J.P. Longtin, Thermosiphon-assisted cooling system for refrigeration applications, *Int. J. Refrig.* (2016), <http://dx.doi.org/10.1016/j.ijrefrig.2016.10.012>.
- [7] A.A. Eidan, S.E. Najim, J.M. Jalil, Experimental and numerical investigation of thermosiphon performance in HVAC system applications, *Heat Mass Transfer* 52 (2016) 2879–2893.
- [8] Kamburova, Veselka & Ahmedov, Ahmed & Iliiev, Iliya & Beloev, Ivan & Pavlović, Ivan. (2018). NUMERICAL MODELLING OF THE OPERATION OF A TWO-PHASE THERMOSYPHON. *Thermal Science.* 22. 1311-1321. 10.2298/TSCI1855311K.
- [9] Yang, K.M. & Cong, Z. & Wang, W.F.. (2016). CFD simulation of flow and heat transfer in a thermosiphon. 1038-1044. 10.1142/9789814749916_0110.
- [10] A. Tarokh, C. Bliss, A. Hemmati, Performance enhancement of a two-phase closed thermosiphon with a vortex generator, *Appl. Therm. Eng.*, 182 (2021), Article 116092, 10.1016/j.applthermaleng.2020.116092
- [11] B. Fadhl, L.C. Wrobel, H. Jouhara, Numerical modelling of the temperature distribution in a two-phase closed thermosiphon, *Appl. Therm. Eng.* 60 (2013) 122–131.
- [12] B. Fadhl, L.C. Wrobel, H. Jouhara, CFD modelling of a two-phase closed thermosiphon charged with R134a and R404a, *Appl. Therm. Eng.* 78 (2015) 482–490.
- [13] Y. Kim, J. Choi, S. Kim, Y. Zhang, Effects of mass transfer time relaxation parameters on condensation in a thermosiphon, *J. Mech. Sci. Technol.* (2015).
- [14] Wang, Xiaoyuan & Wang, Yinfeng & Chen, Haijun & Zhu, Yuezhao. (2020). A combined CFD/visualization investigation of heat transfer behaviors during geyser boiling in two-phase closed thermosiphon. *International Journal of Heat and Mass Transfer.* 121. 10.1016/j.ijheatmasstransfer.2018.01.005.
- [15] S.C.K. De Schepper, G.J. Heynderickx, G.B. Marin, Modeling the evaporation of a hydrocarbon feedstock in the convection section of a steam cracker, *Computers & Chemical Engineering* 33 (2009) 122-132.
- [16] H.K. Versteeg, W. Malalasekera, *An Introduction to Computational Fluid Dynamics; the Finite Volume Method*, second ed., Prentice-Hall, Harlow, 2007.
- [17] J.D. Anderson, *Computational Fluid Dynamics the Basics with Applications*, McGraw-Hill, New York, 1995.
- [18] ANSYS FLUENT, *Theory Guide (Release 13.0). Multiphase Flows*, ANSYS, Inc., November 2010, pp. 455-568 (chapter 17).
- [19] H. Jouhara, A.J. Robinson, Experimental investigation of small diameter two-phase closed thermosyphons charged with water, FC-84, FC-77 and FC-3283, *Appl. Therm. Eng.* 30 (2–3) (2010) 201–211.
- [20] J.U. Brackbill, D.B. Kothe, C. Zemach, A continuum method for modeling surface tension, *J. Comput. Phys.* 100 (2) (1992) 335–354.
- [21] W.H. Lee, Pressure iteration scheme for two-phase flow modeling, *Multi-phase Transp. Fundam. React. Safety, Appl.* 1 (1980) 407–431.

ANALYSIS OF C–H···O INTERACTION BETWEEN ANION AND CATION OF 1,3-DIMETHYLIMIDAZOLIUM METHYLSULPHATE USING NATURAL BOND ORBITAL METHOD

Nihal KUŞ

Department of Physics, Science Faculty, Eskisehir Technical University, 26470, Eskisehir, Turkey

ABSTRACT

It is clear that more studies should be done on ionic liquids, as the usage areas and importance of ionic liquids have increased considerably. Therefore, a study on ionic molecule was planned. In this study, geometry optimizations, charge density and natural bond orbital (NBO) analysis of 1,3-dimethylimidazolium and methylsulphate (DIMIM-MS) ionic liquid in cation and anion form were carried out at the Becke, 3-parameter, Lee, Yang-Parr (B3LYP) version with 6-311++G(2d,2p) basis set. Stabilization energies due to the C–H···O weak hydrogen bonds orbital interactions are calculated from the second-order perturbation approach using Fock matrix equation. Donor-acceptor interactions and hybridization for the C–H···O interaction between anion and cation orbital interactions of DIMIM-MS were analyzed and orbital electron density schemes were plotted. HOMO-LUMO, Mulliken charges and NBO charges were calculated and interpreted using DFT-B3LYP/6-311++G(2d,2p) method.

Keywords: Ionic liquid, orbital interaction, stabilization energy, 1,3-dimethylimidazolium methylsulphate, NBO.

1. INTRODUCTION

Ionic liquids (ILs) are salts that exist as liquids at between room temperature and around 100 °C. They are in the form of molten salt at these temperatures [1]. Very low vapor pressures also increased their use as a solvent [2]. The first example of ILs is the ethyl ammonium nitrate [EtNH₃] [NO₃] compound, synthesized in 1914 and melting point of 12 °C [3]. Because of its physical and chemical properties, it is very common in the usage areas of ILs. It is used as a solvent and catalyst for many reactions [4] and a battery in the field of electrochemistry. [5]. They have been used as electrolytes for solar cells [6] as well as supplements for the binding of enzymes [7]. ILs are used as a molding agent for the synthesis of nano-materials [8]. Kolancılar [9] reported an extensive review on the usage areas of ILs.

ILs consist of poor binding of positively and negatively charged ions and are highly polar solvents. Therefore, it is a good solvent for a large part of both inorganic and organic substances. [10]. Zhou et al. [11] produced ammonia in ionic liquid, with an electrochemical reduction of nitrogen gas in the atmosphere, with a yield of up to 60% at room temperature and pressure. This technique has a source of hope for renewable energy while developing previous nitrogen reduction approaches. Recently, there are a lot of researches and reports about ILs. Among the most currently used ILs, imidazolium based ones have been shown to have definite advantages for biologic applications, such as excellent transfection profiles and low cytotoxicity [12-15]. Chang et al. [16] observed frequency shifts in the imidazolium C–H bands of dimethylimidazolium methyl sulphate in their studies with infrared spectroscopy. They said that these shifts related to with pressure and the C–H···O hydrogen bonding. Single crystal X-ray analysis of DIMIM-MS molecules were studied by Holbrey and co-workers [17]. In this study, C–H···O interactions of ionic liquids consisting of 1,3-dimethylimidazolium cation and methyl

sulphate anion form [DIMIM]⁺ - [MS]⁻ were investigated using natural bond orbital (NBO) method. Stabilization energies in orbital states were found by taking into account donor and acceptor interactions for hydrogen bonds. Hybrid orbital shapes were plotted depending on surface conditions. In addition, Highest Occupied Molecular Orbital (HOMO) and Lowest Unoccupied Molecular Orbital (LUMO), Mulliken and natural charges were calculated.

2. THEORETICAL CALCULATIONS

The structure of the DIMIM-MS was optimized at the density functional theory (DFT) using B3LYP/6-311++G(2d,2p) level [18, 19]. NBO [20, 21] analysis for DIMIM-MS were performed. Gaussian 09 program [22] was used for all the calculations. Orbital schemes were plotted using the form check files of the NBO analysis results. High energy stabilization conditions were determined depending on donor and acceptor orbitals using perturbation theory energy analysis.

3. RESULTS AND DISCUSSION

As a result of the calculations using B3LYP/6-311++G(2d,2p) level, the optimized form of the DIMIM-MS is given in Fig. 1 with the selected atomic numbers.

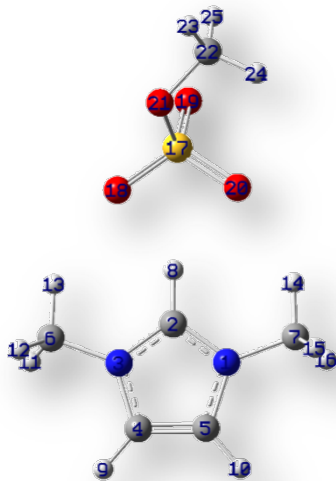


Figure 1. Optimized structure of DIMIM-MS ionic liquid cation-anion pairs with adopted atom numbers.

For the system under study, according to the NBO results, the formation of the H bond occurs depending on charge transfer from an oxygen lone-pair orbital of proton acceptor to non-Lewis valence antibonding orbital of the C-H bond of the proton donor: $n(\sigma)O \rightarrow \pi^*C-H$.

Resonance interactions between donor and acceptor due to hydrogen bonding are given by filled (donor) and unfilled (acceptor) (Lewis and non-Lewis type NBOs), using second-order perturbation theory (Table 1). Stabilization energy (Table 2) is calculated from the second-order perturbation approach (where q_i is the population of the lone-pair orbital of the proton acceptor, F_{ij} is the relevant off-diagonal Fock matrix element and $(\epsilon_j - \epsilon_i)$ is the energy difference between the interacting NBOs) (Fig. 2) [21].

$$E(2) = \Delta E_{ij} = q_i \frac{F_{ij}^2}{\epsilon_j - \epsilon_i} \quad (1)$$

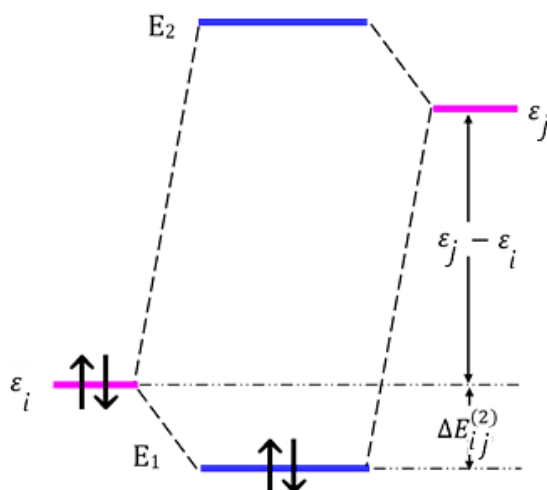


Figure 2. A filled donor and an unfilled acceptor interactions of two electrons: Perturbation theory energy analysis.

Table 1. The selected NBO second-order interaction energies ($\Delta E_{ij}=E(2)$) obtained from B3LYP/6-311++G(2d,2p) calculations*.

Donor NBO (<i>i</i>)	Acceptor NBO (<i>j</i>)	E(2) (kJ mol ⁻¹)	$\epsilon(j)-\epsilon(i)$ (a.u.)	F_{ij} (a.u.)
LP(1)O18	$\sigma^*(C2-H8)$	5.40	1.18	0.035
LP(2)O18	$\pi^*(C2-H8)$	13.81	0.67	0.043
LP(3)O18	$\pi^*(C2-H8)$	2.55	0.66	0.019
LP(1)O20	$\sigma^*(C2-H8)$	11.92	1.19	0.052
LP(2)O20	$\pi^*(C2-H8)$	20.08	0.67	0.052
LP(3)O20	$\pi^*(C2-H8)$	14.02	0.67	0.044
Total		67.78		
LP(1)O18	$\sigma^*(C6-H13)$	12.01	1.17	0.052
LP(2)O18	$\pi^*(C6-H13)$	2.72	0.66	0.019
Total		14.73		
LP(1)O20	$\sigma^*(C7-H14)$	1.21	1.15	0.016
Total		1.21		

* See atom numbering in Fig. 1. LP, lone electron pair orbital.

Table 1 shows that the orbital interaction energy between LP(2)O20 and $\pi^*(C2-H8)$ is the strongest one. The enhanced negative charges at O20 and O18 atoms reveal a decreased s character and an increased p character of the σ -type lone electron pairs. LP(2)O18, LP(3)O18, LP(2)O20 and LP(3)O20 are the p-rich π -type lone pairs (all LP are nO(π); 99.32%, 99.62%, 99.23% and 99.43% p-character, respectively), perpendicular to the bond axis.

Table 2. Total Lewis and non-Lewis occupancies (valence, core, and Rydberg shells).

Core	33.99202 e (99.977%)
Valence	73.72875 e (97.012%)
Lewis	
Total Lewis	107.72077 e (97.928%)
Valence	1.88706 e (1.716%)
non-Lewis	
Rydberg	0.39217 e (0.357%)
non-Lewis	
Total non-Lewis	2.27923 e (2.072%)

(e=1.60217646×10⁻¹⁹ C)

Table 2 summarizes percentage of the occupancies of the core, valence and Rydberg of orbitals due to Lewis and non-Lewis for DIMIM-MS. These results show delocalization of electron densities between donor and acceptor orbitals depend on Lewis and non-Lewis NBO orbitals. Total Lewis and non-Lewis were calculated 97.921% and 2.079%, respectively.

Table 3. Lewis (unstarred) and non-Lewis type (starred) NBO Hybrid composition

$\sigma(\text{C}_2\text{H}_8)$	$= 0.816(\text{sp}^{1.44})_{\text{C}} + 0.579(\text{s})_{\text{H}}$
$\sigma^*(\text{C}_2\text{H}_8)$	$= 0.579(\text{sp}^{1.44})_{\text{C}} - 0.816(\text{s})_{\text{H}}$
$\sigma(\text{C}_6\text{H}_{13})$	$= 0.801 (\text{sp}^{2.63})_{\text{C}} + 0.600(\text{s})_{\text{H}}$
$\sigma^*(\text{C}_6\text{H}_{13})$	$= 0.603 (\text{sp}^{2.69})_{\text{C}} - 0.798(\text{s})_{\text{H}}$
$\sigma(\text{C}_7\text{H}_{14})$	$= 0.800 (\text{sp}^{3.02})_{\text{C}} + 0.601(\text{s})_{\text{H}}$
$\sigma^*(\text{C}_7\text{H}_{14})$	$= 0.602 (\text{sp}^{2.67})_{\text{C}} - 0.798(\text{s})_{\text{H}}$

The data of Table 3 can be explained as follows:

in-phase “Lewis-type” NBO:

$$\sigma_{\text{AB}} = c_{\text{A}}h_{\text{A}} + c_{\text{B}}h_{\text{B}}, \quad h_{\text{A}}, h_{\text{B}} \text{ [natural hybrid orbitals]}$$

out-of-phase “non-Lewis” NBO,

$\sigma^*_{\text{AB}} = c_{\text{A}}h_{\text{A}} - c_{\text{B}}h_{\text{B}}$, c_{A} , c_{B} [polarization coefficient] Depending on the values of these coefficients, a bond NBO may range between covalent ($c_{\text{A}} = c_{\text{B}}$) and ionic ($c_{\text{A}} \gg c_{\text{B}}$) limits. "2-center" σ_{AB} of highly polar form ($c_{\text{A}} \gg c_{\text{B}}$) and a "1-center" nA ($c_{\text{A}} = 1$, $c_{\text{B}} = 0$).

The p character of the hybrid orbital increases if the donor orbital better “overlaps” the acceptor p than the s orbital [21]. Lone-pair-bearing bases (:O), leading to “hydrogen-bond” of the form



The donor-acceptor orbital interactions of the energy values given in Table 1, are plotted and given in Fig. 3. Both the NBO second-order perturbative analysis and natural charges on atoms reveal, in agreement with previous structural data, that the most important anion-cation interactions involve the lone-electron pairs of the two sulphate oxygen atoms that are located closer to the cation and the hydrogen atom of this

latter species which is bonded to C2 (through the C-H antibonding orbital).

Since the transition state from n to n is not possible, orbital interactions in this state ($n(\pi)LP(3)(O18) \rightarrow n(\pi)BD^*(1)(C6-H13)$) are not observed (Fig.3.)

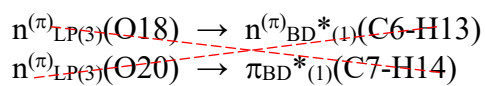
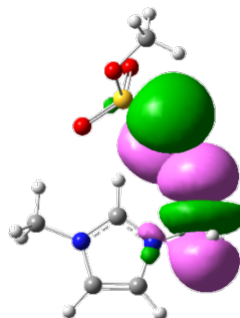
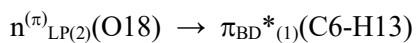
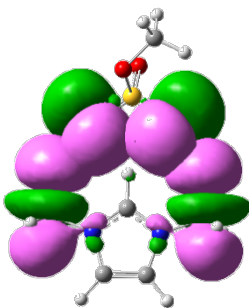
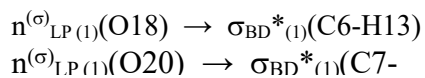
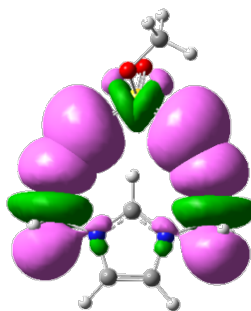
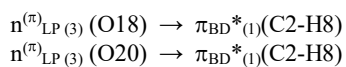
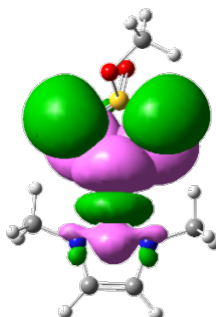
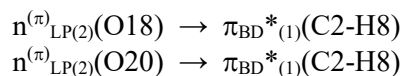
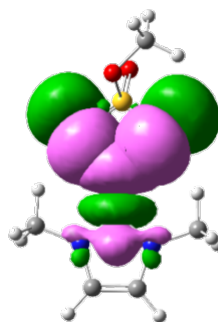
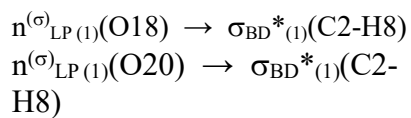
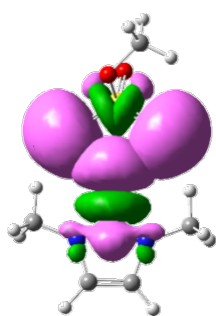


Figure 3. The most important anion-cation interactions (see Table 1). Isovalues of the electron densities are equal

to 0.02 e. Pink and green colors correspond to positive and negative wave function signs.

LP(1)O20 is the s-rich σ -type $sp^{0.31}$ lone pair ($nO(\sigma)$; 75.21% s character), directed along the bond axis. LP(2)O20 and LP(3)O20 are the p-rich π -type lone pairs ($nO(\pi)$ and $nO(\pi)$; 99.37% and 99.55% p-character, respectively), perpendicular to the bond axis. LP(1)O18 s-pair ($nO(\sigma)$; 74.54% s character), directed along the bond axis.

Table 4. The orbital type, occupancy values.

type	hybrid orbital	occupancy (e)	hybridization and ($e=1.60217646 \times 10^{-19}$ C).
LP(1)O18	$sp^{0.32}$	1.97477	
LP(2)O18	$spd^{0.87}$	1.85350	
LP(3)O18	$spd^{16.72}$	1.82714	
LP(1)O20	$sp^{0.31}$	1.97732	
LP(2)O20	$spd^{0.71}$	1.85532	
LP(3)O20	$spd^{1.44}$	1.83005	
BD*(1)C2-H8	$sp^{1.44}$ -s	0.04561	
BD*(1)C6-H13	$sp^{2.63}$ -s	0.00994	
BD*(1)C7-H14	$sp^{3.02}$ -s	0.00402	

All anti-bonding orbitals cause weak delocalization and make no comparatively contribution to occupancies NBOs (Table 4).

The NBO method can be used to study charge transfer, electronic transitions and atomic interactions in molecules. The Mulliken and natural charges for the DIMIM-MS are tabulated in Table 5. The highest positive and lowest minimum natural atomic charge values are seen in S and O20 atoms, respectively. The interaction between the dipoles associated with the highly polarized S-O bond and charges on S and O20 are of ca. +2.565 e and ca. -1.055 e, respectively.

Table 5. The calculated natural and Mulliken charges of the DIMIM-MS, using B3LYP/6-311++G(2d,2p) level.

Atom	Natural (e)	Mulliken (e)
N1	-0.35771	0.018381
C2	0.30524	-0.032845
N3	-0.35789	0.013968
C4	-0.02751	-0.115477
C5	-0.02751	-0.115836
C6	-0.36452	-0.160200
C7	-0.36568	-0.165558
H8	0.30433	0.276245
H9	0.23077	0.127709

H10	0.23068	0.127422
H11	0.20679	0.119031
H12	0.20576	0.121904
H13	0.27047	0.195639
H14	0.27215	0.200419
H15	0.20515	0.119403
H16	0.20624	0.120059
S17	2.56500	1.292751
O18	-1.03880	-0.635530
O19	-0.96767	-0.640994
O20	-1.05476	-0.738040
O21	-0.76358	-0.374047
C22	-0.21122	-0.082639
H23	0.17564	0.097364
H24	0.17308	0.105522
H25	0.18556	0.125350

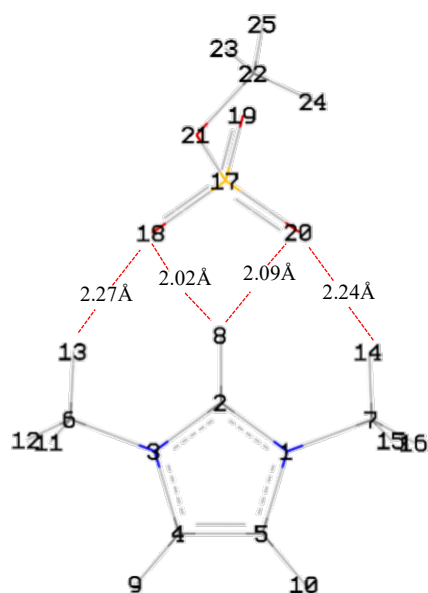


Figure 4. Calculated H bond lengths C-H \cdots O of DIMIM-MS.

The H bond lengths between methylsulphate anion and dimethylimidazolium cation are given in Fig. 4. C6-O18, H8-O18, H8-O20 and H14-O20 hydrogen bond lengths are found 2.27, 2.02, 2.09 and 2.24 Å, respectively.

The energy difference between the HOMO and LUMO of DIMIM-MS was calculated using B3LYP/6-311++G(2d,2p) level, and found to be ca. 4.78 eV. Fig. 5 is shown electron density HOMO-LUMO surfaces of energy for DIMIM-MS. Calculated HOMO-LUMO energy gap was corresponds to the transition $\pi \rightarrow \pi^*$ state.

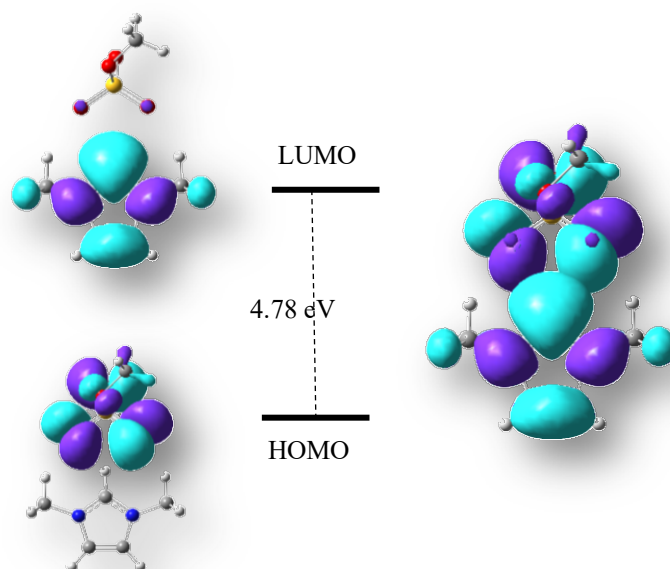


Figure 5. Electron density HOMO-LUMO surfaces of energy for DIMIM-MS.

4. CONCLUSIONS

The NBO and donor-acceptor orbital interactions of DIMIM-MS were investigated using DFT-B3LYP/6-311++G(2d,2p) method. Stabilization energies and significant orbital interactions between anion and cation pairs were calculated using NBO method and presented. The strongest hydrogen bonding orbital interaction energy was ca. 68 kJ mol⁻¹. These interactions associate with the electronic charge back-donation from the MS oxygen pi-type lone electron pairs (LP(2,3) O18 and LP(2,3) O20) and sigma-type lone electron pairs (LP(1) O18 and LP(1) O20) to the DIMIM C2-H8 bond. HOMO-LUMO energy difference was found ca. 4.78 eV. NBO charges and Mulliken charges were calculated for DIMIM-MS with respect to Schrödinger equation.

ACKNOWLEDGMENT

This work was supported by the Eskisehir Technical University Commission of Research Project under grant no: 23ADP042.

REFERENCES

- [1] Seddon, K. R. 2003. Ionic liquids: a taste of the future. *Nat. Mater.*, 2, 363-365.
- [2] Marsh, K. N., Devv, A., Wu, A. C.-T., Tran, E., Klamt, A. 2002. Room temperature ionic liquids as replacements for conventional solvents. *Korean J. Chem. Eng.*, 19(3), 357-362.
- [3] Walden, P. 1914. Molecular weights and electrical conductivity of several fused salts. *Bull. Acad. Imp. Sci. (St.Peterburg)*, 1800, 405-422.
- [4] Jain, N., Kumar, A., Chauhan, S., Chauhan, S. M. S. 2005. Chemical and biochemical transformations in ionic liquids. *Tetrahedron*. 61, 1015-1060.
- [5] Gerfi, A., Dontigny, M., Charest, P., Petitclerc, M., Lagace, M., Vijh, A., Zaghib, K. 2010. Improved electrolytes for Li-ion batteries: Mixtures of ionic liquid and organic electrolyte with enhanced safety and electrochemical performance. *J.Power Sources.*, 195, 845-852.
- [6] Xue, B. F., Wang, H. X., Hu, Y. S., Li, H., Wang, Z. X., Meng, Q. B., Huang, X. J., Sato, O., Chen, L. Q., Fujishima, A. 2004. An alternative ionic liquid based electrolyte for dye-sensitized solar cells. *Photochem. Photobiol. Sci.*, 3, 918-919.
- [7] Feher, E., Major, B., Belafi-Bako, K., Gubicza, L. 2009. Semi-continuous enzymatic production and membrane assisted separation of isoamyl acetate in alcohol ionic liquid biphasic system. *Desalination.*, 241, 8-13.
- [8] Chum, H. L., Koch, V. R., Miller, L. L., Osteryoung, R. A. 1975. An electrochemical scrutiny of organometallic iron complexes and hexamethylbenzene in a room temperature molten salt. *J. Am. Chem. Soc.*, 97, 3264-3267.
- [9] Kolancılar, H. 2010. Klasik Çözücülere Bir Alternatif; İyonik Sıvılar. *Trakya Univ J Sci*, 11(2), 90-100.
- [10] Welton, T. 1999. Room-temperature ionic liquids. Solvents for synthesis and catalysis. *Chem. Rev.*, 99, 2071-2083.
- [11] Zhou, F., Azofra, L. M., Ali, M., Kar, M., Simonov, A. N., M.-Worth, C., Sun, C., Zhang, X., MacFarlane, D. R. 2017. Electro-synthesis of ammonia from nitrogen at ambient temperature and pressure in ionic liquids. *Energ. Env. Sci.*, 10, 2516-2520.
- [12] Pernak, J., Sobaszekiewicz, K., Mirska, I. 2003. Anti-microbial activities of ionic liquids. *Green Chem.*, 5, 52-56.
- [13] Scammells, P. J., Scott, J. L., Singer, R. D. 2005. Ionic Liquids: The Neglected Issues. *Aust. J. Chem.*, 58(3), 155-169.
- [14] Gathergood, N., Scammells, P. J. 2002. Design and Preparation of Room-Temperature Ionic Liquids Containing Biodegradable Side Chains. *Aust. J. Chem.*, 55(9), 557-560.

- [15] Wasserscheid, P. 2006. Volatile times for ionic liquids. *Nature*, 439, 797.
- [16] Chang, H-C. Jiang, J-C., Tsai, W-C., Chen, G-C., Lin S. H. 2006. "Hydrogen Bond Stabilization in 1,3-Dimethylimidazolium Methyl Sulfate and 1-Butyl-3-Methylimidazolium Hexafluorophosphate Probed by High Pressure: The Role of Charge-Enhanced C-H \cdots O Interactions in the Room-Temperature Ionic Liquid. *J. Phys. Chem. B*, 110, 7, 3302-3307.
- [17] Holbrey, J. D.; Reichert, W. M.; Swatloski, R. P.; Broker, G. A.; Pitner, W. R.; Seddon, K. R.; Rogers, R. D. 2002. Efficient, halide free synthesis of new, low cost ionic liquids: 1,3-dialkylimidazolium salts containing methyl- and ethyl-sulfate anions. *Green Chem.*, 4, 407-413.
- [18] Becke, A. D. 1988. Density-functional exchange-energy approximation with correct asymptotic behavior. *Phys. Rev. A*, 38, 3098-3100.
- [19] Lee, C. T., Yang, W. T., Parr, R. G. 1988. Development of the Colic-Salvetti correlation-energy formula into a functional of the electron density. *Phys. Rev. B*, 37, 785-789.
- [20] Reed, A. E., Curtiss, L. A., Weinhold, F. 1988. Intermolecular interactions from a natural bond orbital, donor-acceptor viewpoint. *Chem. Rev.*, 88, 899-926.
- [21] Weinhold, F., Landis, C. R. 2005. *Valency and Bonding. A Natural Bond Orbital Donor-Acceptor Perspective*, Cambridge University Press: New York.
- [22] Frisch, M. J., *et al.* 2009, Gaussian 09, Revision A.0.2, Gaussian, Inc., Wallingford CT.

DOI: [10.5281/zenodo.8220297](https://doi.org/10.5281/zenodo.8220297)

INVESTIGATION OF TRANSFORMATION' SYMMETRIC MOLECULES WITH CLIFFORD ALGEBRA

Abidin KILIÇ

Physics Department, Faculty of Science, Eskisehir Technical University, Eskisehir, Turkey

ABSTRACT

When solving a Physics problem, there is a need for a mathematical system in which the problem is defined and an algebra in which the solution of this problem can be defined. Physicists also used Clifford's self-titled algebra for this purpose.

Clifford (1878) introduced his 'geometric algebras' as a generalization of Grassmann algebras, complex numbers and quaternions. Lipschitz (1886) was the first to define groups constructed from 'Clifford numbers' and use them to represent rotations in a Euclidean space.

It is possible to describe perfectly symmetric molecules with Clifford's Algebra. In addition, the symmetry operations of these perfectly symmetric molecules can be represented by Clifford Algebra. In this study, the transformation matrices of perfectly symmetric molecules, also known as Platonic Solids, were studied..

Anahtar Kelimeler: Clifford Algebra, Symmetry Operations, Platonic Solids.

Introduction

The geometric algebra produces the new fields of view in the modern mathematical physics, definition of bodies and rearranging for equations of mathematics and physics. The new mathematical approaches play an important role in the progress of physics.

The exponential form of complex numbers is useful in the theory of rotational motions. The quaternion algebra, which was defined by Sir W. R. Hamilton, was generalized for the three dimensional complex numbers [1]. The quaternion algebra is the Clifford algebra of the two- dimensional anti-Euclidean space. Quaternions in the three-dimensional spaces have more use- ful appearances for the subalgebras of Clifford algebra. In the n-dimensional spaces, Grassmann carried on the studies for the multi-dimensional bodies and defined the central product, which includes the both interior and exterior products. The Grassmann's central product is the Clifford product of vectors. This result was found by Grassmann independently from Clifford. Clifford tried to combine the Grassmann's algebra and quaternions in a mathematical system.

Today, Clifford algebra has an important role in the investigations of the symmetry properties of systems, crystallography, molecular and solid state physics.

Clifford Algebra and Symmetry Operations

Clifford algebra in physics is used for the studies of symmetry. There are three basic units e_i ($i=1, 2, 3$) in Clifford algebra such that

$$e_i e_j + e_j e_i = 2\delta_{ij}, \quad (1)$$

which are equivalent to

$$e_i e_j = 1, \quad (2)$$

$$\mathbf{e}_i \mathbf{e}_j = -\mathbf{e}_j \mathbf{e}_i. \quad (3)$$

Using \mathbf{e}_1 , \mathbf{e}_2 and \mathbf{e}_3 , which are the terms of second and third rank, $\mathbf{e}_i \mathbf{e}_j$ and $\mathbf{e}_i \mathbf{e}_j \mathbf{e}_k$, can be defined as follows [7]:

$$\mathbf{e}_1 \mathbf{e}_1 = 1, \quad (4)$$

$$(\mathbf{e}_2 \mathbf{e}_1)(\mathbf{e}_2 \mathbf{e}_1) = \mathbf{e}_2 \mathbf{e}_1 \mathbf{e}_2 \mathbf{e}_1 = -\mathbf{e}_2 \mathbf{e}_1 \mathbf{e}_1 \mathbf{e}_2 = -1, \quad (5)$$

$$(\mathbf{e}_1 \mathbf{e}_2 \mathbf{e}_3)(\mathbf{e}_1 \mathbf{e}_2 \mathbf{e}_3) = -1. \quad (6)$$

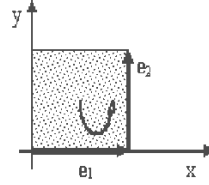


Fig. 1. Directional area with \mathbf{e}_1 and \mathbf{e}_2

The result of $\mathbf{e}_1 \mathbf{e}_2$ product is neither scalar nor vector. This product is called bivector. The $\mathbf{e}_1 \mathbf{e}_2$ product is represented by \mathbf{e}_{12} that shows the oriented plane area of the square with sides \mathbf{e}_1 and \mathbf{e}_2 .

1, \mathbf{e}_1 , \mathbf{e}_2 , \mathbf{e}_3 form the basis of the Clifford algebra Cl_2 of the vector plane \mathbb{R}^2 . An arbitrary element of Cl_2 is

$$\mathbf{u} = u_0 + u_1 \mathbf{e}_1 + u_2 \mathbf{e}_2 + u_{12} \mathbf{e}_{12}, \quad (7)$$

where $u, u_1, u_2, u_{12} \in \mathbb{R}$. The Clifford algebra Cl_2 is the four-dimensional linear space and its basis elements have the multiplication Table 1 as follows:

Table 1. The basis of Clifford Algebra

	\mathbf{e}_1	\mathbf{e}_2	\mathbf{e}_{12}
\mathbf{e}_1	1	\mathbf{e}_{12}	\mathbf{e}_2
\mathbf{e}_2	$-\mathbf{e}_{12}$	1	$-\mathbf{e}_1$
\mathbf{e}_{12}	$-\mathbf{e}_2$	\mathbf{e}_1	-1

The Clifford product of two vectors, namely \mathbf{a} and \mathbf{b} , with components;

$$\mathbf{a} = a_1 \mathbf{e}_1 + a_2 \mathbf{e}_2, \quad (8)$$

and

$$\mathbf{b} = b_1 \mathbf{e}_1 + b_2 \mathbf{e}_2, \quad (9)$$

is given by

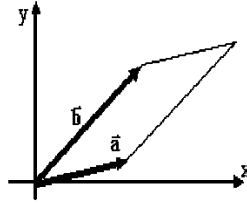


Fig. 2. The geometrical meaning of $\mathbf{a} \wedge \mathbf{b}$.

$$\mathbf{a} \mathbf{b} = \mathbf{a} \cdot \mathbf{b} + \mathbf{a} \wedge \mathbf{b} = a_1 b_1 + a_2 b_2 + (a_1 b_2 - a_2 b_1) \mathbf{e}_{12}, \quad (10)$$

where " \wedge " is called as the wedge product [11]. The bivector $\mathbf{a} \wedge \mathbf{b}$ represents the oriented plane segment of the parallelogram with sides \mathbf{a} and \mathbf{b} .

The reflection of \mathbf{r} across the line \mathbf{a} , namely the mirror image \mathbf{r}' of \mathbf{r} with respect to \mathbf{a} , is given by

$$\mathbf{r}' = \mathbf{a} \mathbf{r} \mathbf{a}^{-1} \quad (11)$$

Equation (11) can be directly obtained from using the commutation properties of Clifford algebra [7]. The composition of two reflections, first across \mathbf{a} and then across \mathbf{b} , is given by

$$\mathbf{r}' = \mathbf{b} \mathbf{r}' \mathbf{b}^{-1} = \mathbf{b} (\mathbf{a} \mathbf{r} \mathbf{a}^{-1}) \mathbf{b}^{-1} = (\mathbf{b} \mathbf{a}) \mathbf{r} (\mathbf{b} \mathbf{a})^{-1} \quad (12)$$

Platonic Solids

The Platonic solids are tetrahedron, cube, octahedron, icosahedron and dodecahedron. Some important numbers for the Platonic solids are shown in Table 2.

Table 2. Numbers for the five Platonic solids

	Number of faces	Number of edges	Number of vertices	Edges per face
Tetrahedron	4	6	4	3
Cube	6	12	8	4
Octahedron	8	12	6	3
Icosahedron	20	30	12	3
Dodecahedron	12	30	20	5

A dodecahedron has twenty-vertices. The vertices of a dodecahedron, whose origin was chosen at the centre of body, are indexed as cartesian coordinates in Table 3.

The special isometric transformations of a cylindrical surface were discovered and studied by Pogorelov [8]. They admit a certain regular structure. To describe them, an auxiliary regular prism with an even number of sides is considered. Let us denote it by Π . It has a vertical axis. On its lateral faces congruent smooth curves $\gamma_1, \dots, \gamma_{2n}$ are drawn (Fig. 3) which are spanned by cylindrical surfaces $Z_1, Z_2, \dots, Z_{2n-1}, Z_{2n}$ with horizontal generators (Fig. 3). It is seen that surface Z isometric to a cylindrical surface. Let it be admitted each curve γ_i has zero curvature at any of its points, that is, every ridge line γ_i actually is a rectilinear edge i , $i = 1, \dots, 2n$. Then we obtain the following three natural special cases: (1) if i partitions the corresponding face of Π into two equal rectangles, then the surface Z is a regular prism, which we denote by P (see Fig. 1); (2) if i partitions the face of Π into two equal trapezoids, then the surface Z consists

of congruent equilateral trapezoids, and we denote it by T (see Fig. 3); (3) if i partitions the face of Π into two equal triangles, then the surface Z is an antiprism, which we denote by A (see Fig. 1).

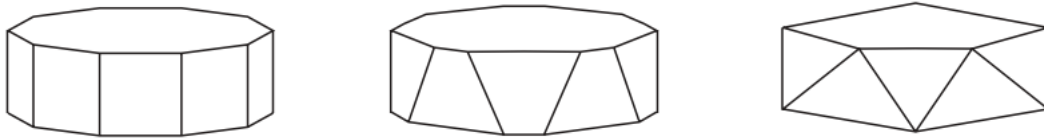


Fig. 3. All intermediate positions on solid surfaces

In the case (2) the segment I can run over all intermediate positions (vacancies) between the two extreme positions (1) and (3). However, among the infinitely many such vacancies for i we henceforth select and fix only one of them.

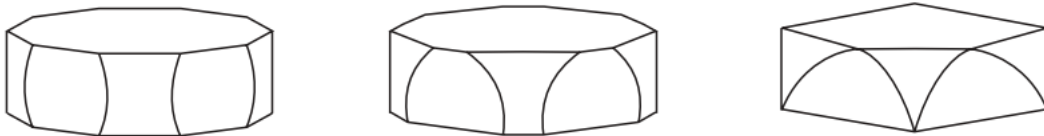


Fig. 4 All intermediate positions on solid surfaces


We apply what has just been said to the surfaces of the Platonic solids. Namely, suppose that a planar cross-section of the surface, perpendicular to an axis of symmetry of the solid, does not contain vertices of the solid and is a closed geodesic line on the surface. Then all such parallel cross-sections constitute a belt cut out of the surface by the two extreme parallel planes going through vertices of the solid. As it turns out, the belt has the form of one of the surfaces P, T or A. Indeed, on the surface of a cube, the belt with an axis of 4th order is the prism P. On the surface of a dodecahedron, the belt with an axis of 3rd order is the surface T. On the surface of a tetrahedron, octahedron, cube, dodecahedron or icosahedron, the belt with an axis of 2nd, 3rd, 3rd, 5th, 5th order respectively, is the antiprism A. Moreover, we replace the piecewise linear belts P, T, and A in the surfaces of the Platonic solids with the isometric piecewise smooth belts $Z = Z(P)$, $Z = Z(T)$, and $Z = Z(A)$ in Figs. 4–6. In all three figures, the extreme left (right) ridge line γ_i projects onto a rectilinear segment. We obtain a piecewise smooth embedding of the surface of the Platonic solid in R^3 . In all cases, the belt Z has the curved lateral edges γ_i . In three cases, new rectilinear edges appear on the surface: 10 of them in the case of a belt with an axis of 5th order for the dodecahedron, and 6 of them in the case of a belt with an axis of 3rd order for the dodecahedron and the cube. Finally, if the curvature of the ridge line γ_i approaches zero at all points of the smooth curves γ_i of the belt Z, then the curved edges γ_i (they are not geodesics on Z; they are arbitrarily chosen on the planes of the lateral faces of Π ; see [1]) with fixed endpoints (the endpoints of the varying edges γ_i are fixed on the bending belt Z, but not in the ambient space R^3) are deformed into the rectilinear edges i (geodesics on Z). We obtain a continuous piecewise smooth bending of the surface of the Platonic solid with a smoothly varying belt Z in R^3 with varying curved edges γ_i [9].

Conclusion

The case of an axis of 2nd order for a tetrahedron is singular, since the belt is the singular antiprism A: its bases are degenerate; they are two opposite edges of a tetrahedron. However, this belt A can be replaced with the piecewise smooth belt $Z(A)$ [10]. Hence the tetrahedron admits a continuous bending where two opposite edges remain rectilinear and the remaining four edges are deformed into curvilinear ones. We thus obtain exclusively piecewise smooth embeddings of the surface of the tetrahedron in three-dimensional Euclidean space R^3 . They are without linear parts: all four triangular faces are non-linear. In this they differ from the other embeddings given above and in [11].

References

- [1] M.Kline: Mathematical Thought from Ancient to Modern Times. Oxford University Press, Oxford (1972)
- [2] W.K.Clifford: Am. J. Math.1 (1878) 350
- [3] S.L.Altmann: Rotations, quaternions, and double groups. Clarendon Press, Oxford (1994)
- [4] J. Funda, R. P. Paul: A Comparison of Transforms and Quaternions in Physics, Proc. 1988 IEEE Int. Conf. Robotics and Automation, Philadelphia, 1988, p. 886

- 
- [5] Fletcher, J.P., Spinor Representations of Clifford Algebra: A Symbolic Approach". 53 (3) (2003) 253
- [6] O. Rodrigues: Journal de Mathématiques Pures et Appliquées 5 (1840) 380
- [7] P. Lounesto: Lectures on Clifford Geometric Algebras. TTU Press, Cookeville, TN, USA (2002)
- [8] A. Kılıç, K. Özdaş, M. Tanışlı, An Investigation of Symmetry Operations With Clifford Algebra, Acta Physica Slovaca, (54), 221, 2004.
- [9] A. V. Pogorelov, Bendings of surfaces and stability of shells, 2nd ed., Naukova Dumka, Kiev 1998; English transl. of 1st ed., Amer. Math. Soc., Providence, RI 1988.
- [10] M. I. Shtogrin, Uspekhi Mat. Nauk 59:5 (2004), 167–168; English transl., Russian Math. Surveys 59 (2004), 979–981.
- [11] M. I. Shtogrin, Special isometric transformations of the surfaces of the Platonic solids, Communications of the Moscow Mathematical Society.